

ESTABLISHMENT OF TRANSPLANTATION PLATFORM FOR DELIVERING MOUSE INDUCED  
PLURIPOTENT STEM CELL-DERIVED INSULIN-PRODUCING CELLS (miPS-IPCs) FOR  
DIABETES TREATMENT



A Dissertation Submitted in Partial Fulfillment of the Requirements  
for the Degree of Doctor of Philosophy in Veterinary Science and technology

FACULTY OF VETERINARY SCIENCE

Chulalongkorn University

Academic Year 2022

Copyright of Chulalongkorn University



การพัฒนารูปแบบการปลูกถ่ายสำหรับการนำส่งเซลล์สังเคราะห์อินซูลินจากเซลล์ต้นกำเนิดพลูริโพเท

นต์ชนิดเหนียวนำของหนูเมาส์เพื่อการรักษาโรคเบาหวาน



วิทยานิพนธ์นี้เป็นส่วนหนึ่งของการศึกษาตามหลักสูตรปริญญาวิทยาศาสตรดุษฎีบัณฑิต

สาขาวิชาวิทยาศาสตร์ทางการสัตวแพทย์และเทคโนโลยี ไม่สังกัดภาควิชา/เทียบเท่า

คณะสัตวแพทยศาสตร์ จุฬาลงกรณ์มหาวิทยาลัย

ปีการศึกษา 2565

ลิขสิทธิ์ของจุฬาลงกรณ์มหาวิทยาลัย



จุฬาลงกรณ์มหาวิทยาลัย  
**CHULALONGKORN UNIVERSITY**

Thesis Title ESTABLISHMENT OF TRANSPLANTATION PLATFORM FOR DELIVERING MOUSE  
INDUCED PLURIPOTENT STEM CELL-DERIVED INSULIN-PRODUCING CELLS  
(miPS-IPCs) FOR DIABETES TREATMENT

By Miss Hong Thuan Tran

Field of Study Veterinary Science and technology

Thesis Advisor Assistant Professor CHENPHOP SAWANGMAKE, D.V.M, Ph.D.

---

Accepted by the FACULTY OF VETERINARY SCIENCE, Chulalongkorn University in Partial Fulfillment of  
the Requirement for the Doctor of Philosophy

.....  
Dean of the FACULTY OF VETERINARY SCIENCE  
(Professor SANIPA SURADHAT, D.V.M., Ph.D.)

DISSERTATION COMMITTEE

.....  
Chairman  
(Associate Professor Pakpoom Kheolamai, M.D., Ph.D.)

.....  
Thesis Advisor  
(Assistant Professor CHENPHOP SAWANGMAKE, D.V.M, Ph.D.)

.....  
Examiner  
(Associate Professor NOPADON PIRARAT, D.V.M., Ph.D.)

.....  
Examiner  
(Assistant Professor THEERAWAT THARASANIT, D.V.M., Ph.D.)

.....  
Examiner  
(Professor Thanaphum Osathanoon, DSS., Ph.D.)

.....  
Examiner  
(Nuttha Klincumhom, D.V.M., Ph.D.)

สอง ตอน ทราน :

การพัฒนาแบบการปลูกถ่ายสำหรับการนำส่งเซลล์สังเคราะห์อินซูลินจากเซลล์ต้นกำเนิดพลูริโพเทนต์ชนิดเหนียวนำของหนูเม้าส์เพื่อการรักษาโรคเบาหวาน. ( ESTABLISHMENT OF TRANSPLANTATION PLATFORM FOR DELIVERING MOUSE INDUCED PLURIPOTENT STEM CELL-DERIVED INSULIN-PRODUCING CELLS (miPS-IPCs) FOR DIABETES TREATMENT) อ.ที่ปรึกษาหลัก : เจนภพ สว่างเมฆ

การปลูกถ่ายเบต้าเซลล์นั้นนับได้ว่าเป็นวิธีการที่มีความเป็นไปได้ในการรักษาโรคเบาหวานชนิดที่ 1 อย่างไรก็ตามมีรายงานถึงการต่อต้านจากภูมิคุ้มกันที่ส่งผลกระทบต่อการทำงานและการสูญเสียของเบต้าเซลล์ที่ปลูกถ่ายในมนุษย์และสัตว์ด้วยเหตุดังกล่าว จึงมีการพัฒนาเบต้าเซลล์ที่มีการเจริญเติบโตอย่างไม่จำกัด และมีความเข้ากันได้ทางชีวภาพรวมถึงรูปแบบการปลูกถ่ายเพื่อแก้ไขปัญหาดังกล่าวในการศึกษานี้เซลล์ต้นกำเนิดพลูริโพเทนต์ชนิดเหนียวนำของหนูเม้าส์ที่ได้จากเนื้อเยื่อเหงือกได้รับการเหนียวนำให้เปลี่ยนแปลงเป็นเซลล์สังเคราะห์อินซูลิน โดยการเหนียวนำด้วยสารเคมีอย่างมีขั้นตอน โดยได้รับการทดสอบยืนยันด้วยวิธีการเพิ่มจำนวนสารพันธุกรรม การวิเคราะห์ระดับซี-เปปไทด์ จากการกระตุ้นด้วยกลูโคส การย้อมทางภูมิคุ้มกัน และการตรวจควมมีชีวิตของเซลล์โดยเซลล์สังเคราะห์อินซูลินที่ผลิตได้จะถูกห่อหุ้มและปลูกถ่ายลงในถุงชั้นใต้ผิวหนังที่ได้รับการสร้างขึ้นและได้รับการตรวจวิเคราะห์ด้านค่าเม็ดเลือด ค่าเคมีของเลือด ระดับ ซี-เปปไทด์ ดัชนีโฮมา ความทนต่อการกระตุ้นด้วยกลูโคสด้วยการฉีดเข้าช่องท้อง ผลทางจุลพยาธิวิทยา และการศึกษาไซโตไคน์ด้วยวิธีทดสอบผ่านแอนติบอดี ตลอดช่วงระยะเวลาการศึกษา ผลการศึกษาพบว่าการสร้างถุงในชั้นใต้ผิวหนังด้วย 10% พลูโรนิค-เอฟ 127 และวิจีเอฟ-165 ประสบผลสำเร็จ โดยพบการสร้างหลอดเลือดในบริเวณรอบถุงใต้ผิวหนัง และการปลูกถ่ายเซลล์สังเคราะห์อินซูลินที่ถูกห่อหุ้มให้กับหนูที่เป็นเบาหวานจากการเหนียวนำด้วยสเตรปโตโซโทซิน ช่วยให้ระดับกลูโคสและการทนต่อการกระตุ้นด้วยกลูโคสอยู่ในระดับดีขึ้น โดยไม่พบการต่อต้านทางภูมิคุ้มกัน และยังสามารช่วยให้อาการเบาหวานมีสุขภาพดีขึ้น และมีช่วงชีวิตที่ยาวนานขึ้น การศึกษานี้เป็นต้นแบบของการพัฒนาวิธีการทางคลินิกเพื่อใช้ในการรักษาโรคเบาหวานชนิดที่ 1 โดยเซลล์บำบัดต่อไป

สาขาวิชา	วิทยาศาสตร์ทางการสัตวแพทย์และเทคโนโลยี	ลายมือชื่อนิสิต .....
	โลยี	
ปีการศึกษา	2565	ลายมือชื่อ อ.ที่ปรึกษาหลัก .....

# # 6278311131 : MAJOR VETERINARY SCIENCE AND TECHNOLOGY

KEYWORD: mouse gingival fibroblast-induced pluripotent stem cells, Insulin-producing cells, differentiation, transplantation, induced diabetic mice

Hong Thuan Tran : ESTABLISHMENT OF TRANSPLANTATION PLATFORM FOR DELIVERING MOUSE INDUCED PLURIPOTENT STEM CELL-DERIVED INSULIN-PRODUCING CELLS (miPS-IPCs) FOR DIABETES TREATMENT. Advisor: Asst. Prof. CHENPHOP SAWANGMAKE, D.V.M, Ph.D.

Pancreatic beta-cell replacement is recognized for feasible type 1 diabetes (T1D) treatment. However, in post-transplantation, the autoimmune destruction incidentally attacks the activity and survival of beta-cells are reported in animal and human. To address these concerns, the generation of immortalized, biocompatible beta-cells, and the engraftment platform are insightfully investigated. The stepwise chemical process was used for *in vitro* Insulin-producing cells (IPCs) production from mouse gingival fibroblast-induced pluripotent stem cells (mGF-iPSCs). The real-time qRT-PCR, glucose stimulation C-peptide/Insulin secretion, immunostaining, and visible cell methods were examined during IPC differentiation. The encapsulated-IPC beads were loaded into subcutaneous pocket space via transplantation platform. Completed blood count, blood chemistry, C-peptide, HOMA indexes, intraperitoneal glucose tolerance test, and histopathology were analyzed at pre-, post-transplantation and at termination. The 40 cytokines were explored via antibody array detection. In this study, *in vitro* IPC differentiation protocol was perceptively dissection. IPC encapsulation achieved to the transplantable capacity. In mice, the catheter insertion and 10% Pluronic-F127 carrying-VEGF-165 (VP) created the subcutaneous pocket formation (SPF), and stimulated angiogenesis and neovascularization surrounding the SPF. Especially, IPC-bead engraftment alleviated hyperglycemia in STZ-induced-diabetic mice-VP + IPC-bead transplantation. In post-transplantation, IPC-bead transplantation showed no immune response, as well as, IPC-bead maintained the health condition in diabetic mice. The obtained results can be applied as a clinical transplantation protocol for T1D treatment using cell-based therapy.

Field of Study: Veterinary Science and technology Student's Signature .....

Academic Year: 2022 Advisor's Signature .....

## ACKNOWLEDGEMENTS

Firstly, I would like to express my gratitude for the Second Century Fund (C2F) of Chulalongkorn University for Doctoral Scholarship, and Veterinary Clinical Stem Cell and Bioengineering Research Unit, Faculty of Veterinary, Department of Pharmacology, Chulalongkorn University for financial support.

I would like to acknowledge the chairman of thesis committee, Associate Professor Pakpoom Kheolamai MD, Ph.D., members of thesis committee, Assoc. Prof. Dr. Nopadon Pirarat, DVM., Ph.D.; Asst. Prof. Dr. Theerawat Tharasanit, DVM., Ph.D.; Prof. Dr. Thanaphum Osathanon, DDS, Ph.D.; Dr. Nuttha Klincumhom, DVM., Ph.D. for kindly providing useful comments to the study.

For the success on the study and thesis project, I would like to express my deepest gratitude to my thesis principle advisor, Assistant Professor Chenphop Sawangmake DVM., MSc, Ph.D. for supporting and taking care of me until reaching the destination.

For other kind supports, I would like to express my appreciation to Professor Prasit Pavasant DDS, Ph.D., Professor Thanaphum Osathanon DDS, Ph.D. Center of Excellence for Regenerative Dentistry, Faculty of Dentistry, Chulalongkorn University; Assoc. Prof. Dr. Sayamon Srisuwatanasagul DVM., Ph.D. Department of Anatomy, Chulalongkorn University; and staffs at Chulalongkorn University Laboratory Animal Center (CULAC) for supporting and helping on research work; the Veterinary Stem Cell and Bioengineering Innovation Center (VSCBIC) (<http://www.cuvscbic.com/>) for providing research facility support. For biggest supporters, I deeply thank my beloved family and my relatives for supporting, encouraging, and giving all their love to me.

จุฬาลงกรณ์มหาวิทยาลัย  
CHULALONGKORN UNIVERSITY

Hong Thuan Tran

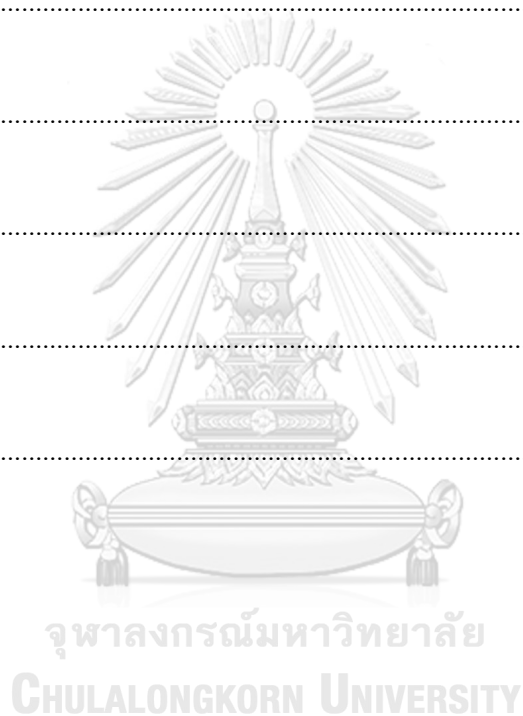


## TABLE OF CONTENTS

	Page
ABSTRACT (THAI).....	iii
ABSTRACT (ENGLISH).....	iv
ACKNOWLEDGEMENTS.....	v
TABLE OF CONTENTS.....	vi
LIST OF TABLES.....	ix
LIST OF FIGURES.....	x
CHAPTER I.....	1
INTRODUCTION.....	1
Importance and rationale.....	1
Objectives.....	4
Hypothesis /research question.....	5
CHAPTER II.....	6
LITERATURE REVIEW.....	6

Conceptual framework.....	32
CHAPTER III.....	34
METHODOLOGY.....	34
CHAPTER IV.....	49
RESULTS AND DISCUSSION.....	49
Establishment and optimization of the effective IPC differentiation using mGF-iPSCs modeling.....	49
In vitro in-house induction protocols yield efficient and long-term survival IPCs ...	56
Trypsin-EDTA causes EBs separating into single cells, nevertheless limits IPC capacity.....	62
Encapsulated IPCs preserve the Insulin secretion capacity and transplantable potential.....	64
Establishment of transplantation platform for safe and efficient IPC installment... 67	
Global exploration of cytokine network in mice receiving blank bead transplantation.....	75
The transplantation platform shows no effect on insulin-dependent tissues.....	78

Subcutaneous IPC-bead transplantation alleviates hyperglycemic condition and sustains survival rate in STZ-induced diabetic mice.....	80
Subcutaneous IPC-bead engraftment shows no immune response in post-transplantation.....	86
DISCUSSION.....	92
CHAPTER V.....	102
CONCLUSION.....	102
REFERENCES.....	2
VITA.....	40



## LIST OF TABLES

	Page
Table 1 Completed blood count parameters in CTRL and VEGF-165+10%Pluronic mice.....	71
Table 2 Blood chemistry parameters in CTRL and VEGF-165+10%Pluronic mice	71
Table 3 Completed blood count parameters in DM-VP + Blank bead Tx and DM-VP + IPC-bead Tx mice.....	83
Table 4 Blood chemistry parameters in DM-VP + Blank bead Tx and DM-VP + IPC-bead Tx mice.....	83

## LIST OF FIGURES

	<b>Page</b>
Figure 1 Establishment and optimization of the effective IPC differentiation using mGF-iPSCs modeling.....	53
Figure 2 In vitro in-house induction protocols yield efficient and long-term survival IPCs.....	60
Figure 3 Trypsin-EDTA made EBs separate in single cells, reduced the capacity of IPCs.....	63
Figure 4 Encapsulated IPCs preserve the Insulin secretion capacity and transplantable potential.....	66
Figure 5 Establishment of transplantation platform for safe and efficient IPC installment.....	70
Figure 6 Global exploration of cytokine network in mice receiving blank bead transplantation.....	76
Figure 7 The mixture of 250 ng/ml VEGF-165 + 10% Pluronic-F127 normally reacted in histopathological insulin-dependent tissues.....	79

Figure 8 Subcutaneous IPC-bead transplantation alleviates hyperglycemic condition and sustains survival rate in STZ-induced diabetic mice ..... 82

Figure 9 Subcutaneous IPC-bead engraftment shows no immune response in post-transplantation ..... 87

Figure 10 Insulin-dependent tissues were performed via H&E staining ..... 89



## CHAPTER I

### INTRODUCTION

#### Importance and rationale

Current benefits of the pancreatic beta-cell generation and replacement is applied for the feasible diabetes treatment (Roep et al. 2021). Production of in vitro immortal induced pluripotent stem cells (iPSCs)-derived from animal biopsy is fashionably concerned (Srivastava and Kilian 2019). Remarkably, gingival tissue is easily obtained and extracted which serves as a promising cell source of the iPSC induction. SNL fibroblast feeder cells are identified to maintain derivation of iPSCs and support their culturation (Egusa et al. 2010; Lai et al. 2011; Zhang et al. 2011; Oh et al. 2012; Lee et al. 2016; Yu et al. 2016; Osathanon et al. 2017; Haridhasapavalan et al. 2019; Wang et al. 2020). Insulin-producing cells (IPCs) are synthesized from various stem cells. Especially, the iPSCs-derived IPC differentiation manifests the more efficiencies and functionalities (Walczak et al. 2016; Kim et al. 2020a).

Notably, the microenvironment of transplantable space is focused on extracellular matrix contents, vascularization, and invaded immune cells (Assoc 2006; Mitrousis et al. 2018; Pomposelli et al. 2021). In post-transplantation, the host autoimmune cells incidentally attack the beta-cell activity and their longevity (Stabler et al. 2019; Roep

et al. 2021). Thus, immunomodulation and biocompatible materials can overcome the bottleneck of autoinflammatory reactions (Andorko and Jewell 2017; Chen et al. 2019). Cell encapsulation is the achievable method for reducing the impacts of cytokine storms and maintaining the engraftment lifelong in post-transplantation animals (An et al. 2018; Kuncorojakti et al. 2020).

According to the completed type 1 diabetes (T1D) model generation, a single dose of streptozotocin (STZ)-high concentration directly invades and damages the pancreatic beta-cells, then entirely provokes the STZ-induced T1D mice with hyperglycemia symptoms (Lipes and Eisenbarth 1990; Ohsugi et al. 1991; Rosmalen et al. 1997; Billotey et al. 2005; Giarratana et al. 2007; Van Belle et al. 2009; Deeds et al. 2011; Graham et al. 2011; Furman 2015; Chen et al. 2020; Hahn et al. 2020; Furman 2021). In the progress of translation of pancreatic islet transplantation therapies, the subcutaneous device-less (DL) is well recommended (Shapiro et al. 2000; Gunawardana et al. 2009; Lee et al. 2012; Kim et al. 2020b; Yu et al. 2020). Due to the surgery manipulation for subcutaneous DL sites is easy, painless, and minimally touch to other organs unexpectedly (Bromberg 2015; Audouard et al. 2021; Cayabyab et al. 2021). This method rapidly enhances vascularization, which permits oxygen and



glucose cargo to transplanted place (Halberstadt et al. 2005; Pepper et al. 2014; Pepper et al. 2015b; Kim et al. 2020b; Vlahos et al. 2021b).

Furthermore, the vascular endothelial growth factors (VEGF)-165 is mixed with the collagen matrix of encapsulated-ovarian-tissue that recruits the network of blood vessels in mice (Henry et al. 2015). In xenograft, VEGF-165 presented in encapsulated-pancreatic rat islets transplanting to diabetic mice, which triggers angiogenesis and decreases macrophage surrounding the membrane of cells; especially, revascularization of islet engraftments in post-transplantation (Sigrist et al. 2003; Rodrigues et al. 2013). VEGF-165 can modulates the inflammation and vascular permeability in rat brain (Proescholdt et al. 1999). Combinedly, Pluronic-F127 is a potential material for cell carrier and improves the angiogenesis in animal (Brunet-Maheu et al. 2009; Zhou et al. 2022). Pluronic-F127 interacts with VEGF and TFG-beta which enhances the wound healing process (Kant et al. 2014). Taken together, the combination of insulin-producing cell production, cell encapsulation, subcutaneous device-less transplantation, angiogenesis stimulation, oxygen, and nutrition demands are strategies for this application.

In this study, we have presented the high capacity of the insulin-producing cell (IPC) differentiation protocols from mGF-iPSCs including accurate endogenous IPC

biosynthesis and function. 10% Pluronic-F127-carrying-VEGF-165 significantly generated the subcutaneous pocket formation, which elevated the blood vessel network surrounding blank or IPC bead location, and subcutaneous pocket boundary. IPC-beads were translated for rescuing the insulin-dependent tissues, blood parameters and alleviating the hyperglycemia symptoms in STZ-induced-diabetic mice-VEGF-165+10%Pluronic + IPC-bead transplantation (DM-VP+IPC-bead Tx mice). The 40 inflammatory cytokines were globally explored in the blood circulation in DM-VP+IPC-bead Tx mice. Moreover, IPC-beads maintained the health condition in diabetic mice. Here, the results are used for a reference strategy of IPC differentiation protocol. The achievement of high-performance IPC engraftment is applied as a clinical protocol for diabetes treatment using cell-based therapy.



### **Objectives**

To establish and optimize the differentiation protocol for insulin-producing cells (IPCs) production from mouse gingival fibroblast-derived induced pluripotent stem cells (mGF-iPSCs)

To establish the transplantation platform for delivering IPCs generated from mGF-iPSCs

To explore the anti-diabetic capacity of the encapsulated mouse induced pluripotent stem cell-derived insulin-producing cells (miPS-IPCs) in type I diabetes (T1D) mouse model

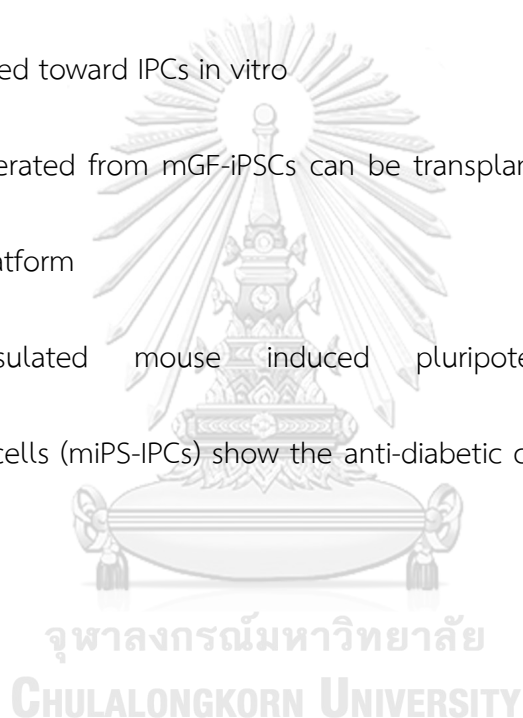
### **Hypothesis /research question**

Whether mouse gingival fibroblast-derived induced pluripotent stem cells (mGF-iPSCs)

can be differentiated toward IPCs in vitro

Whether IPCs generated from mGF-iPSCs can be transplanted using the established transplantation platform

Whether encapsulated mouse induced pluripotent stem cell-derived insulin-producing cells (miPS-IPCs) show the anti-diabetic capacity in type 1 diabetes mouse model



## CHAPTER II

### LITERATURE REVIEW

#### Diabetes disease

In the type 1 diabetes (T1D) patients, the hyperglycemia is caused by a probable defection of beta cells in pancreas or insulitis phenomenon (Katsarou et al. 2017). The etiology of T1D is a multifactorial disease from crosstalk between i) genetic factors, ii) epigenetic factors, and iii) exogenous factors. Consequently, the destruction of autoimmune T-cell-mediated innocently attacks and destroys to pancreatic beta cells (Manov 1991; Stankov et al. 2013). In initial events, dendritic cells, T cells, macrophages target to insulin antigens via major histocompatibility complex (MHC) presentation. Continuously, the infiltration of inflammatory cytokines and leukocytes provokes the beta cell failure including interleukin-1b (IL-1b), interferon gamma (IFN-gamma), tumor necrosis factor-a (TNF-a) (Faideau et al. 2005; Roep and Peakman 2012; Blanter et al. 2019; Roep et al. 2021). On the other hand, susceptible event to T1D is considered by interplay between some genetic loci (allelic variants) and exogenous risk factors (Roep et al. 2021). To maintain the euglycemia (normal blood glucose levels) in the bloodstream, which is controlled by two functionally opposite proteins, insulin and glucagon (Steineck et al. 2019). The glucose levels in blood

periodicity are supervised by the critical pancreatic islets where is produced insulin hormones. The interaction or relationship between insulin and diabetes is properly regulated via the insulin transduction pathway (Ho et al. 2016). In diabetes patient, this pathway which is abnormally increasing the absorbance of glucose into fat and muscle cells, as well as dysfunctional glycogenesis of glycogen in liver by glucagon (McCrimmon and Sherwin 2010; Bode et al. 2020).

#### **Detection of diabetes disease via insulin secretion signaling pathway**

The glucose-stimulated insulin releasing pathway initially starts with binding of glucose on the glucose transporter (GLUT2) which is a transmembrane receptor of beta cells. In the metabolism of glycolysis, the energy ATP is generated from glucose resulting in the high level of ATP/ADP ratio which inhibits the K<sup>+</sup> channels. Therefore, the K<sup>+</sup> currents outward is downed and impulse the membrane depolarization; thus, opening the voltage-dependent Ca<sup>+</sup> channels (VDCCs) for uptake the Ca<sup>+</sup> and, eventually accumulates the high level of Ca<sup>+</sup> inward. Subsequently, the vesicles of insulin fuse in membrane and release the contents (Henquin 2000; Roder et al. 2016; Carrageta et al. 2021; Henquin 2021). To mimic the insulin secretion signaling pathway, the glucose-stimulated insulin secretion test is developed for checking the in vitro IPC function.

## Regulation of insulin production by cAMP/PKA pathway in pancreatic beta cells

In pancreatic beta cells, the insulin production is regulated by cAMP/PKA cascade. Initially, Glucagon-like peptide 1 (GLP-1) binds to GLP-1 receptor which stimulates the alteration from ATP to cAMP. cAMP energy supplies to the activation of protein kinase A (PKA). Then, activated PKA triggers to the transcription of insulin; besides, it helps insulin secretion by phosphorylation of vesicle-associated snapin protein. Otherwise, insulin is also released by binding to A-kinase anchoring proteins (AKAPs). Correspondingly, PKA phosphorylates the transcription factor of CREB, inhibits glucose transporter GLUT2, inhibits ATP-sensitive potassium channel (KATP), activates L-type voltage-gated calcium channels (LTCC) for secretory insulin modulation. MAFA is transcribed by an activated CREB regulation, then MAFA (a transcription factor) provokes the transcription of insulin. In hyperglycemia, insulin secretion in a long-term is attacked by the induction of the intrinsic PKA inhibitor B (PKIB). The effect of PKA on insulin release is also dependent on its subcellular localization (Hussain et al. 2006; Tengholm 2012; Yang and Yang 2016).

### **Insulin-mediated glucose uptake cascade**

The insulin receptor (IR) is a heterotetramer including two  $\alpha$  subunits and two  $\beta$  subunits. Insulin molecule directly binds to the insulin receptor via disulfide bridge at

$\alpha$  subunit. When  $\alpha$  subunit of insulin receptor is triggered, it activates auto-phosphorylation of the  $\beta$  subunit. Thus, three tyrosine residues (Tyr-1158, Tyr-1162, and Tyr-1163) are phosphorylated and amplified the number of the kinase activity. The insulin receptor substrate (IRS) proteins are phosphorylated by insulin-mediated stimulation. The insulin receptor substrate (IRS) proteins are phosphorylated and the activation of the list of downstream molecules consist of phosphatidylinositol 3-kinase (PI3-kinase), PIP2, PIP3, protein kinase B (PKB), Akt. Thus, PKB induces glucose transporter 4 (GLU4) which continuously moves to cell surface importing the glucose into cells (Lanner et al. 2006; Lanner et al. 2008; Saini 2010; Satoh 2014).

### **Induced pluripotent stem cells (iPSCs) from somatic cells**

The development of induced pluripotent stem cells (iPSCs) represents a milestone step in the stem cells studies. From 1980s, mouse embryonic stem cells (mESCs) were indefinitely proved the ability to maintain pluripotency which directly and spontaneously differentiated into all three germ layers (endoderm, mesoderm, ectoderm) (Takahashi and Yamanaka 2006; Yamanaka and Blau 2010). Eventually, ESCs was cultured in large population associating with feeder cells. The researchers began to develop in 1990s, the new technologies of somatic cell nuclear transfer (SCNT), cell

fusion, and induced pluripotent stem cells (iPSCs) were generated to serve the evolution of scientific researches and clinical therapy (Yamanaka 2013). However, the human and animal eggs were used in the SCNT technique that regarding to ethical issues while these decades, SCNT is being investigated extensively. Subsequently, in 2006, the iPSCs generation was exciting reported in genetically reprogramming from adult somatic cells causing by the transduction of four transcription factors (OCT4, SOX2, c-MYC, KLF4) into mouse fibroblasts (Takahashi and Yamanaka 2006). From a cocktail of Yamanaka, Takahashi and Tanabe et al., 2007 successfully generated the human iPSCs using retroviral system. Besides, three separated groups also showed the somatic cells reprogramming to iPSCs by OCT4, NANOG, SOX2, LIN28 using lentiviral system (Thomson factor) (Takahashi et al. 2007a; Takahashi et al. 2007b; Yu et al. 2007).



To generate iPSCs from differentiated somatic cells, the delivering reprogramming factors to source cells approach are reported with the multiplicity of integrating and non-integrating manipulation. The robust and efficient integrative techniques such as retroviruses infect to any somatic cell types and achieve a stable transgene expression. Initially, the viral delivery of retrovirus is used to generated iPSCs which cargos four transcription factors into fibroblasts of mouse and human (Seki and Fukuda 2015;



Shahjalal et al. 2018). The activation of retroviral silencing vector is stop when pluripotent cells are full formation (Gram et al. 1998; Hotta and Ellis 2008). In full-reprogramming stage, iPSCs reporters are strong detection. iPSCs makers consisted of Nanog, Oct3/4, Sox2, Eras, Rex1, Klf4, c-Myc are increased the mRNA levels. In pluripotency distinction, the activity of Nanog and Oct3/4 promoters are elevated via the bisulfide sequencing validation. In gold standard for pluripotent identity, iPSCs are injected into animals for teratoma formation (Yu et al. 2020).

The strategy on combination of Doxycycline-inducible lentiviruses brings a new interesting manipulation with temporal control. Here, the researchers also proved iPSCs formation using inducible virus highly (Lai et al. 2011). But these methods permanently cause genetic material modifications due to transgene integration randomly which is a reason of insertional mutagenesis or tumorigenesis. Eventually, it causes the limitation on the generated iPSCs for clinical applicability. Besides, the genetic endogenous of the iPSCs are inefficient silencing, and eventually activation of transgenes being affected (Zhou et al. 2009; Gunaseeli et al. 2010; Xiao et al. 2016; Cherkashova et al. 2020; Amimoto et al. 2021). To solve this problem, a transgene excision method can be excised out from the iPSCs. In the challenges, this excision event can remove randomly some neighbor elements in the genome and cause thus

a mutagenesis, subsequently, this approach is limited for clinical treatment (Kusumoto et al. 2011).

To make iPSCs applying in practical clinic, the techniques of non-viral, DNA-free reprogramming involving recombinant proteins, mRNA, miRNA and small molecules are promising without the possibility of transgene integration or genomic modifications in long-term. However, these approaches are very restricted according to the low efficiency and/or difficulty of the techniques. Therefore, the application of each technique is facing different problems and must be overcome the bottlenecks for obtaining efficient result (Lai et al. 2011; Zhang et al. 2011; Oh et al. 2012; Haridhasapavalan et al. 2019; Wang et al. 2020).

Furthermore, in the developing of scientific researches and clinical demanding, the delivering techniques are definitely modified and explored the novel approaches for improving the activation of the induced transcriptional program in an efficient cell manner (Yamanaka and Blau 2010). The advantageous iPSCs are particularly obtained. First, the iPSCs modeling comes from biopsy of patient-derived that breakthrough the ethical issues and immunological rejection. Besides, in the iPSCs stage, the gene editing can be manipulated with different aims or the gene expression and signaling can be studied as well. Rapidly, iPSCs undergo differentiated duration to become the

interested cell types. Second, these iPSCs-based disease models can be carried out drug screening in vitro. Third, the technique of viral vector integration overcomes the tumorigenic potential which is concerned for cell therapy (Shahjalal et al. 2018) Yamanaka and Blau 2010; Charles C. Hong et al. 2014). Here, the mGF-iPSCs were generated using retroviral silencing vectors which was a kindly gift from Prof. Egusa Hiroshi, Tohoku University, Japan. The mGF-iPSCs were well characterized and differentiated to osteoclasts (Egusa et al. 2010).

#### **Chemical strategies for induced insulin producing cells differentiation**

#### **Embryoid bodies and definitive endoderm development from iPSCs**

During many decades for IPC synthesis trajectories, the strategies of IPC chemical induction are divided into two main ways: i) synchronized embryoid bodies (EBs) formation, ii) direct definitive endoderm development (Kim et al. 2010; Mfopou et al. 2014).

Embryoid bodies generation: EBs are three-dimensional (3D) cell aggregation that mimic a spherical organization of embryonic stem cells in embryogenesis period which immediately designs to differentiate precursors of three layers of germinal lineages consist of endoderm, mesoderm, ectoderm (Rungarunlert et al. 2009; Brickman and Serup 2017). The capacity of EBs initially dictates lineage-specific downstream

differentiation towards many target lineages including neural, cardiomyocyte, hepatocyte etc. (Son et al. 2011). Besides, the outcomes of target cell differentiation are based on the quality of EBs that is controlled by spatial and temporal culture such as medium condition, number of cells and EB parameter (Pettinato et al. 2014a). During EB development, the pluripotency of EB markers are decreased in expression. Correspondingly, its morphology are changed by fluid infiltration; the following days, the cavity structure and additional appendages are formed (Carpenedo et al. 2007; Zeevaert et al. 2020). The manner of EB size can dependently decide the yield of target cells. While the small size of EBs is not alive in the long duration as well as, too large EBs gradually create core necrosis (Zeevaert et al. 2020). Duration of EB formation, the EBs considerably undergo cell-cell interaction via cell junction and activated cell signaling mechanism for maturation pathway (Pettinato et al. 2015). It means the gene expression in EB maturation is decreasing in the network of pluripotency levels and increasing in germ layer specification (Zeevaert et al. 2020). Additively, in suspension culture, the agglomeration events are randomly occurred preventing partly the colony proliferation and differentiation (Carpenedo et al. 2007). There are several methods for generate EBs from iPSCs such as enzymatic treatment, micro-well arrays, hanging drop, 3D printing, spin-EB, hydrogel (Chen et al. 2008; Lin

and Chen 2008; Pettinato et al. 2014b). The regular approach is simply used to detach the iPSCs by enzyme and then, they are maintained in the suspension medium, either in non-bacterial grade petri plates or ultra-low attach plates (Carpenedo et al. 2007; Zeevaert et al. 2020). Expectedly, in vitro EB synchronization is formed in suspension media and low-attach plates which mainly reduces the heterogeneous of iPSCs, feeder cells matrix, and remove the feeder cells for 3D formation. This method helps the integrity of terminal IPC differentiation be more uniform and efficient. In the results, IPC termination indicates pro-insulin or C-peptide and insulin expression that performs correct the process of insulin generation (Wei et al. 2013).

Definitive endoderm formation: skipping the EB development and directly induce to definitive endoderm (DE) from iPSCs-derived is obtained some achievements (Liu et al. 2010; Wei et al. 2013; Jaafarpour et al. 2016). In this method, the cells are treated with the induction media including Activin A, Wnt3a or TGF- $\beta$ , etc, for immediately forming DE and strong expresses mRNA levels of FoxA2, Cxcr4, Goosecoid, Sox17, and Bmp2 (Kubo et al. 2004). This protocol is required a quite short time for IPC generation. In several researches, they proved the insulin production that is not completed synthesis with lacking pro-insulin protein (Kubo et al. 2004). Stepwise, the scientists demonstrated the successful engraftment of these IPCs in streptozotocin (STZ) treated

mice which corrected the hyperglycemia or recused the diabetic phenotype, however, some organs as kidney, spleen be coming to tumorigenesis (Raikwar and Zavazava 2009).

### **Procedure of mouse induced pluripotent stem cell-derived insulin-producing cells (miPS-IPCs) synthesis**

In fact, pancreatic beta cell procedure is directly differentiated from ESCs which live in inner cells mass (ICM) of blastocyst during embryonic development (Murry and Keller 2008). Then, ICM can develop to three layers of endoderm, mesoderm, ectoderm targeting to any expected cells by suitable induction medium (Murry and Keller 2008; Oliver-Krasinski and Stoffers 2008). Here, we apply this workflow to make three-dimensional (3D) embryoid bodies from iPSCs in un-attached plates with ES medium. In detail, the differentiation into pancreatic beta cells is generally divided into 6 steps including 1) EB generation, 2) DE stage for toward to pancreatic beta cells formation, 3) progenitor cells stage that can be different to any target cells, 4) pancreatic endocrine stage, 5) early pancreatic beta cells or early IPCs, and 6) matured IPCs stage (Hosoya et al. 2012; Pagliuca et al. 2014; Liu et al. 2021). The stage-specific biomarkers are detected such as the pluripotent stem cells (Oct4, Sox2, Nanog, Rex1, cMyc, Ssea1); definitive endoderm (Cxcr4, Goosecoid, FoxA2, Sox17, Bmp2); pancreatic

progenitor cells (Pdx1, Nkx6.1, Sox9, Gp2, Hnf6); pancreatic endocrine cells (Ngn3, NeuroD1, Maf-B, Nkx-2.2, Pax6, Pax-4); and pancreatic beta cell or IPCs (Insulin, Glucagon, Nkx-6.1, Maf-A, Isl-1, Glut-2, Glp-1r) (Fig 1) (Escurat et al. 1991; Oliver-Krasinski and Stoffers 2008; Liu et al. 2021). Stepwise differentiation procedures are guided by optimized small and large chemical treatment.

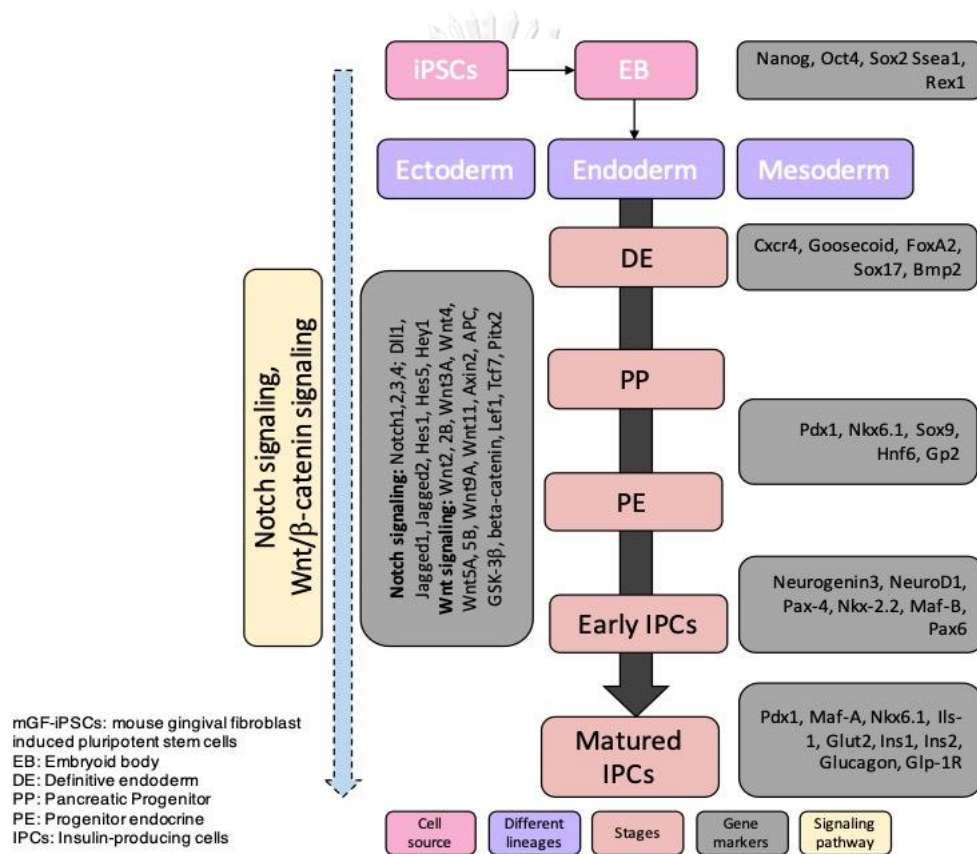


Figure i Scheme of miPS-IPC synthesis workflow

On the other hand, expression of matured IPCs can be manipulated on the specific transcription factors. They find the combination between Pdx1 and Pax4 that is increased the develop of pancreatic beta cells. However, overexpression of Pdx1 or

Pax4 expression tend to cytotoxicity (Raikwar and Zavazava 2009). Remarkably, the convenience and efficiency of doxycycline-inducible technique helps induce various genes of pancreatic transcription factors (Nkx2.2, Ngn3, Nkx6.1...); these factors can solve toxic problems. However, the present of doxycycline in cells still is not clear the negative side effects (Raikwar and Zavazava 2009).

### **Small and large chemicals are used for IPC induction**

Pluripotent stem cells are potential model for biomedical researches, and translational clinical therapeutics. The differentiation of IPCs is a mile-step in diabetes treatment via stem cell-based therapy (Charles C. Hong et al. 2014). In the DE generation step, activating the transforming growth factor (TGF)-beta signaling, activin A is a strong factor to stimulate endoderm lineage differentiation in the low fetal bovine serum (FBS) concentration (Sulzbacher et al. 2009; Takeuchi et al. 2014). Because activin A is a homodimer complex with two beta-A subunits, not expressed during the embryogenesis (Kumar et al. 2014). Activin A is also a non-glycosylated cytokine that is involved in TGF-beta family and expresses in diversely biological processes (Su et al. 2018; Xie et al. 2020). Therefore, activin A plays a key role in various mechanism (Kumar et al. 2014). Its properties trigger the differentiated progress including pancreas, neural, mesoderm, etc. Some researchers showed the



combination between activin A and sodium butyrate to induce differentiation of hESCs to pancreatic beta cells (Kumar et al. 2014; Pan and Liu 2019). Besides, activin A and WNT3A are added in the DE induction medium to improve the meso-endodermal lineage from hESCs (Pan and Liu 2019). Recently, the activin A and wortmannin complex stimulates to DE formation with highly efficient pancreatic cells synchronization. At the nutshell, activin A is known as an extremely important factor for differentiation of hESCs toward DE with promoting the expression of DE markers (Pavathuparambil Abdul Manaph et al. 2019; Thakur et al. 2020).

Retinoic Acid (RA) is a retinaldehyde dehydrogenase that is an essential enzyme for PDX1 gene expression in both mouse and human ES cells during pancreatic cell production (Kumar et al. 2014). Meaningfully, RA is implied joining in signal transduction but its activities are still unknown in the various mechanism during pancreatic cell formation (Huang et al. 2014). Obtaining from many researches, RA is used alone and not integrating with other chemicals, the PDX1 expression is decreased significantly; so the progressive combination of RA and nicotinamide gained the expression of PDX1 up to 80% yield (Ma and Zhu 2017). Some studies demonstrated that the failure of transcription factors (Ins, Ngn3, Pdx1, and glucagon) expression is detected in the lacking RA supplement (Ostrom et al. 2008; Brun et al.

2015) Ma and Zhu 2017). Hence, the optimal amount of RA and well associate with other ingredients are useful for producing the pancreatic progenitor cells effectively.

Nicotinamide is belonged to vitamin B3 family that promotes Nkx6.1-positive (Nkx6.1+) pancreatic progenitor cell differentiation. In human pancreatic progenitor period, nicotinamide attends to several metabolic mechanisms because it inhibits two classes of enzymes in poly-ADP-ribose polymerases (PARPs) family. It also administrates the cellular pool of nicotinamide adenosine deoxynucleotide (NAD<sup>+</sup>); the alteration of NAD<sup>+</sup>/NADH ratio enhances Pdx1 expression (Amjad et al. 2021). Besides, Nicotinamide can prolong the survival of human pluripotent stem cells (Kumar et al. 2014; Jiang et al. 2017; Meng et al. 2018).

Taurine is a 2-aminoethanesulfonic acid that belongs to cryo-protective agent attending in numerous physiological functions. It can interact with calcium signaling, then taurine alters the potential of cell membrane and effects on ion currents, which helps insulin secretion (Pavathuparambil Abdul Manaph et al. 2019).

Fibroblast growth factor (FGF) has seven different receptors controlling the transition and differentiation. However, FGF is insufficient effect when it is alone. The combination of FGF and other small and/or large molecules can enhance the pancreatic endoderm (PE) specification as well as increasing the number of PE cells.

FGF and endothelial growth factor (EGF) promote the expansion of PDX1+ pancreatic progenitor cells from human ES cell differentiation. Moreover, the upregulation of EGF expression improves the proliferation of PDX1+ cells (Zhang et al. 2009; Kumar et al. 2014).

Notch signaling suppresses Ngn3 transcription factor.

N-[N-(3,5-difluorophenacetyl)-L-alanyl-S-phenylglycine t-butyl ester (DAPT) is a chemical of Notch signaling inhibitor leading to transition of pancreatic beta cells differentiation. Consequently, the expression of insulin, Pdx1, Nkx6.1, NeuroD1 is performed significantly (Qu et al. 2013; Thakur et al. 2020).

Glucagon like peptide-1 (GLP-1) is a peptide that is the most popular and effective stimulator for insulin secretion by glucose stimulation. GLP-1 is rapidly released to response the meal intake via metabolism by inactivated using dipeptidyl-peptidase-4.

In mouse embryonic stem cells (mESs), GLP-1 enhances insulin production in in vitro IPC induction (Bai et al. 2005). The achieved integration of GLP-1, nicotinamide, or Notch signaling inhibitors gained the maturation of IPCs with high expression of EB markers consist of islet-like 1 (Isl1), insulin, C-peptide (Pavathuparambil Abdul Manaph et al. 2019).

Levodopa (L-DOPA) belongs to dopamine family that is a dopamine precursor being active as a neurotransmitter. With responsible dosage of L-DOPA, it affects to insulin releasing directly and modifies the population of pancreatic beta cells. Actively, L-DOPA triggers to block the  $K^+$  channels and open  $Ca^{2+}$  channels for insulin secretion. In experimental condition, L-DOPA half-life is short around 36-72h (Garcia Barrado et al. 2015).

In conclusion, the wise integration of chemicals will generate a sustainable medium at each step during miPS-IPC synthesis in this study.

**Strategy of subcutaneous device-less establishment for implantation and transplantation**

**Transplant models**

In the late 1970s and early 1980s, the discovery of animal models of Type 1 Diabetes (T1D) was properly known (Van Belle et al. 2009). They have generated the genetics, aetiology, pathogenesis and particularly the non-obese diabetic (NOD) mouse (Van Belle et al. 2009; Driver et al. 2011). Later, the develop of transgenic and gene-targeting technologies were explored to reduce genetic and pathogenic complexity in many T1D models (Matsuoka et al. 2013). Currently, there are four main T1D models such as: pathogen-induced models, spontaneous models (NOD mice,

double-Tg, BDC2.5/B6g7 mice models), transfer models of autoimmune diabetes (transfer into immunodeficient mice, transfer of BDC2.5 TCR Tg CD4 T-cells in NOD neonates mice, transfer of P14/Smarta LCMV-specific CD8 or CD4 into RIP-GP and humanized mouse models), pharmacological intervention (Alloxan and streptozotocin) (Lipes and Eisenbarth 1990; Ohsugi et al. 1991; Rosmalen et al. 1997; Billotey et al. 2005; Giarratana et al. 2007; Van Belle et al. 2009; Chen et al. 2020). To precisely generate the T1D models with ease to practice and painless manipulation, pharmacological induction (PI) is fashionably selected in T1D models (Deeds et al. 2011; Graham et al. 2011; Furman 2015; Hahn et al. 2020; Furman 2021). In PI way, the streptozotocin (STZ) drug is a glucose analogue which potentially transport to pancreatic beta cells through glucose transporter 2 (GLUT2) (Deeds et al. 2011; Graham et al. 2011). In beta cells, H<sub>2</sub>O<sub>2</sub> is created and induces expression of glutamic acid decarboxylase (GAD) autoantigens. GAD is a strong trigger of beta cell-specific autoimmunity, both in experimental diabetes models, and in humans that has been performed to require a Th1-dependent inflammatory reaction (Van Belle et al. 2009). Single dose of STZ-high concentration directly invades and damages the beta cells, then provokes the STZ-treated T1D with hyperglycemia symptom (Deeds et al. 2011; Graham et al. 2011; Furman 2015; Hahn et al. 2020; Furman 2021). The mouse model

will be chosen in this study. Because the mouse has the genetic background as similar as human, ease to nursing and manipulation (Justice and Dhillon 2016; Perlman 2016). The eleven-week age of mice are homologous with adult human that are healthy, immortality, stable weigh and plague survival maintenance (Justice and Dhillon 2016). To apply the functionality of in vitro pancreatic IPCs in in vivo for diabetes treatment, we will generate a T1D mice model by STZ injection, the STZ-treated diabetes mice will be transplanted by the encapsulated IPCs for recovering hyperglycemia.

### **Biomaterials**

Current benefits of the cell replacement for diabetes treatment focus on investigating the microenvironment of transplantation sites, including their extracellular matrix content, vascularization and invaded immune cells (Assoc 2006; Mitrousis et al. 2018; Pomposelli et al. 2021). Nowadays, an increasing amount of research is focusing on engineered biomaterials, promote angiogenesis and protect the graft from the immune system (Mitrousis et al. 2018). Biocompatible materials and immunomodulation can overcome these limitations (Ishihara et al. 2018). To date, cell encapsulation is the promising method for effective and long-term engraftment in diabetes animal (An et al. 2018). Basing on size-pore, there are two main ways for encapsulation including immune-protective and revascularization approaches that

active as vesicles or exosomes in tissues (Dufrane and Gianello 2012). In microporous construct, the encapsulated beads are surrounded by blood vessels where supply the oxygen and nutrients to the islets; moreover, the immune cells cannot get into the encapsulated beads. In macro-porous construct, the blood vessels invade to the beads and directly connect with islets; therefore, immune cells smoothly move into the encapsulated beads (Souza et al. 2011; Dufrane and Gianello 2012; Omami et al. 2017; White et al. 2020a). In biomaterial selection, alginate is a biomaterial which is applied in various biomedical sciences with less difficult manipulation, efficient immune-barrier, and preserved cell viability (Lee and Mooney 2012; Sun and Tan 2013). Besides, Pluronic-F127 is a potential non-toxicity chemical for coating the alginate surface with promoting the collagen generation and improving the angiogenesis (Diniz et al. 2015). The double layers of alginate and Pluronic-F127 brings the outstanding achievement for conserving the endogenous gene expression and functionality (Kuncorojakti et al. 2020).

On the other hand, the biomaterial of implantation is diverse composition (Yue et al. 2016; Ishihara et al. 2018). There are many names either tubes or catheter with different outer and inner diameter. In transplantation fields, the surface compatibility with surrounding matrix in host animal is extremely critical (Sakiyama-Elbert and

Johnson 2012). Since it can be decreased or increased the immune response (Tomei et al. 2014). The composition of biomaterials can be butyl rubber, Fluorinated ethylene, silicone (polydimethylsiloxane), nylon (aramid) (Pepper et al. 2015a). In term of subcutaneous implantation, the researchers proved the correlation between nylon composition and reversal of diabetes that was high level of 91.3% (Krevelen and Hoftzyer 1976). In the regenerative medicine toolkit, biomaterials are an essential component. To improve cell survival and integration, regeneration and clinical translation, the communication between donor cells, biomaterial and host body should be further elucidated and coordinated (Mitrousis et al. 2018).

### **Vascular endothelial growth factor (VEGF)-165**

The role of VEGFs in transplantation is critical to improve the angiogenesis or stimulate the other important pathways. In angiogenesis cascade, VEGF and VEGFR interaction is a major role regulating vasculogenesis and blood vessel formation from precursor cells, embryogenesis duration, early and late stage of angiogenesis (Shibuya 2011).

Transplantation of mesenchymal stem cells (MSC)-VEGF to Alzheimer's disease (AD) transgenic animals forms neovascularization and amyloid-beta peptides in hippocampus (Garcia et al. 2014). In transgenic Amyotrophic lateral sclerosis (ALS) mice, delivering the human neural stem cells (hNSCs) and VEGF gene overexpression



significantly generates the delayed disease onset. Correspondingly, it prolongs the survival of transgenic ALS mice (Hwang et al. 2009). Mixture of adenovirus-mediated vascular endothelial growth factor and fat tissue are transplanted to nude mice. Here, they report the VEGF gene enhances the longevity and graft's quality of fat tissue because of angiogenesis induction (Yi et al. 2007). In post-transplantation, VEGF level is identified as monitoring the risk of severe transplant-relative mortality (Min et al. 2006).

A recombinant adeno-associated virus carrying human VEGF-165 is transduced to human adipose derived stromal cells; then, the expression of VEGF-165 stimulates revascularization in intramuscular post-transplantation (Shevchenko et al. 2013). In ischemic hind limbs New Zealand rabbits, they proved that VEGF-165 transfected to endothelial progenitor cells (EPC) which significantly higher the level of angiogenesis comparing with EPC alone (Wang et al. 2015). In case of xenotransplantation in mice, VEGF-165 is mixed with the collagen matrix of encapsulated ovarian tissue that recruits the network of blood vessels (Henry et al. 2015). VEGF-165-transfected vascular endothelial cells and islets are grafted into the diabetic rats which elevated islet revascularization and increase the islet graft survival (Cheng et al. 2007).

Pancreatic rat islets are encapsulated with the presentation of VEGF-165 for transplanting to diabetic mice. VEGF triggers angiogenesis and decrease macrophage

surrounding the membrane of cells; especially, revascularization of islet engraftments in post-transplantation (Sigrist et al. 2003).

### **Transplantation sites**

In the progress of translation of subcutaneous islet transplantation therapies, the experimental approaches used to optimize the subcutaneous (sc) space for experimental transplantation (Shapiro et al. 2000; Gunawardana et al. 2009; Lee et al. 2012; Kim et al. 2020b; Yu et al. 2020). In 1996, Juang JH and colleagues used mouse transplant model for islet transplantation; however, they faced the intervention of previsualization by implantation of polymer (Juang et al. 1996). Subsequently, in 1999, the other researchers used a mouse model to apply for subcutaneous transplantation with macro-encapsulated islet that was challenged in instant blood mediated inflammatory response (IBMIR) and inflammatory response in blood circulation (Tatarkiewicz et al. 1999). Normally, beta cell transplantation is lost the vascularized and extracellular matrix in the host body which can cause the risks of animal strokes (Stendahl et al. 2009; Pepper et al. 2015b; Vlahos et al. 2021b). Therefore, the scientists built many transplant sites for consideration including intra-portal/portal vein, renal subcapsular, omentum/intraperitoneal, pancreas, spleen, gastric submucosa, bone marrow, brain, testis, thymus, anterior chamber of eye,

intramuscular, subcutaneous (sc) and subcutaneous device-less (Audouard et al. 2021; Cayabyab et al. 2021). Individually, there are advantages and disadvantages of transplantation.

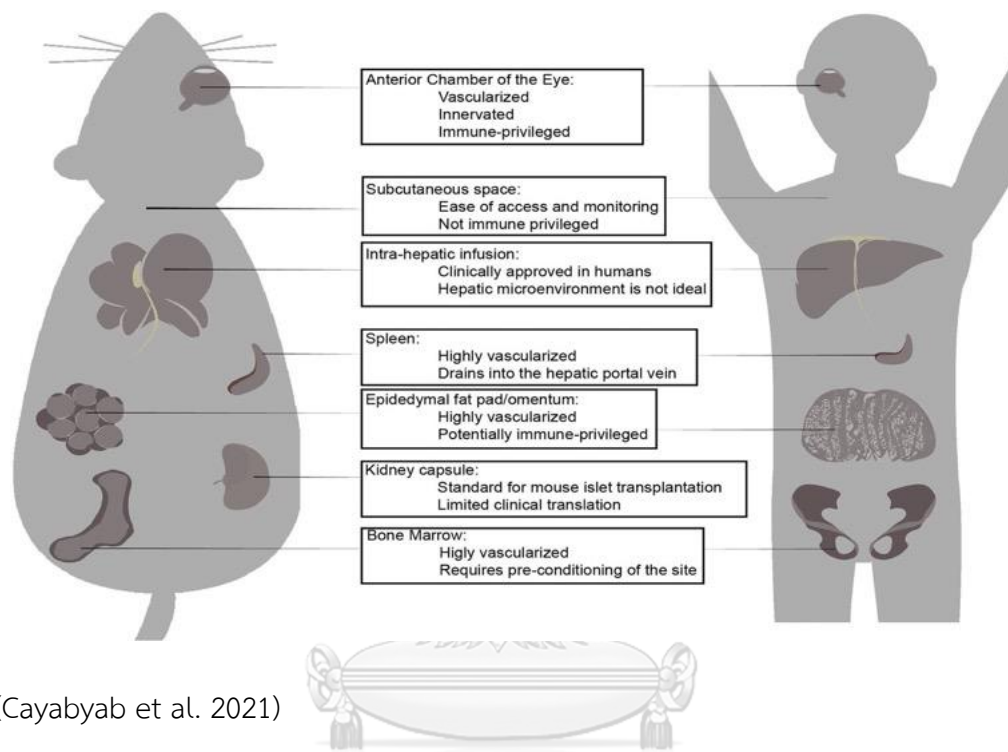


Figure ii Summary of islet transplantation areas in mouse models and mammalian models.

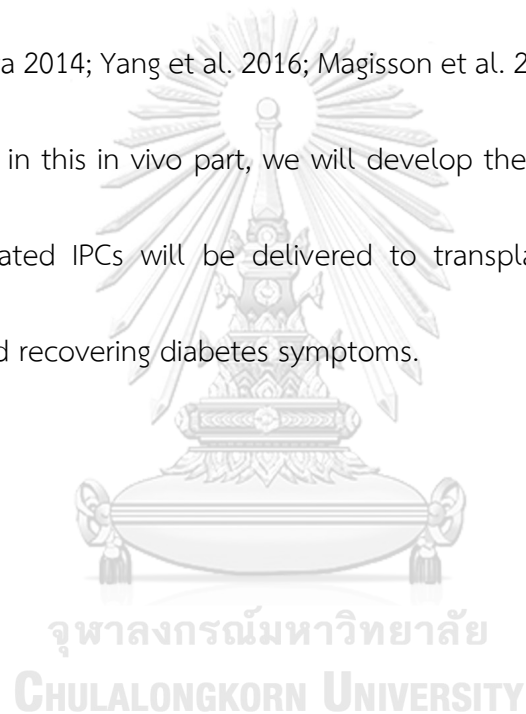
In post-transplantation, the beta cell engraftment should be supplied the oxygen, nutrition, and physical supports via the new blood vessel system (Bromberg 2015).

The blood vessel regeneration is formed from the host body and/or additional injection of the vascular endothelial growth factors (VEGFs) (Pepper et al. 2015b; Smink and de Vos 2018; Vlahos et al. 2021b). Importantly, the success of beta cell

transplantation mainly depends on 1) the capacity of tissue volume, amount of IPCs, and velocity of injection, 2) blood vessel networks, 3) the potential of crosstalk between the engraftment place and physiologically systemic circulation in relative manner, 4) facilitate the grafting invasion, 5) minimally reduce the inflammation and attack of immunogenicity, and 6) improve the transplantation survival in the long time (Janowski et al. 2013; Yu et al. 2020; Pomposelli et al. 2021). Accordingly, transplantation into the subcutaneous backside is recommended. Because the manipulation of surgery is easy, painless, and minimally touch to other organs unexpectedly (Bromberg 2015). Additionally, functional monitor of the engraftment is simply checked through imaging under in vivo microscope (Lee et al. 2012). Currently, the approach of scalable device-less is fashionably developed for islet transplantation in the subcutaneous (sc) space. This method enhances rapid vascularization, which permits oxygen and glucose cargo to transplanted place (Halberstadt et al. 2005; Pepper et al. 2014; Pepper et al. 2015b; Kim et al. 2020b; Vlahos et al. 2021b). In the procedure, the strategy of sc transplantation is consisted of two stepwise 1) sterile prepare the “pocket” in the subcutaneous area via implantation, and 2) safe transplantation of islets into the preformed “pocket”. In previous research using the mouse model, the methacrylic acid (MAA)-based biomaterials were used to coat the

islets which helped the immunosuppression, prolong the survival engraftment, and vessels generation at implantation site (Bromberg 2015; Vlahos et al. 2021a).

Conclusively, the combination of biocompatible biomaterials, IPC encapsulation, subcutaneous device-less, growth factors, angiogenesis stimulation, oxygen and nutrition demands are strategies for implantation and transplantation approach (Calafiore and Basta 2014; Yang et al. 2016; Magisson et al. 2020; White et al. 2020b; Yu et al. 2020). Thus, in this in vivo part, we will develop the way to safe implantation. Besides, encapsulated IPCs will be delivered to transplantation space with rapid vascularization and recovering diabetes symptoms.



## Conceptual framework

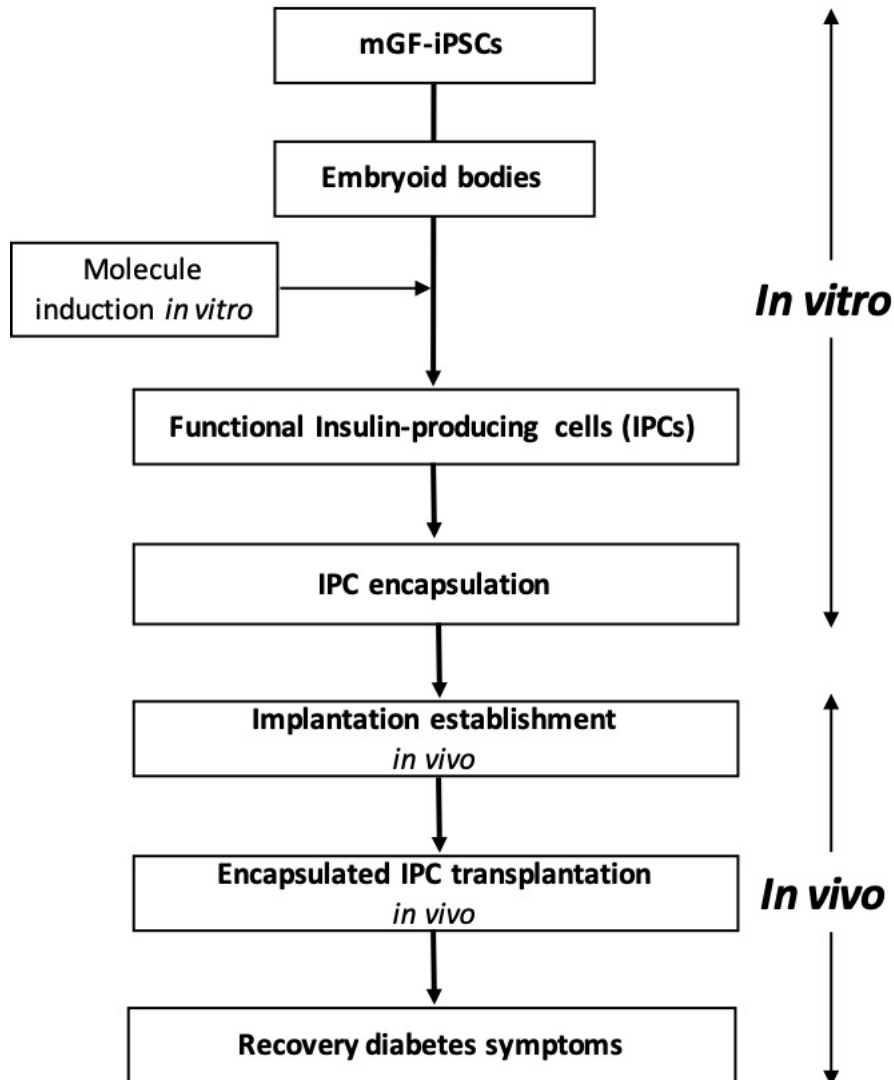


Figure iii Conceptual framework of IPCs induction from mGF-iPSCs modeling.

To generate the IPC lineage, we use the stem cell potential of mGF-iPSCs as a good modeling that can make a high yield of beta cell mass in pancreas (Fig.2). To form the completed synthesis of IPCs, EBs are conceptualized basing on their development. To establish the highly efficient protocol, we will optimize the induction protocol using in

in vitro molecule treatment. To show the IPC performance, we will check the phenotypic and genotypic alteration by proving the morphology and gene/protein expression. To confirm the IPC function, we will test the glucose stimulation C-peptide secretion (GSCS), and C-peptide/insulin production. To address the IPC biocompatibility in mice, IPCs will be encapsulated totally. To reverse the hyperglycemia in diabetes mice, encapsulated IPC engraftment will be applied, the blood glucose level is normally maintained in post-transplantation.



## CHAPTER III

### METHODOLOGY

#### Animal husbandry

All the protocols and animals were followed the ARRIVE guidelines and were approved by the Institutional Animal Care and Use Committee (IACUC), Chulalongkorn University Laboratory Animal Center (CULAC), Faculty of Veterinary Science, Chulalongkorn University (Protocol No. 2173018). All male C57BL/6NJcl mice were purchased from the Nomura Siam International Co., Ltd, Thailand. The mice were housed in cages with suitable space for enabling free movement, generating social contact. They were fed a standard pellet mouse diet and had water ad libitum, and they will be monitored the clinical condition of animals and weighted every week. The animals will be kept in the optimally controlled environment according to CULAC management. Briefly, room temperature  $23 \pm 2^{\circ}\text{C}$ , humidity 40-60%, 12/12 h, light/dark cycle, bedding provided and changed accordingly to the guideline, clean cages and water bottles change weekly otherwise the facility manager mentions. Non-diabetic mice will be treated with the standard protocol mentioned above but the diabetic mice will be closely monitored and be provided extra care and consumables depending on their conditions such as extra bedding change. Most of



the animal procedures were less painful and distressed to the mice. A cardiac puncture was performed once under anesthesia, then the mice are sacrificed. Tissues/organs were harvested consequently.

### **mGF-iPSC culture and embryoid bodies generation**

mGF-iPSCs were induced by the factors of Oct3/4, Klf4, Sox2 via the retroviral system and completely characterized as previous publication (Egusa et al. 2010). Firstly, the feeder cells were seeded in the medium consisting of high-glucose Dulbecco's Modified Eagle Medium (DMEM) (Thermo Fisher Scientific, USA) with 1% of Antibiotics-Antimycotic (Thermo Fisher Scientific, USA), 1% GlutaMAX™ (Thermo Fisher Scientific, USA), and 7% fetal bovine serum (FBS) (Thermo Fisher Scientific, USA) until reach 80% confluence. The feeder cells were in-activated by 6  $\mu$ g/ml Mytomicin C (Nacalai Tesque, Japan). Next, the mGF-iPSCs were cultured on the feeder cells layer, continuously. They were kept in the E1 media including high-glucose Dulbecco's Modified Eagle Medium (DMEM) (Thermo Fisher Scientific Corporation, USA) with 1% of Antibiotics-Antimycotic (Thermo Fisher Scientific Corporation, USA), 1% GlutaMAX™ (Thermo Fisher Scientific, USA), and 15% fetal bovine serum (FBS) (Thermo Fisher Scientific, USA), 2% beta-mercaptoethanol (Sigma-Aldrich, USA), 1x non-essential amino acids (NEAAs) (Sigma-Aldrich, USA) as supplements. All cultured cells were in

37°C, 5% CO<sub>2</sub> and humidified condition. The medium was changed every 2 days. mGF-iPSCs colonies maturation was trypsinized and formed to embryoid bodies (EBs) into low-attach plates. The EB colonies were maintained in E1 media and changed every 2 days for serving in the further experiments.

### **Pancreatic IPC production**

The protocol was modified following the previous researchers (Jeon et al. 2012). The cells were re-suspended in the serum free media (SFM)\_R1: GlutaMax™ (Thermo Fisher Scientific, USA), 0.1% BSA (Sigma-Aldrich, USA), 50 ng/mL Activin A (Sigma-Aldrich, USA). They were seeded into the 60 mm low-attached dishes (Eppendorf™ Cell Culture Dishes, Non-Treated, USA) for protocol I, in MicroQC™ Petri Dish (MicroQC, Thailand) for protocol II, and in Sterilin™ Petri Dish (Corning, France) for protocol III, IV, V, VI, VII, VIII, IX; then incubated for 72 h. After that, they were maintained in SFM/F12\_R2: 0.5% BSA (Sigma-Aldrich), 1% ITS (Invitrogen, USA), 2 mM retinoic acid (Sigma-Aldrich, USA) for 48 h. And complex of R3 media: DMEM-low glucose (Invitrogen, USA), 0.5% BSA (Sigma-Aldrich, USA), 1% ITS (Invitrogen, USA), 10 ng/mL bFGF (R&D, USA), 20 ng/mL EGF (Sigma-Aldrich, USA) for 72 h. For next 72 h, R4 media: DMEM/F12 (Invitrogen, USA), 1% ITS (Invitrogen, USA), 10 ng/mL bFGF (Merck, USA), 10 nM Nicotinamide (Sigma-Aldrich, USA). The morphology of IPCs were

observed under a microscope before changing the media. The miPS-IPCs maturation were collected for evaluating IPC-related genes, proteins and functional properties.

Modified protocols of IV, VI, VII with Dopamine hydrochloride (Sigma-Aldrich, USA) at early IPCs stage. In protocol V, 100 nM glucagon-like peptide (GLP)-1 (Sigma-Aldrich, USA) and 1  $\mu$ M DAPT (Sigma-Aldrich, USA) were added at progenitor endocrine stage and early IPC stage.

In the optimized protocol of VIII, SFM\_R1: 2% beta-mercaptoethanol (Sigma-Aldrich, USA), 1x NEAAs (Sigma-Aldrich, USA), 1x GlutaMax<sup>TM</sup> (Thermo Fisher Scientific, USA), 0.1% BSA (Sigma-Aldrich, USA), 50 ng/mL Activin A (Sigma-Aldrich, USA) are incubated in 3 days; the SFM\_R2: 2% beta-mercaptoethanol (Sigma-Aldrich, USA), 1x NEAAs (Sigma-Aldrich, USA), 0.5% BSA (Sigma-Aldrich, USA), 1% ITS (Invitrogen, USA), 2 mM retinoic acid (Sigma-Aldrich, USA), 1 mM Taurin (Sigma-Aldrich, USA), 10 nM Nicotiamide (Sigma-Aldrich, USA) were maintained for 2 days; the DMEM/F12 media of R3: 2% beta-mercaptoethanol (Sigma-Aldrich, USA), 1x NEAAs (Sigma-Aldrich, USA), 0.5% BSA (Sigma-Aldrich, USA), 1% ITS (Invitrogen, USA), 10 ng/mL bFGF (R&D, USA), 20 ng/mL EGF (Sigma-Aldrich, USA) and 1  $\mu$ M DAPT (Sigma-Aldrich, USA) were kept for 3 days; the DMEM/F12 media of R4: 2% beta-mercaptoethanol (Sigma-Aldrich, USA), 1x NEAAs

(Sigma-Aldrich, USA), 1  $\mu\text{M}$  DAPT (Sigma-Aldrich, USA), 100 nM (GLP)-1 (Sigma-Aldrich, USA) were added and changed every two days.

### **Reverse transcription-quantitative polymerase chain reaction (RT-qPCR)**

The IPC samples were collected and interpreted by using RT-qPCR system. The total RNA was stored in the solution of TRIzol-RNA isolation reagent (Thermo Fisher Scientific, USA), and extracted using DirectZol-RNA extraction kit (Zymo Research, USA) following to the optimized protocol. Subsequently, the complementary DNA (cDNA) was converted by the kit of ImProm-TM Reverse Transcription System (Promega, USA). Next, the pancreatic IPC-related targeted genes with the specific primer sets were showed in Table S1. They were amplified and detected by the material of FastStart Essential DNA Green Master (Roche Diagnostics, Switzerland) running into the machine of CFX96TM real-time PCR detection system (Bio-Rad, USA). The ribosomal Protein L13 (Rlp13A), was served as the housekeeping gene, and the fold changes in gene expression levels were normalized with Rlp13A and calculated following this formula:  $2^{-\Delta\Delta\text{CT}}$ , where  $\Delta\Delta\text{CT} = [\text{Ct}_{\text{target gene}} - \text{Ct}_{\text{Rlp13A}}]_{\text{treated}} - [\text{Ct}_{\text{target gene}} - \text{Ct}_{\text{Rlp13A}}]_{\text{control}}$  (Ct referred to cycle threshold).

Supplementary Table 1. Primer sequence

No.	Gene	Accession # (mRNA)	Forward Primer sequence	Reverse Primer sequence	Primer size
1	Rex-1	NM_009556.3	GGAGGAAATAGGTAGAGCGCA	AGTGAGGCGATCCTGCTTTC	21
2	Nanog	NM_001289828.1	GGTGTCTTGCTCTTCTGTGG	TGTCAGTGTGATGGCGAGG	21
3	Oct-4	NM_001252452.1	GCAGATAGGAACCTGCTGGGT	AAGCGACAGATGGTGGTCTG	21
4	Sox-2	NM_011443.4	TTGGGAGGGGTGCAAAAAGA	TTCTAGTCGGCATCACGGTT	20
5	Ssea1 (Fut4)	NM_010242.3	ACGTGTCTGTGGACGTGTTT	ACGTGCCGTGAGTTCTCAA	20
6	Cxcr4	NM_001356509.1	GCGTTTGGTGTCCGGTAAC	GAAGCAGGGTTCCTTGTGGGA	20
7	Goosecoid (Gsc)	NM_010351.1	TCCAGGAGACGAAGTACCCA	TCGGCGTTTTCTGACTCCTC	20
8	FoxA2	NM_001291065.1	ATGCACTCGGCTTCCAGTATG	TGTTTCATGCCATTATCCCCA	21
9	Sox17	NM_001289464.1	CCCCAAGGCTAGCTTCCGAT	TCTGGTGTGACTGGCGTAT	20
10	Bmp2	NM_007553.3	GCTAGATCTGTACCGCAGGC	GAAGTTCCTCCACGGCTTCT	20
11	Pdx1	NM_008814.4	CCTTTCCCGAATGGAACCGA	TCCGCTGTGTAAGCACCTC	20
12	Sox9	NM_011448.4	AAGAGACCCTTCGTGGAGGA	ATGTGAGTCTGTTCCGTGGC	20
13	Hnf6 (Onecut1)	NM_008262.3	GCAACGTGAGCGGTAGTTTC	GTCCTTGCTGGGAGTTGTGA	20
14	Gp2	NM_025989.4	CTGGGCAGGGAGGAAGGATAC	TCACAACCCACCATCCTTTTCA	21
15	Ngn-3	NM_009719.6	GCTGCTTGACACTGACCCTA	AGGTGGGGTGAATTGGAAC	20
16	NeuroD1	NM_010894.3	GCCTTTACCATGCACTACCCT	GATGGCATTAAAGCTGGGCAC	21
17	Pax-4	NM_001159925.1	CACAGCTGCCAGGATCATCT	ATAGGCTGGGATGAGGTGT	21
18	Nkx-2.2	NM_001077632.1	TCGCTACAAGATGAAACGTGC	CTTGCGGACACTATGGGCA	21
19	Maf-b	NM_010658.3	GGCAACTAACGCTGCAACTC	CGGAAGGGACTGAACACCA	20
20	Pax-6	NM_001244198.2	GCTTTGAGAAGTGTGGGAACC	AATACGGGGCTCTGAGAACTG	21
21	Nkx-6.1	NM_144955.2	GCACGCTTGGCCTATTCTCT	TTCGGGTCCAGAGGTTTGTT	20
22	Isl1	NM_021459.4	CCCAGAGTCATCCGAGTGTG	GAGTTCCTGTATCCCTGG	20
23	Mafa	NM_194350.2	CGCACCCGACTTCTTTCTGT	CAGAGTCTGAACCGAGACCG	20
24	Glut2	NM_031197.2	ACCGGGATGATTGGCATGTT	GGACCTGGCCCAATCTCAA	20
25	Insulin1 (Ins1)	NM_008386.4	AATGGGCCAAACAGCAAAGT	TAGGAAGTGCACCAACAGGG	20
26	Insulin2 (Ins2)	NM_001185083.2	GCAAGCAGGAAGGTTATTGTTCA	CACACACCAGGTAGAGAGCC	24
27	Glucagon	NM_008100.4	TCTACACCTGTTGCGAGCTC	GTCCTCATGCGCTTCTGTCT	20
28	Glip1 receptor (Glip1r)	NM_021332.2	GGGCCAGTAGTGTGCTACAA	CTTCACACTCCGACAGGTCC	20
29	Dll1	NM_007865.3	AGATAACCCTGACGGAGGCT	ACCGGCACAGGTAAGAGTTG	20
30	Jagged1	NM_013822.5	CGGGGGTAACACCTTCAATCT	TCCACCAGCAAAGTGTAGGAC	21
31	Jagged2	NM_010588.2	CCTCGTCGTACTTCCCTTCA	CAGCTCCTCATCTGGAGTGGT	21
32	Hes1	NM_008235.2	AGAAAGATAGCTCCCGGCAT	GTCACCTCGTTCATGCACTC	20
33	Hes5	NM_001370755.1	AAGGCCGACATCCTGGAGAT	GTGCAGGGTCAGGAACTGTA	20
34	Hey1	NM_010423.2	GTAACTCCTCCTTGCCCGC	TCGTTGGGGACATGGAACAC	20
35	Lef1	NM_001276402.1	GACTTCAGGTGGTAAGAGAAGC	TGTCAGTGTCTTGGGGTTC	22
36	Tcf7	XM_030245770.1	TTTCCCGGACAAACTTCCAGA	GTTATGCAGCGGGGGTTGAG	21
37	Rpl13a	NM_009438.5	TGAATACCAACCCCTCCCGA	CTCTCTTGGTCTTGTGGGGC	20

**Rex1**, reduced expression 1; **Nanog**, Nanog homeobox; **Oct-4**, octamer transcription factor 4; **Sox-2**, SRY (sex determining region Y)-box 2; **Ssea1**, Stage-specific embryonic antigen 1; **Cxcr4**, C-X-C chemokine receptor type 4; **Goosecoid (Gsc)**, Homeobox protein goosecoid; **FoxA2**, Forkhead box protein A2; **Sox17**, SRY-box transcription factor 17; **Bmp2**, bone morphogenetic protein 2; **Pdx1**, pancreatic and duodenal homeobox 1; **Sox9**, SRY-Box Transcription Factor 9; **Hnf6**, ONECUT1 one cut homeobox 1; **Gp2**, glycoprotein 2; **Ngn-3**, Neurogenin-3 is a marker of embryonic-type endocrine progenitor cells; **NeuroD1**, neurogenic differentiation 1; **Pax-4**, Paired Box 4; **Nkx-2.2**, Homeobox protein; **Maf-b**, MAF bZIP transcription factor; **Pax-6**, paired box 6; **Nkx-6.1**, NK6 homeobox 1; **Isl1**, ISL LIM homeobox 1; **Mafa**, MAF BZIP Transcription Factor; **Glut2**, Slc2a2 solute carrier family 2; **Insulin1 (Ins1)**, **Insulin2 (Ins2)**, **Glucagon**, **Glip1 receptor (Glip1r)**, glucagon-like peptide 1 receptor; **Dll1**, delta like canonical Notch ligand 1; **Jagged1**, jagged canonical Notch ligand 1; **Jagged2**, jagged canonical Notch ligand 2; **Hes1**, hairy and enhancer of split-1 or hes family bHLH transcription factor 1; **Hes5**, hairy and enhancer of split-5 or hes family bHLH transcription factor 5; **Hey1**, hes related family bHLH transcription factor with YRPW motif 1; **Lef1**, lymphoid enhancer binding factor 1; **Tcf7**, transcription factor 7, T cell specific; **Rpl13a**, ribosomal protein L13A.

Immunocytochemistry staining

The IPC encapsulation samples were dissolved or the naked IPCs are collected. Fixation was performed by 100% cold methanol (-20°C) with 15 minutes at 4°C, the samples were permeabilized for 1 minute using 0.1% Triton®X-100 (VWR life science, USA) in PBS at room temperature. The samples were blocked in 10% donkey serum (in PBS) incubating for 1 hour at 4°C. For the primary antibodies, the monoclonal of mouse clone Pro-Insulin C-Pep-01 (Millipore, USA) and anti-mouse Insulin monoclonal (Merck, USA), were stained with dilution at 1:100 (in 1% BSA) incubating for 24 hours at 4°C. After around 24 hours, the samples were washed with PBS and incubated with a secondary antibody of goat anti-mouse IgG conjugated to fluorescein isothiocyanate isomer 1 (Bio-rad, USA) at 1: 1,000 dilution (in 1% BSA), in the dark condition of room temperature for 1 hour. Nucleus marker was stained using DAPI (0.4 µg/mL) (Sigma-Aldrich, USA). The samples were detected and analyzed under 10x and 20x magnification of a fluorescent microscope incorporated with Carl Zeiss™ Apotome.2 apparatus (Carl Zeiss, Germany).

#### **Live/Dead cells staining**

The IPC encapsulation, naked IPCs, and control samples were collected and evaluated by double staining. Calcein AM chemical (Thermo Fisher Scientific, USA), and propidium iodide chemical (Sigma-Aldrich, USA) were used with 1: 1,000 dilution

for 30 minutes incubation. Then, the samples were rinsed into PBS. The results were indicated under 10x objective of a fluorescent microscope incorporated with Carl Zeiss<sup>TM</sup> Apotome.2 apparatus (Carl Zeiss, Germany).

### **Functional tests for IPCs**

During IPC induction, the samples were tested by the approach of glucose-stimulated C-peptide secretion (GSCS). The buffer was used by Krebs-Ringer bicarbonate HEPES (KRBH buffer) mixture of 120 mM NaCl, 5 mM KCl, 2.5 mM CaCl<sub>2</sub>, 1.1 mM MgCl<sub>2</sub>, 25 mM NaHCO<sub>3</sub>, and 10 mM HEPES, then adjust pH 7.4 value by NaOH solution was served as the normal control. The glucose anhydrous (Sigma-Aldrich, USA) for stimulation at concentration 5.5 mM (99 mg/dL) and 22 mM (396 mg/dL) were prepared. The samples were challenged in series of concentration for 60 minutes into the solution of control, 5.5 mM Glucose, and 22 mM Glucose, respectively. The Insulin secretion levels were indicated via C-peptide quantitation, the C-peptide into supernatant was measured using Rat/mouse C-peptide enzyme-linked immunosorbent assay kit (Millipore, USA) according to the supplied protocol. Two factors consist of total DNA (ng) and stimulated time (minute) were normalized the levels of C-peptide secretion.

### **Double layers of IPC encapsulation**

For IPC encapsulation, matured IPC generation were collected and resuspended with prepared 2% (w/v) alginate solution. Double encapsulation of IPCs was created by completed 30% (w/v) of Pluronic-F127 as beads with two layers following to optimized protocol. In aseptic condition, the beads were maintained in induction solution at 37°C and 5% CO<sub>2</sub> condition. The blank beads were as control for further experiments.

#### **Alginate/Pluronic-F127 bead dissolution**

The pancreatic encapsulated IPCs were dissolved by incubating in dissolving buffer (0.2 M C<sub>6</sub>H<sub>5</sub>Na<sub>2</sub>O<sub>7</sub>·2H<sub>2</sub>O, pH 7.4 and 0.1 M EDTA) for 5m, in 37°C. The layers of beads were degraded and then, they were washed in PBS buffer (three times/3 minutes each) and processed for further manipulation (RT-qPCR or Immunocytochemistry staining).

#### **Subcutaneous pocket formation technique**

The mice were divided into two groups: i) Tested group, and ii) Sham group. In Tested group, the mice were subcutaneously implanted with 18-G catheter (Nipro, Thailand) at the back with an aseptic technique. The space-retaining solution consisted of a sterile mixture of 250 ng/mL Vascular Endothelial Growth Factor-165 (VEGF-165) (GenScript, USA) and 10% Pluronic-F127 (Sigma-Aldrich, USA) was injected through the



catheter. The subcutaneous pocket formation period was set up for 14 days. For mock-up transplantation, the pre-made sterile mock-up beads were made from alginate and Pluronic-F127. These beads were transplanted into the pocket using aseptic technique. Approximate twenty to twenty-five beads were assigned to this transplantation (~250 IPCs). After that the skin were closed by suturing. They were observed for 21 days (short-term study) and 42 days (long-term study). For Sham group, the mice were applied as Tested group, except the infiltration of space-retaining solution and the transplantation of the mock-up beads. The mice were weighted and blood withdrawal for fasting glucose levels (FGLs) and HOMA-IR/beta analysis before intraperitoneal (ip) 1.5 g/kg of glucose (Sigma-Aldrich, USA) for injection glucose tolerance testing (IPGTT). At termination, they were cardiac blood collected under generalized anesthesia for complete blood count (CBC), blood chemistry, and cytokine analysis. The sacrificed mice were harvested pancreas, implantation site (skin and all subcutaneous tissue at the insertion area), kidney, and brain for histological analysis. Cardiac puncture blood was stored in lithium heparin tube (BD Vacutainer®, Thailand) (suitable for blood chemistry and cytokines technique) for anticoagulant function. Blood for CBC is contained in lavender top (EDTA) tubes (BD Vacutainer®, Thailand). The blood is short stored on ice or 4oC until

the next processing. All animals were checked for their health and weight every week.

All mice were 6h water and feed deprivation before blood collection.

### **Diabetic induction and encapsulated IPC transplantation**

Two groups were divided for this study consisting of i) STZ-induced diabetes mice + encapsulated IPC transplantation, and ii) Sham group (STZ-induced diabetes mice + non-IPC transplantation). Then, they were separated into two study periods: 21-day (short-term transplantation) and 42-day (long-term transplantation).

The normal FGLs (<11.1 mM) mice were rendered diabetic through administration of an intraperitoneal injection of streptozotocin (STZ) (Sigma-Aldrich, USA) at 180 mg/kg (in Citrate buffer, pH 4.5, Sigma-Aldrich, USA). Animals were considered diabetes when their non-fasting blood glucose levels exceeded a pre-established value of 20 mM for post STZ administration. Only animals meeting this inclusion criterion were selected for transplantation. Then, the implantation process was applied as Phase I. At the time of transplantation, 250 or 500 IPC colonies equivalents were added into a subcutaneous pocket under anesthesia. In post-transplantation, the mice were checked fasting glucose levels (FGLs) and HOMA-IR/beta analysis before intraperitoneal (ip) 2 g/kg of glucose for injection glucose tolerance testing (IPGTT). At termination, they were cardiac blood collected under generalized anesthesia for CBC,

blood chemistry, and cytokine analysis, and sacrificed for harvesting pancreas, implantation site (skin and all subcutaneous tissue at the insertion area), kidney, and brain for histological analysis.

All animals were monitored their health and weight every week. All mice were 6h water and feed deprivation before blood collection.

#### **HOMA index and QUICKI index checking**

HOMA index consists of HOMA-beta, HOMA-IR and QUICKI are based on the levels of C-peptide in the plasma. C-peptide levels are detected using Rat/mouse C-peptide enzyme-linked immunosorbent assay kit (Millipore, USA) according to the supplied protocol. The value is calculated follow the formula: HOMA-beta: fasting C-peptide x 20/(FGLs-3.5) or HOMA-beta (diabetes): fasting C-peptide x 20/(FGLs-3.5)+50 and HOMA-IR = fasting C-peptide x FGLs/22.5; QUICKI = 1/[log(HOMA-IR)]. The unit of C-peptide and FGLs values are  $\mu$ IU/mL, and (mmoL/mL), respectively.

#### **Intraperitoneal injection glucose tolerance test (IPGTT)**

The mice are fasted for 6h to keep them in a low blood glucose status. After fasting, an initial blood draw was done prior to each glucose challenge. For the glucose challenge, mice were intraperitoneal injection with glucose (1.5 g/kg). FGLs are

checked at 15, 30, 60 and 120 min after glucose injection. Glucose in the blood was measured by glucose meter (Accu-Chek, Roche, Switzerland).

### **Completed blood count (CBC) and Blood Chemistry**

The whole blood was withdrawn into the lavender top (EDTA) tubes or heparin (BD Vacutainer®, Thailand) for anticoagulant. The plasma was collected after centrifuge at 2500 rpm, 15 m, 4°C. The parameter of blood chemistry was checked in the panel of comprehensive cards by biochemistry analyzer, Vetscan VS2 machine (Abaxis, Zoetis, UK). The CBC was detected in CBC panel by RIA company, Bangkok, Thailand.

### **Cytokine analysis**

Cardiac puncture blood was stored in lithium heparin tube for anticoagulant function. Using multiplex protein detection and semi-quantitation methods of mouse inflammation antibody array with protein targets were assayed. The profile of proteins in plasma samples were progressed following the commercial manufacturer's kit (ab133999, abcam, USA). Briefly, antibody array membranes were blocked in 2 mL of blocking buffer for 30 m, and then incubated with 1 mL of the samples overnight at 4 °C. The sample solution were then discarded from each container, and the membranes were large washed with 20mL of wash buffer. Next, adding more three times with 2 mL of wash buffer at room temperature with shaking. The membranes

were then incubated in 1:1000 diluted streptavidin–horseradish peroxidase at room temperature for 2 h, and the membranes were washed thoroughly and exposed to a peroxidase substrate before imaging. Chemiluminescence was imaged using a Amersham imager 600 (UV), Japan with 2-minute exposure. In inflammation panel, this panel will allow simultaneous analysis of 40 biomarkers. In result, the list of proteins' detections in the membrane array is matched with the cytokine's map. The intensity of dot clots was automatically measured by ImageJ software (National Institutes of Health, NIH). Heatmap was generated using R software (Bell Lab, GNU project). The intensity was calculated by formula  $(X = (X(y)\text{-negative}) * P1/P(y))$  following the manufactory supply.

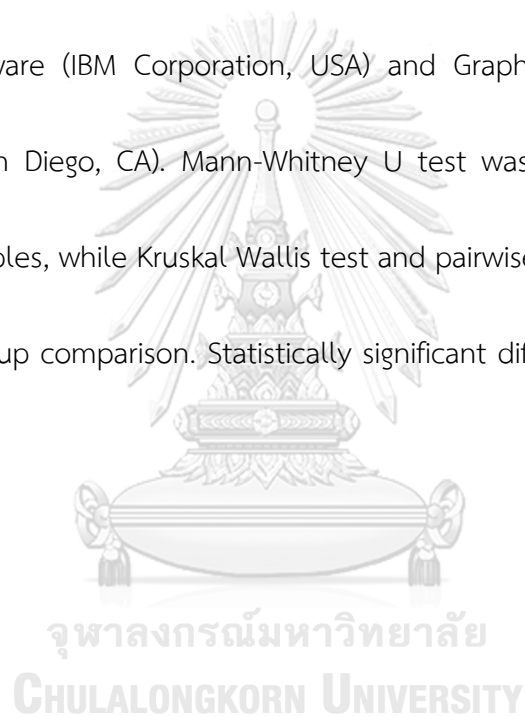
### **Histopathology**

The animals were euthanized by inhalation administration of CO<sub>2</sub>. Their death was confirmed by lack of heartbeat, cervical dislocation and removing vital organs. Tissues were collected and rinsed with 1X phosphate buffered saline (PBS), pH 7.4, and fixed in 4% Paraformaldehyde (PFA) for 24 h. Then, the tissues were dehydrated in a graded ethanol series, embedded in paraffin wax, and next sectioned at a thickness of 3 μm for histology. Three serial sections of each sample were stained with haematoxylin and eosin (H&E) for histological examination. Stained slides were digitally taken the

pictures using a Olympus microscope (Olympus Group, Japan). The evaluation was performed by independent examiners who were blinded to the experimental group. Three sections from each sample were randomly selected and evaluated.

### **Data analysis**

All results were illustrated as dot plot. Statistical analysis is determined using SPSS statistics 22 software (IBM Corporation, USA) and GraphPad Prism 9.0 (GraphPad Software, Inc., San Diego, CA). Mann-Whitney U test was used for comparing two independent samples, while Kruskal Wallis test and pairwise comparison was used for three or more group comparison. Statistically significant difference (\*) is recognized if p-value <0.05.



## CHAPTER IV

### RESULTS AND DISCUSSION

#### Establishment and optimization of the effective IPC differentiation using mGF-iPSCs modeling

The mGF-iPSCs were a kind gift from Prof. Egusa Hiroshi (Tohoku University, Japan) that was well-established and well-characterized (Egusa et al. 2010). The mGF-iPSCs were validated the morphology, the mRNA levels of stemness markers, and alkaline phosphatase (ALP) expression before examining the experiments (Fig.S1). Embryoid bodies (EBs) were initially synthesized into a suspension medium. They were maintained in the low-attached Eppendorf™ Cell Culture Dishes (Non-Treated), MicroQC™ Petri Dish, and Sterilin™ Petri Dish respectively. Sufficiently, 4-day EBs demonstrated the morphology were variant when using the different containers (Fig.S2). The IPC differentiation was generally divided into 6 steps including: [1] EB generation (4 days), [2] definitive endoderm (DE) stage (3 days), [3] pancreatic progenitor (PP) cell stage (2 days), [4] pancreatic endocrine stage (3 days), [5] 11-day (early) IPC stage (3 days), [6] 13-day (matured) IPC stage (2 days) (Fig.1A). To prove the plasticity of IPC development from early IPCs to mature IPCs, the glucose stimulation C-peptide secretion (GSCS) of IPCs was examined with basal, 5.5 mM, and 22 mM

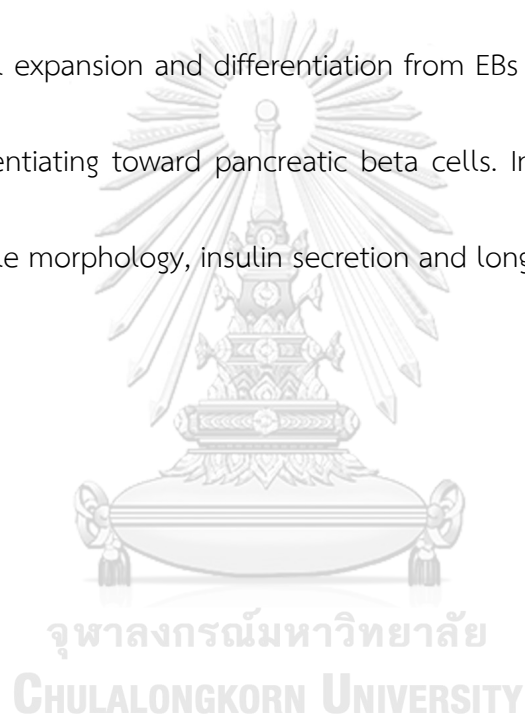
glucose concentration respectively. It implied that the high glucose concentration (Glu) induced the high of C-peptide of IPCs to extracellular solution. The C-peptide level was detected by ELISA technique in extracellular solution. Three protocols (I, II, III) were used the same chemical of IPC induction; however, they were different containers for EB formation. Using Sterilin™ Petri Dish, the colonies of EBs elucidated the round shape, less agglomeration (Fig.1B-III). Expectedly, IPCs have raised up 3.5 folds at 13-day IPCs compared with 11-day IPC duration via the expression of C-peptide. The C-peptide secretion were elevated from Glu of basal to 5.5mM, 22 mM (Fig.1C-III). In whiles, EBs were small size into Eppendorf™ Cell Culture Dishes and much agglomeration and appendages into MicroQC™ Petri Dish (Fig.1B-I, II). In Eppendorf™ Cell Culture Dishes, from 11-day IPCs (early) to 13-day IPCs (matured) that presented the sensitivity of IPCs with Glu 5.5 mM and 22 mM. However, it was slightly increased up 1.5-fold the level of C-peptide from 11-day to 13-day (Fig.1C-I). Likewise, when EBs were created into MicroQC™ Petri Dish, the C-peptide levels were not significantly changed either series of Glu or 11-day, 13-day of IPC periods (Fig.1C-II). Here, the morphology and intracellular formation of EB aggregation was an essential role in determination of the IPC maturation and function.



To enhance C-peptide secretion, basing on the condition of protocol III, protocol IV was supplied 30  $\mu\text{M}$  Dopamine hydrochloride (DA) at 11-day (D11) for 48 h; the protocol V was added 100  $\mu\text{M}$  glucagon-like peptide (GLP)-1 and 1  $\mu\text{M}$  gamma-secretase inhibitor (DAPT) at D11 and 13-day (D13). The protocol VI was built on protocol V ingredients that was added with 30 $\mu\text{M}$  DA at D11 (Fig.1A). In morphology, there were not significantly different between protocols IV, V, and VI (Fig.1B-IV, V, VI). Otherwise, when series of glucose concentration (Glu) triggered to C-peptide secretion that was clearly distinct with/without (w/wo) DA supply at Glu 22 mM. In the 13-day IPC of protocol IV and VI, C-peptide detection was higher level at Glu 22 mM compared with Glu 5.5 mM. However, from 11-day IPCs to 13-day IPCs, the level of C-peptide expression was grown up 2-3.5 folds; and this performance was equivalent levels between these protocols (Fig.1C-IV, V, VI).

To obtain more achievement of IPCs as autologous beta cells, we optimized the protocol VII from protocol VI, by adding in 1mM Taurin and 10mM Nicotiamide at pancreatic progenitor cell step, and enclosed 1 $\mu\text{M}$  DAPT in pancreatic endocrine step. To gain the survival of in vitro IPC, 1% non-essential amino acids (NEAAs) and 2%  $\beta$ -mercaptomethanol (b-met) were added in every step during IPC induction that was described as protocol VII (Fig.1A). However, the morphology and C-peptide expression

were not expected performance as protocol VI (Fig.1B-VII). Surprisingly, protocol VIII without 30  $\mu$ M DA, the number of IPC colonies was well maintained. The colony's morphology was similarly kept in diameter from early IPC (D11) generation to 60-day (D60) (Fig.1B-VIII). C-peptide detection was increased 4 folds from 11-day IPCs to 13-day IPCs, and higher at Glu 22 mM compared with Glu 5.5 mM (Fig.1C-VIII). Here, the cells were parallel expansion and differentiation from EBs to 11-day IPCs; then, they focused on differentiating toward pancreatic beta cells. In overall, the protocol VIII showed responsible morphology, insulin secretion and long survival.



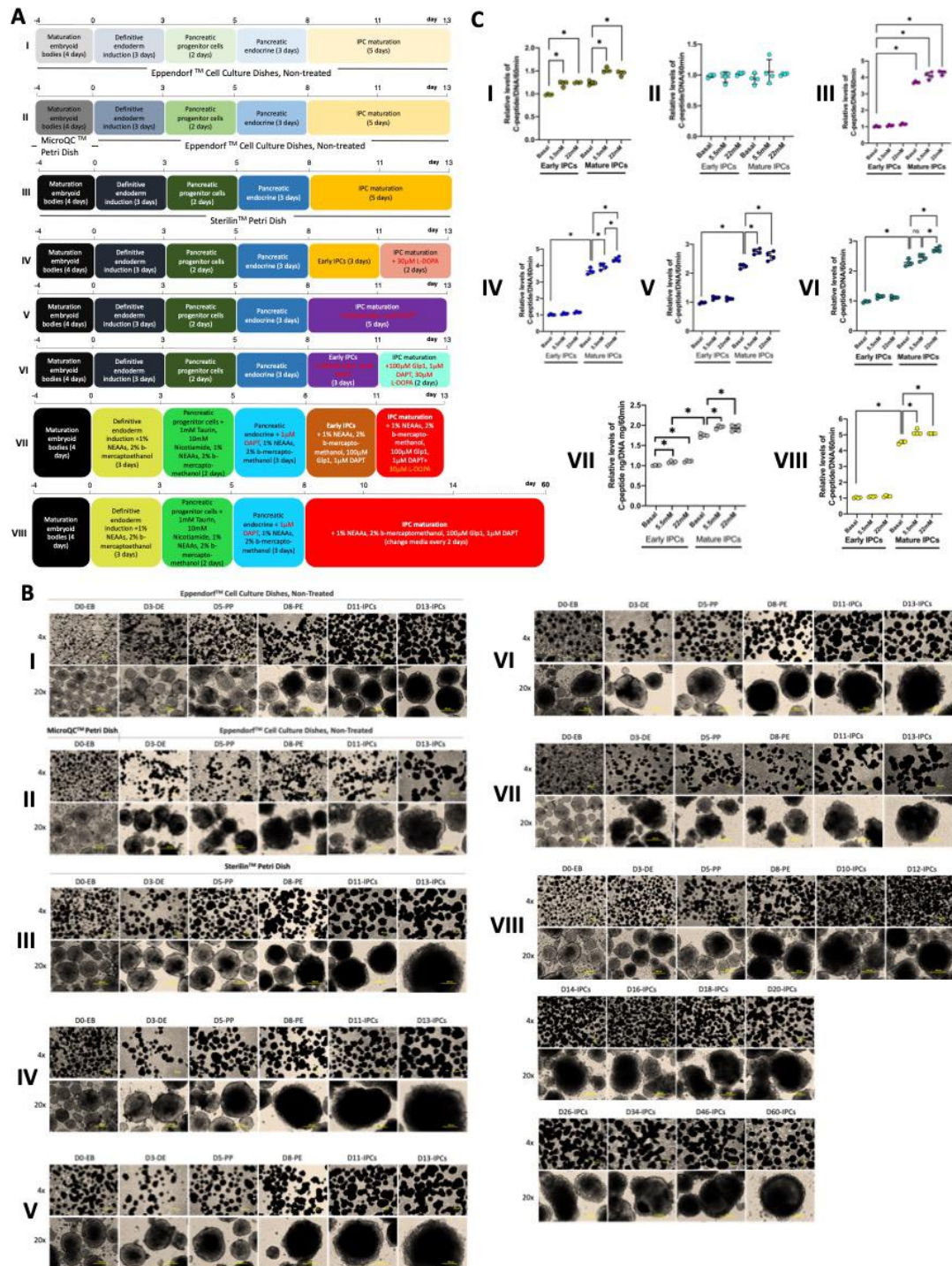


Figure 1 Establishment and optimization of the effective IPC differentiation using mGF-iPSCs modeling

(A) Scheme of seven protocols; protocol I-III was same chemical supply and different untreated containers during EBs and IPCs induction. Protocol IV, V, VI were based on the condition of protocol III, protocol IV was supplied 30mM DA at 11-day (D11) for 48 h; the protocol V was added 100mM Glp1 and 1mM DAPT at D11 and 13-day (D13). The protocol VI was built on protocol V ingredients that was modified with 30mM DA at 13-day. Protocol VII was optimized of the protocol V by putting in 1mM Taurin and 10mM Nicotiamide solution at the step of pancreatic progenitor cells, and enclosed 1mM DAPT in pancreatic endocrine duration. 1% non-essential amino acids (NEAAs) and 2% b-mercaptomethanol were added in every step during IPC development and maturation. (B) The variant morphology of IPCs were showed with stepwise chemical adding for individual protocol; protocol I-VI: 13-day induction; protocol VII: 60-day induction. Magnification = 4x, 20x. (C) Glucose stimulation C-peptide secretion (GSCS) was checked all of three protocols at 11-day or early IPCs and at 13-day or matured IPCs. The IPCs were challenged with basal, 5.5 mM, 22 mM glucose concentration and then using the ELISA technique to detect the C-peptide secretion. The level of C-peptide releasing was calibrated on DNA concentration and 60 minutes of secreting timing. DNA concentration was measured by QUBIT kit.

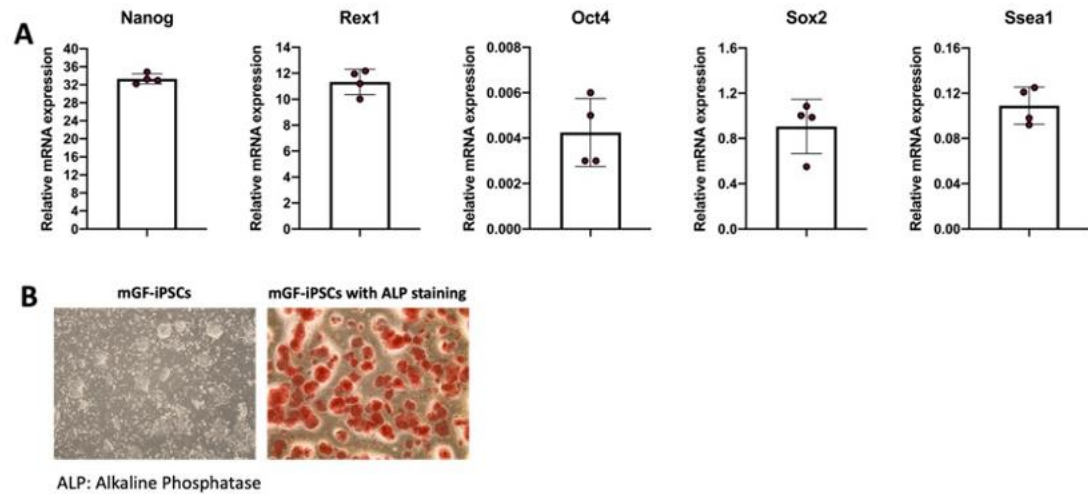


Figure S1 Characterization of mGF-iPSCs. A) The mRNA expression of Nanog, Rex1, Sox2, Oct4, Ssea1 were elucidated in mGF-iPSCs. B) The colonies of mGF-iPSCs were stained by ALP test. Red colonies displayed the high activity of ALP in cells.

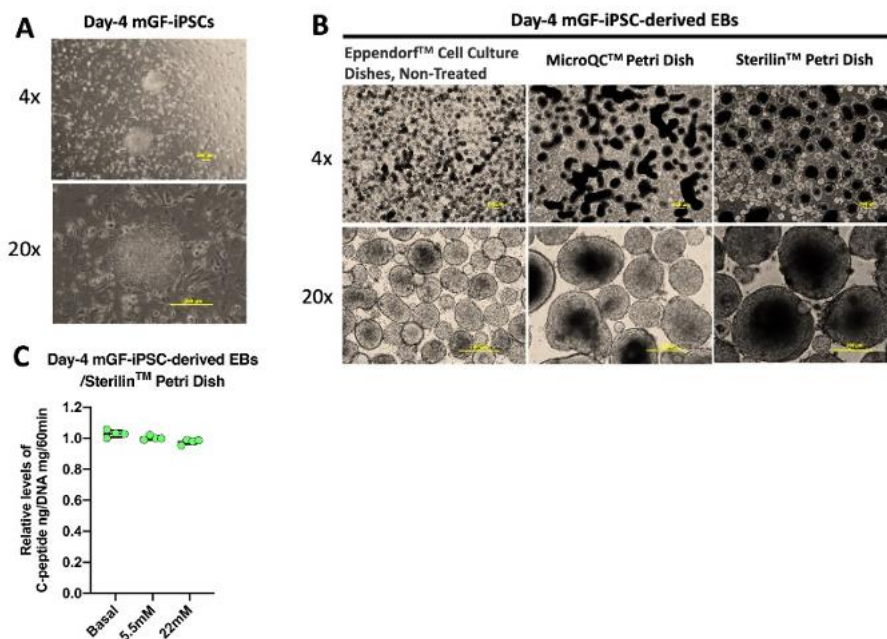


Figure S2 Embryoid bodies were created in different containers making be altered morphology. A) mGF-iPSCs were matured on day 4. B) The morphology of EBs

was differently generated in different un-attached containers including low-attached Eppendorf TM Cell Culture Dishes (Non-Treated), MicroQC TM Petri Dish, and SterilinTM Petri Dish.

### **In vitro in-house induction protocols yield efficient and long-term survival IPCs**

To determine the correction of gene expression in IPC formation, the mRNA levels were checked at EBs, D8, D14, D20, D27, D34, D48 by using real-time RT-qPCR method.

The primer sets were designed and validated as the attached table (Table.S1). In the stem-ness markers, EBs were shown the high expression of Nanog, Sox2, Oct4, Ssea1, and Rex1 that were gradually decreased the level during IPC development. Especially, Nanog and Sox2 were extremely high levels at the EB stage. Besides, the mouse pancreas (C57BL/6NJcl strain) was isolated serving as a positive control. In the mouse pancreas, the levels of stemness markers were low expression. Surprisingly, the mRNA level of Rex1 in mouse pancreas and IPC colonies were higher than EB stage. It implied

that Rex1 might interplay with the pancreatic beta-cell developmental process (Fig.2A).

In the definitive endoderm makers, the same pattern of Sox17 and Foxa2 expression were risen from EBs to D20, and then, it was steadily fallen at D27, D34, D48. The genes of Cxcr4 and Gsc were similar in the manner of decreasing levels from EBs to D48. Besides, Bmp2 gene was the different performance that was risen 15 folds at D34

compared with EB stage and dramatically gone down at D48 (Fig.2B). In pancreatic progenitor markers, Sox9 gene was slowly increased from EBs to D48 and was not detected in mouse pancreas. Hnf6 gene was not much active from D8 to D48 and the similar manner of the mouse pancreas. Pdx1 gene was exceptionally increased in IPCs collating with mouse pancreas. Nkx6.1 gene was a dynamic expression and higher than the levels in mouse pancreas. Remarkably, the mouse pancreas needed a lot of Gf2 for functionality and activity (Fig.2C). In early IPC markers, Ngn3, Nkx2.2, NeuroD, Pax6 genes were equivalent to the pattern of mRNA levels that were increased up to D27 and gradually low until D48. Mafb gene was variant between the periods. Pax4 gene was grown at D48. In mouse pancreas, the genes of early IPC markers were shown comparable activity with IPC generation (Fig.2D). In matured IPC markers, Ins2, Glut2 genes were risen at D27 and extremely top in mouse pancreas. Ins2, Mafa, Glp1r, Isl1, Nkx6.1, and glucagon mRNA levels were produced in IPC colonies comparable with mouse pancreas (Fig.2E). The target genes of Wnt/beta-catenin signaling and Notch signaling were oscillated presentation from EB to D48 timepoint (Fig.2F, 2G). They were indicated that mouse pancreas required the low levels of Wnt and Notch signaling for activity and function. In this study, the results revealed that the molecular intracellular expression was correct and sufficient transition and extremely dynamic.

The gene expression of IPCs were generated that can be comparable with mouse pancreas.

Correspondingly, the IPCs were induced from protocol VIII which were collected at D14, D20, D27, D34, D48. The C-peptide detection was increased about 3.5 folds from D14 to D20; interestingly, decreased 1.5 folds at D27 compared with D20. Consequently, it was fallen down at D34 and D48 collating with C-peptide level at D20 (Fig.2H). Additionally, IPCs were stimulated the glucose concentration (Glu) at basal, Glu 5.5mM, Glu 22mM for exocytosis of C-peptide proteins. It was significantly lifted the levels of C-peptide detection at Glu 5.5mM and Glu 22mM solution rather than a basal solution (Fig.2H). Besides, to reveal the total C-peptide endogenous IPCs, we collected the IPCs at D14, D20, D27, D34, D48 time points for the C-peptide protein extraction. Then, C-peptide levels were measured by ELISA technique as well. Connectively, the total C-peptide of IPCs were associated with the levels of C-peptide of GSCS test. During IPC survivals, the total C-peptide was not notably different between D27, D34, and D48 (Fig.2I). It implied that Glut2 gene or Insulin-releasing dependent genes might be reduced the expression.

To determine Pro-Insulin/C-peptide and Insulin proteins expressed into matured IPCs, the IPC colonies were stained Pro-Insulin and Insulin antibodies by



immunocytochemistry (ICC) test. The IPC colonies strongly expressed Pro-Insulin and Insulin which were located in the center rather than the boundary of colonies (Fig.2J). In visible cell examination, the IPCs presented the dead cells that were not much reduced from D18 to D60 (Fig.2K). Here, IPC termination indicated Pro-Insulin and Insulin expression that performed the correct process of Insulin generation. Moreover, we obtained lots of live cells during IPC development without significantly decreasing the expressed levels of intracellular C-peptide and Insulin proteins. However, the results of GSCS test were manifested the helping genes (Glut2 or Insulin-releasing dependent genes) of C-peptide/Insulin secretion pathway that might be degraded the expression and activity. In conclusion, we supposed that IPCs produced the correct Pro-Insulin, Insulin and IPC markers; otherwise, exogenesis was reduced due to degradation of Glut2 or Insulin-releasing dependent genes.

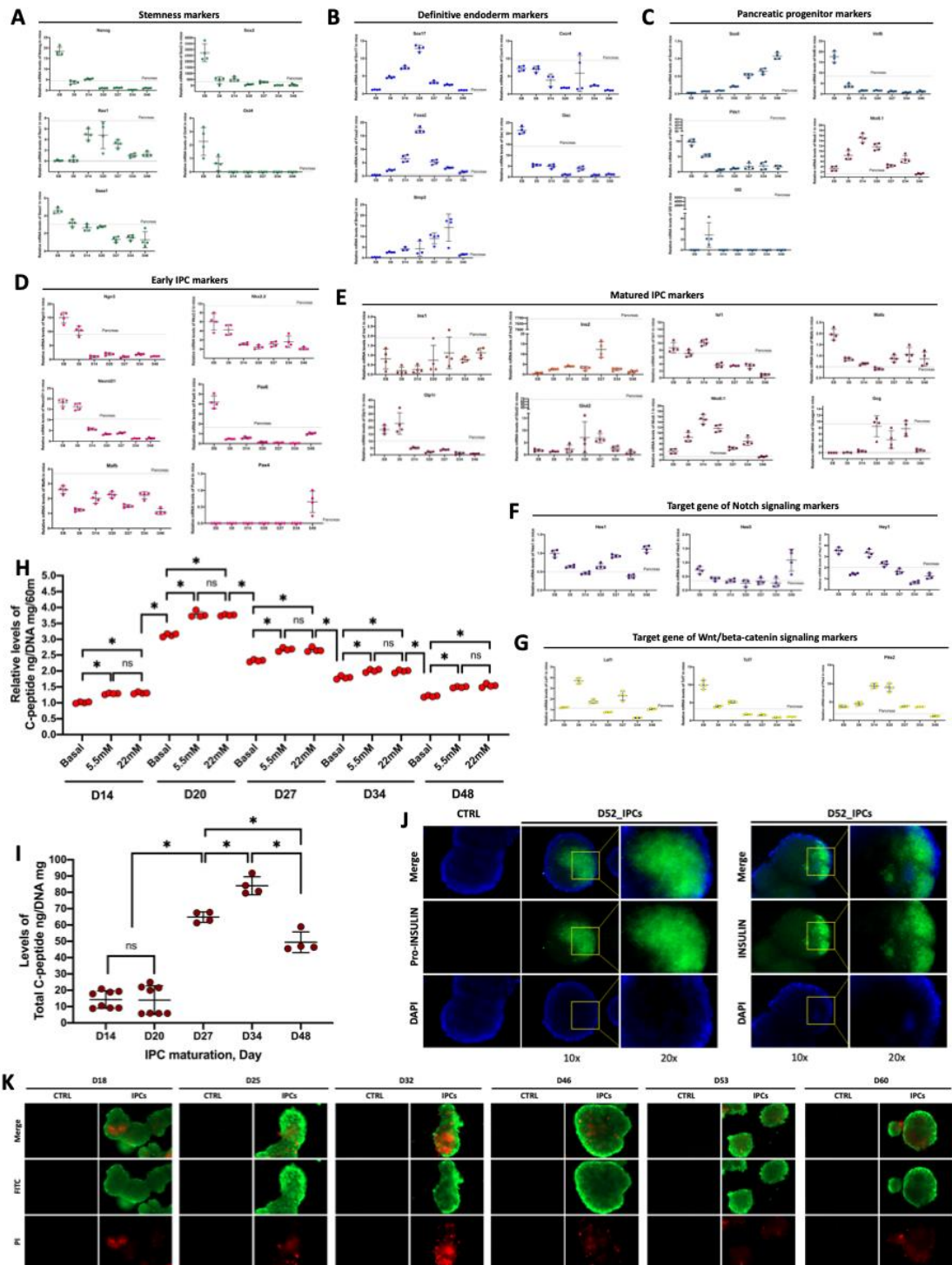


Figure 2 In vitro in-house induction protocols yield efficient and long-term survival IPCs

(A), (B), (C), (D), (E), (F), (G) Oscillation mRNA levels during IPC differentiation. The samples were collected at EB, D8, D14, D20, D27, D34, D48. Pancreas line was the levels of gene expression in mice's pancreas. The mRNA levels were demonstrated with stem-ness, definitive endoderm, pancreatic progenitor, early IPCs, matured IPCs, targeted genes of Notch signaling, targeted genes Wnt signaling, respectively. The mRNA expression levels were detected by real time qRT-PCR technique. (H) GSCS test was checked the protocols at 14-day, 20-day, 27-day, 34-day, 48-day of matured IPCs. The IPCs were challenged with basal, 5.5 mM, 22 mM glucose concentration and then using the ELISA technique to detect the C-peptide secretion. The level of C-peptide releasing was calibrated on DNA concentration and 60 minutes of secreting timing. (I) The total C-peptide in IPCs were kept in protease-free solution and used sonication for extracting C-peptide. C-peptide was detected by ELISA technique. The level of C-peptide releasing was calibrated on DNA concentration. DNA concentration was measured by QUBIT kit. (J) Matured IPCs were staining with pro-Insulin and Insulin antibodies with isotype as a control. (K) Matured IPCs were shown with the live/dead staining at D18, D25, D32, D46, D53, D60. Magnification = 4x, 20x.

## Trypsin-EDTA causes EBs separating into single cells, nevertheless limits IPC

### capacity

To produce the small scale of IPCs and remain their functionality, we modified protocol VIII. Then, trypsin-EDTA stimulated EB colonies (D4) to single cells before IPC induction (Fig.3A). The single cells were properly created, some EB colonies were still survived. Eventually, the single cells were formed into small colonies into the induction medium, survived EBs were continuously bigger diameter, and lots of single cells were poorly died. Thus, the number of IPCs of protocol IX were synthesized that were less than the IPC number of protocol VIII (Fig.3B). The potential of glucose stimulation C-peptide/Insulin secretion and total C-peptide expression were significantly less than protocol VIII as well (Fig.3C, 3D). These IPCs were expressed IPCs's markers including Ins1, Glut2, Isl1, Glucagon, Glp1r, Pdx1, Maf-a, Nkx6.1, Pax6, Ngn3. In whiles, the levels of Glut2, Glp1r, Pdx1, Nkx6.1 were lower than the protocol VIII. Moreover, this protocol was not detected the level of Ins2 expression (Fig.3E). Here, the IPCs can be induced without sufficiently endogenous gene expression.

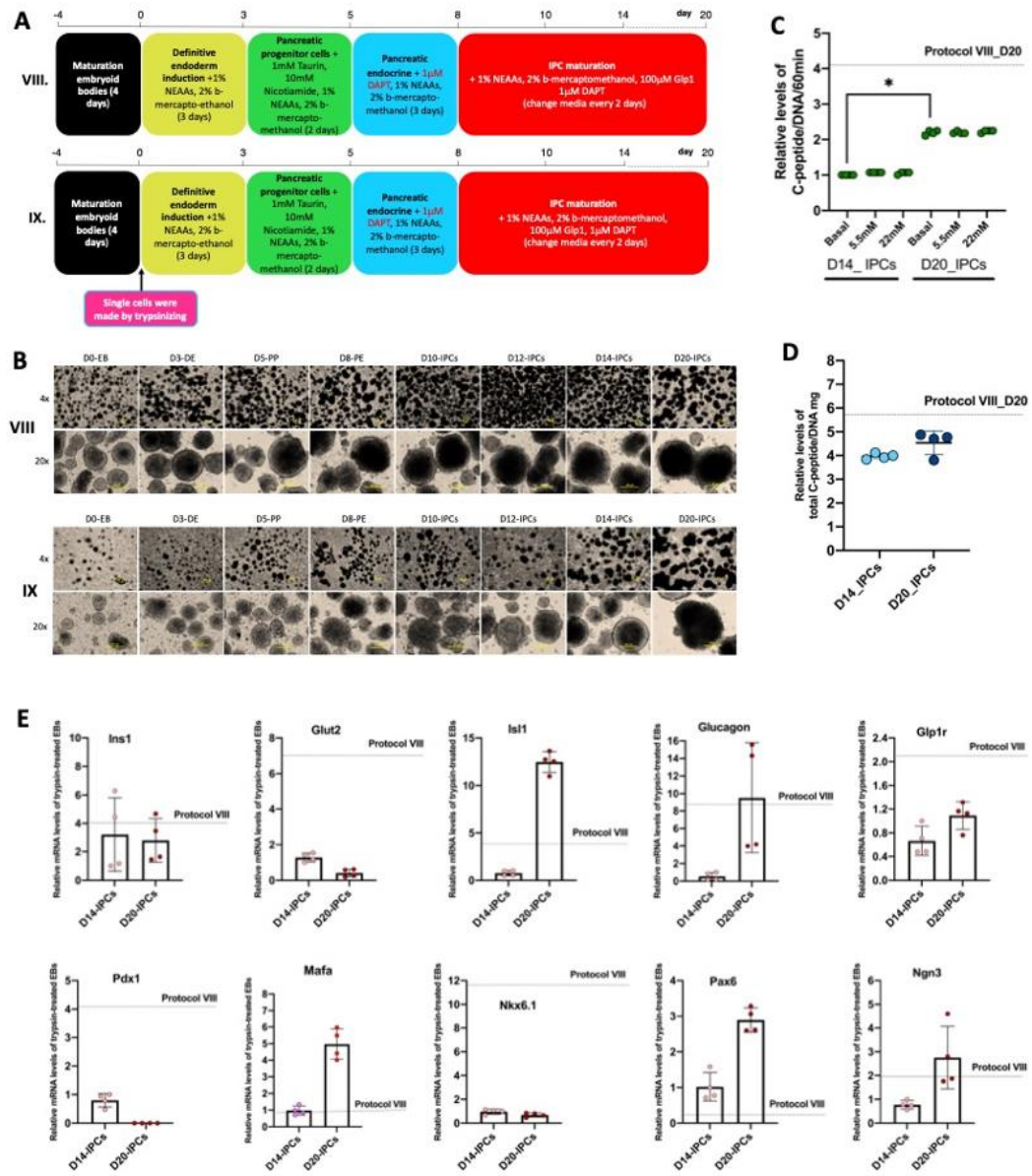


Figure 3 Trypsin-EDTA made EBs separate in single cells, reduced the capacity of IPCs

(A) Scheme of protocol VII and added trypsin-EDTA solution to the matured EBs for protocol VIII. (B) Morphology of protocol VIII was compared with protocol VII. (C) GSCS

test was checked all of three protocols at 14-day and at 20-day. The IPCs were challenged with basal, 5.5 mM, 22 mM glucose concentration and then using the ELISA technique to detect the C-peptide secretion. The level of C-peptide releasing was calibrated on DNA concentration and 60 minutes of secreting timing. (D) Total C-peptide was measured, and the level of C-peptide releasing was calibrated on DNA concentration. DNA concentration was measured by QUBIT kit. (E) The samples were collected at early IPCs and matured IPCs. The mRNA levels of Ins1, Glut2, Isl-1, Glucagon, Glp1r, Pdx1, Maf-a, Nkx6.1, Pax6, Ngn3 were checked.

### **Encapsulated IPCs preserve the Insulin secretion capacity and transplantable potential**

To minimize the autoimmune response in the host model, we applied the double biomaterial layers of alginate/Pluronic-F127 for encapsulation of IPCs. The IPCs were differentiated to D13 following the integrative protocol VIII. Then, 13-day IPCs were encapsulated by alginate/Pluronic-F127 biomaterials (Fig.4A). IPCs were stayed inside beads that were validated the potential of C-peptide/Insulin secretion, and gene expression. The mRNA levels of IPC biomarkers were remaining the endogenous gene expression from D13 to D20 and comparing with mouse pancreas (Fig.4B). In post-encapsulation, IPCs were collected the colonies at D14, D20, D27, D34, D48 that

were tested the capacity of C-peptide/Insulin secretion and total intracellular C-peptide. Remarkably, at D27, C-peptide of IPCs were excessively grown up 6 folds and slightly decreased 2 folds at D34 and D48. Besides, the C-peptide detection tended to susceptibly increase combining with increasing glucose concentration (Fig.4C). At D27, D34, D48, total C-peptide intracellular was significantly different with highest level at D48 (Fig.4D). Meanwhile, the sensors of IPC membrane were reduced the sensitivity with glucose. To provoke the evidence of C-peptide/Insulin expression, encapsulated IPCs were randomly picked to stain with Pro-Insulin/C-peptide and Insulin antibodies. Those colonies symbolized the presentation of Pro-Insulin and Insulin proteins (Fig.4E). To prove the survival of IPCs into the beads, encapsulated IPCs were stained by live/dead cells technique. The dead cells were not risen until D47 of post-encapsulated days (Fig.4F). Here, the encapsulated IPCs were prolonged maturation. The IPC beads were conserved the expression of intracellular molecules and susceptible C-peptide/Insulin secretion that were requested of transplantable criteria.

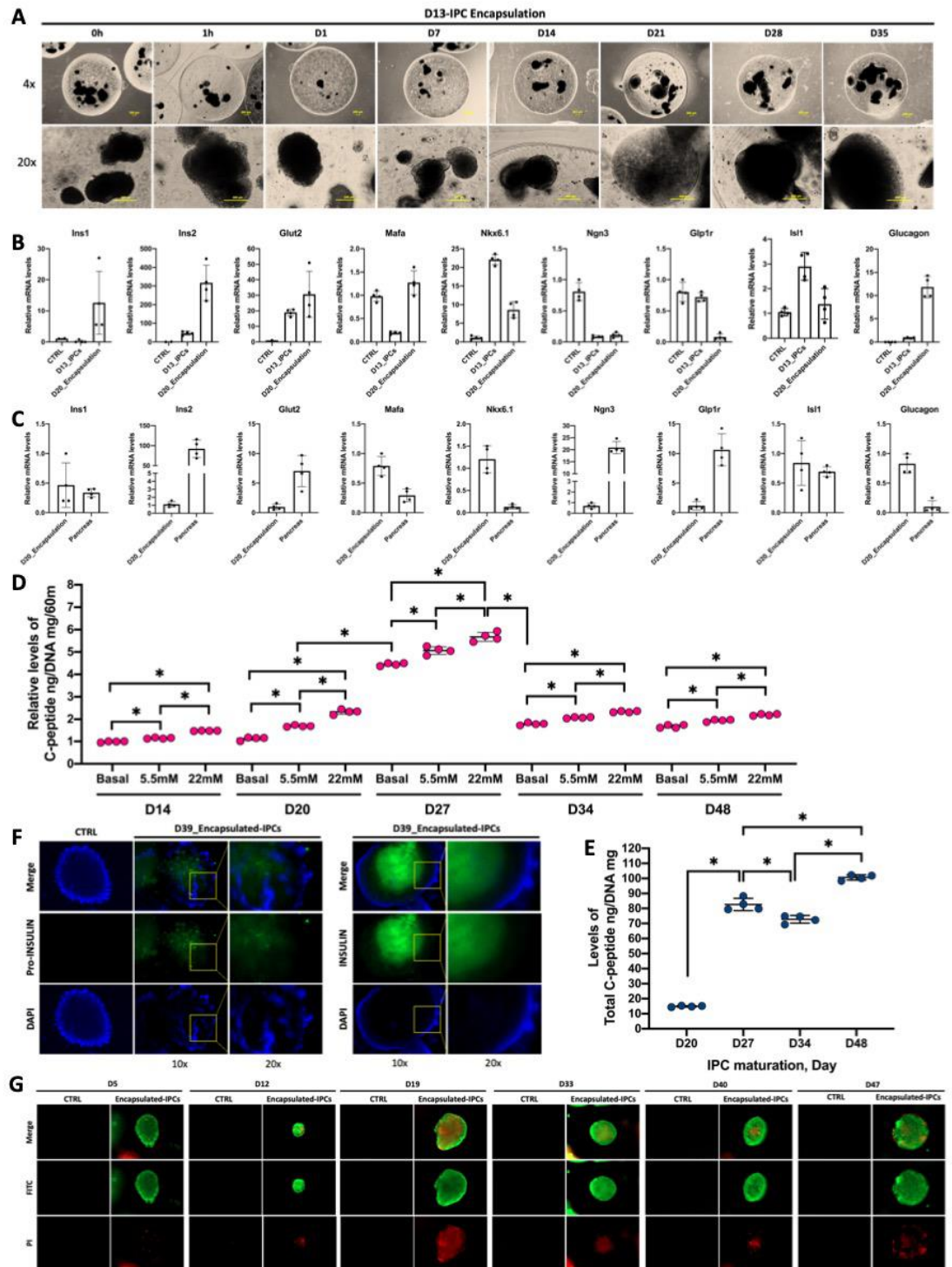


Figure 4 Encapsulated IPCs preserve the Insulin secretion capacity and transplanted potential



(A) At 13-day of IPC induction, matured IPCs were encapsulated by double layers of alginate/Pluronic-F127. Morphology of beads were checked at post-encapsulation of 1h, D1, D7, D14, D21, D31. (B) The mRNA levels of IPCs were maintained as the naked IPCs of protocol VII. (C) GSCS test was checked at D14, D20, D27, D34, D48. The IPCs were challenged with basal, 5.5 mM, 22 mM glucose concentration and then using the ELISA technique to detect the C-peptide secretion. The level of C-peptide releasing was calibrated on DNA concentration and 60 minutes of secreting timing. (D) The colonies were collected at D14, D20, D27, D34, D48 and dissolved them into dissolving buffer. The naked IPCs were sonicated into the protease-free solution; then, they were detected C-peptide and the levels of C-peptide releasing was calibrated on DNA concentration. DNA concentration was measured by QUBIT kit. (E) Matured IPCs were staining with pro-Insulin and Insulin antibodies with isotype as a control. (F) Matured IPCs were shown with the live/dead staining at D18, D25, D32, D46, D53, D60.

Magnification = 4x, 20x.

### **Establishment of transplantation platform for safe and efficient IPC installment**

To establish the subcutaneous pocket formation for delivering encapsulated cells, the animal experiments were conducted at CULAC following the ethics approval. This study with thirty-six (36) C57BL/6NJcl mice in total that was divided into two groups: i)

Tested group--18 mice and ii) Control (CTRL) group--18 mice. In tested groups and CTRL mice, the mice were also subcutaneously implanted with 18-G catheter at the back under generalized anesthesia using isoflurane (day -14) (with aseptic technique). After insertion, in tested group, the stylet was taken out; then, the sterile mixture of 250 ng/ml VEGF-165 + 10% Pluronic-F127 (VP) was injected through the catheter for space-retaining pocket. The subcutaneous pocket formation period was set up for 14 days. When subcutaneous pocket formation was set up (at day 0), the pocket was ready for the blank bead transplantation. Then, the skin was closed by suturing, and they were observed for 21 days (short-term study) and 42 days (long-term study) (Fig.5A). The body weight of CTRL and VEGF-165 + 10% Pluronic group were grown up for 9 weeks (Fig.5B). Fasting blood glucose level were variant in animal groups (Fig.5C). Otherwise, the completed blood count (CB), and blood chemistry (BC) parameter were standardly indicated in Table 1, and Table 2. The C-peptide level or relative C-peptide level was increased from day-0 to day-42 (Fig.5D, 5E). The function of pancreatic beta-cells was showed as HOMA-beta, which elevated the expression (Fig.5F). HOMA-IR or insulin resistance displayed the decreasing levels (Fig.5G). Besides, QUIKI or  $1/\log(\text{HOMA-IR})$  also displayed the opposite site of insulin resistance (Fig.5H). Intraperitoneal glucose tolerance test (IPGTT) was examined in both groups. The

pattern of fasting blood glucose levels was similar in CTRL and VEGF-165 + 10% Pluronic group (Fig.5I, 5J). Especially, in VEGF-165 + 10% Pluronic mice, number of blood vessels at subcutaneous pocket formation was improved after 2 weeks (Day-0) and significantly elevated at day-21 and day-42 (Fig.K, Fig.S5). The skin biopsy revealed distinguishing tubular foreign body or an 18-G catheter in deep dermal layer surrounding by hyperplastic fibroblastic cells. There were mild or moderate histiocytic cells, lymphocytes and occasionally macrophages were also displayed hyperplastic fibroblastic tissue, neutrophilic infiltration (Fig.L, Fig.S5). Furthermore, in CTRL group, the thick layer of connective tissues was around the catheter insertion; in whiles, in VEGF-165 + 10% Pluronic mice, adipose layer appearance and thin layer of connective tissues were surrounded subcutaneous pocket (Fig.L). Blood vessel network was generated at the boundary of subcutaneous pocket and invaded around the blank beads (Fig.L). Here, the blank beads were maintained in subcutaneous pocket until day-42. VEGF-165 + 10% Pluronic promoted angiogenesis and neovascularization, which may improve the health condition of mice.

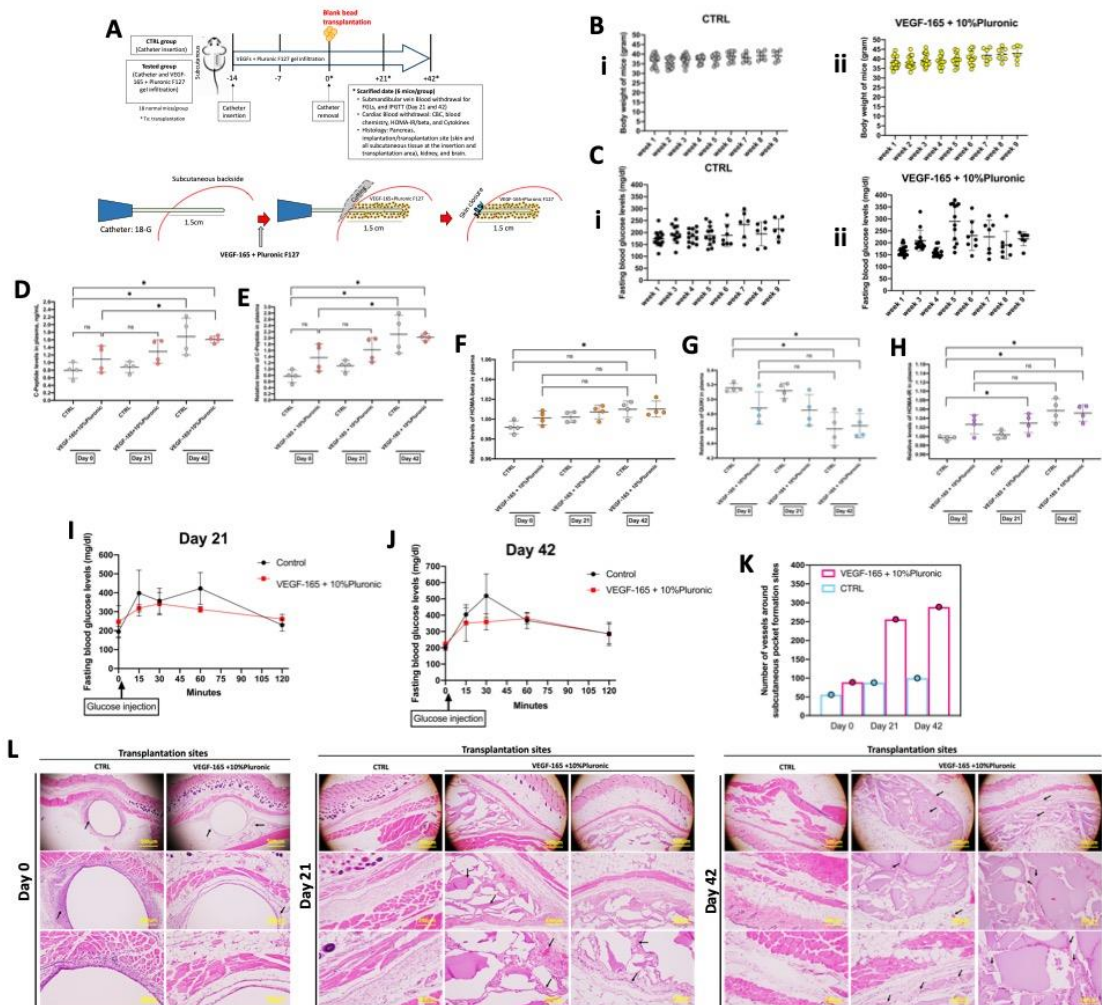


Figure 5 Establishment of transplantation platform for safe and efficient IPC

installment

(A) The scheme of subcutaneous pocket formation procedure. (B) The body weight of

all mice was measured by a digital weight machine, gram (g). (C) Fasting blood glucose

levels were checked by a glucose meter, dL/mg. (D), (E), (F), (G), (H) The C-peptide

levels, relative C-peptide levels, HOMA-beta, HOMA-IR, QUIKI indexes. (I), (J) The mice

were examined intraperitoneal glucose tolerance test (IPGTT) at day-21 and day-42. (K) Number of blood vessels were counted around subcutaneous pocket formation area in CTRL and VEGF-165 + 10% Pluronic mice. (L) The process of subcutaneous pocket post-transplantation from day-0 to day-42 was indicated via H&E staining.

**Table 1 Completed blood count parameters in CTRL and**

**VEGF-165+10%Pluronic mice**

**Table 2 Blood chemistry parameters in CTRL and VEGF-165+10%Pluronic mice**

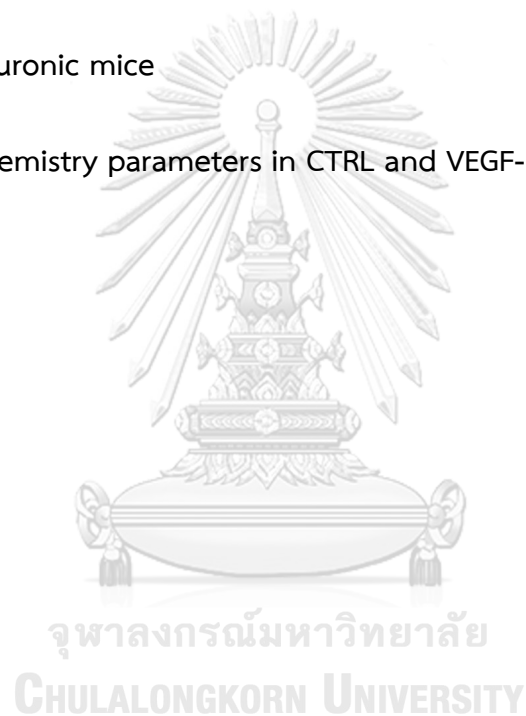


**Table 1.** Completed blood count (CBC) parameters were demonstrated in CTRL and VEGF-165 + 10%Pluronic mice during day 0, day 21, day 42 after 2-week catheter implantation and VEGF-165 + 10%Pluronic infiltration.

Parameter	Day 0		Day 21		Day 42		Ranges	Units
	CTRL (n=3)	VEGF-165 +10%Pluronic (n=3)	CTRL (n=3)	VEGF-165 +10%Pluronic (n=3)	CTRL (n=1)	VEGF-165 +10%Pluronic (n=1)		
<b>HB</b>	14.10 ± 0.643	12.70 ± 1.686	13.70 ± 0.987	14.40 ± 0.681	14.90	13.70	6.10 - 21.70	g/dL
<b>HCT</b>	50.20 ± 2.685	45.00 ± 6.322	49.40 ± 4.537	52.70 ± 3.721	53.40	48.90	16.70 - 69.80	%
<b>WBC animal count</b>	7.50 ± 1.957	6.10 ± 0.185	6.10 ± 0.606	7.10 ± 1.735	6.46	6.22	1.06 - 56.08	10 <sup>3</sup> *cell/μL
<b>RBC animal count</b>	9.60 ± 0.604	8.70 ± 1.089	9.30 ± 0.707	10.10 ± 0.627	10.05	9.92	3.57 - 15.2	10 <sup>6</sup> *cell/μL
<b>PMN</b>	3.00 ± 1.000	2.70 ± 0.577	3.00 ± 0.000	3.70 ± 0.577	2.00	10.00	4.27 - 18.48	%
<b>LYMPHOCYTE</b>	92.00 ± 1.000	91.30 ± 0.577	91.70 ± 0.577	88.30 ± 2.082	77.00	78.00	71.77 - 89.94	%
<b>MONOCYTE</b>	0.30 ± 0.577	0.70 ± 0.577	0.70 ± 0.577	1.00 ± 0.000	1.00	1.00	0.00 - 5.08	%
<b>EOSINOPHIL</b>	0.30 ± 0.577	0.00	0.00	0.70 ± 1.155	0.00	1.00	0.00 - 2.03	%
<b>BASOPHIL</b>	4.30 ± 0.577	5.30 ± 0.577	4.70 ± 0.577	6.30 ± 0.577	20.00	10.00	0.00 - 2.33	%
<b>RBC MORPHOLOGY</b>								
	<b>Normochromic/Normocytic</b>							
<b>MCV</b>	52.10 ± 0.896	51.60 ± 1.058	52.90 ± 1.193	52.20 ± 1.179	53.10	49.30	39.00 - 90.8	fL
<b>MCH</b>	14.60 ± 0.252	14.60 ± 0.231	14.70 ± 0.173	14.30 ± 0.300	14.80	13.80	12.6.0 - 31.00	pg
<b>MCHC</b>	28.00 ± 0.252	28.20 ± 0.200	27.80 ± 0.611	27.40 ± 0.651	27.90	28.00	27.00 - 37.60	g/dL
<b>BLOOD PARASITE</b>								
	<b>Not found</b>							
<b>PLATELET COUNT</b>	504.00 ± 45.738	238.30 ± 257.115	258.33 ± 22.85	315.00 ± 96.161	974.00	978.00	59.00 - 2633.00	10 <sup>3</sup> *cell/μL

HB: Hemoglobin; HCT: Hematocrit; WBC: White Blood Cells; PMNs: Polymorphonuclear leukocytes; RBC: Red Blood Cells; MCV: Mean Corpuscular Volume; MCH: Mean Corpuscular Hemoglobin; MCHC: Mean Corpuscular Hemoglobin Concentration.

**Table 2.** Blood Chemistry parameter were demonstrated in CTRL and VEGF-165 + 10%Pluronic mice during day 0, day 21, day 42 after 2-week catheter implantation and VEGF-165 + 10%Pluronic infiltration.

Parameter	Day 0		Day 21		Day 42		Ranges	Unit
	CTRL (n=3)	VEGF-165 +10%Pluronic (n=3)	CTRL (n=3)	VEGF-165 +10%Pluronic (n=3)	CTRL (n=3)	VEGF-165 +10%Pluronic (n=3)		
<b>ALB</b>	4.80 ± 0.173	4.60 ± 0.100	4.90 ± 0.153	4.30 ± 0.354	4.57 ± 0.321	4.367 ± 0.321	2.6-5.4	g/dL
<b>ALP</b>	62.30 ± 7.506	47.30 ± 11.930	33.70 ± 20.744	32.00 ± 12.728	42.00 ± 24.576	19.00 ± 5.568	16-200	U/L
<b>ALT</b>	40.00 ± 4.583	107.30 ± 60.715	58.70 ± 22.301	48.50 ± 6.364	253.70 ± 191.398	136.00 ± 104.312	22-133	U/L
<b>AMY</b>	994.00 ± 70.633	1442.70 ± 820.488	991.70 ± 52.205	900.00 ± 2.828	1587.00 ± 942.813	975.33 ± 44.015	608-2000	U/L
<b>TBIL</b>	0.30 ± 0.000	0.30 ± 0.058	0.20 ± 0.058	0.30 ± 0.071	0.28 ± 0.058	0.23 ± 0.058	0.1-0.9	mg/dL
<b>BUN</b>	19.70 ± 1.155	19.30 ± 1.528	18.00 ± 1.000	20.00 ± 0.000	26.00 ± 5.292	18.33 ± 3.215	2.0-71	mg/dL
<b>CA</b>	11.60 ± 0.586	11.50 ± 0.520	11.50 ± 0.451	10.50 ± 1.273	10.60 ± 2.343	10.07 ± 3.272	6.8-11.9	mg/dL
<b>PHOS</b>	18.20 ± 3.053	16.40 ± 2.411	9.00 ± 1.580	10.10 ± 0.354	14.13 ± 2.223	14.53 ± 2.055	6.0-11.3	mg/dL
<b>CRE</b>	0.30 ± 0.058	0.20 ± 0.058	0.20 ± 0.115	0.40 ± 0.071	0.43 ± 0.058	0.10 ± 0.100	0.1-1.8	mg/dL
<b>GLU</b>	142.70 ± 17.559	181.70 ± 26.388	278.00 ± 60.893	211.50 ± 38.891	288.67 ± 54.930	339.67 ± 44.072	114-279	mg/dL
<b>NA<sup>+</sup></b>	161.30 ± 4.163	161.30 ± 2.309	151.00 ± 2.646	144.50 ± 10.607	154.67 ± 3.055	154.00 ± 1.000	153-175	mmol/L
<b>K<sup>+</sup></b>	10.20 ± 1.234	10.50 ± 0.404	10.80 ± 0.451	10.50 ± 0.778	9.87 ± 1.305	9.70 ± 0.265	6.5-9.7	mmol/L
<b>Total Protein</b>	5.90 ± 0.173	5.70 ± 0.173	5.90 ± 0.252	5.30 ± 0.849	6.00 ± 0.265	5.80 ± 0.173	4.6-7.3	g/dL
<b>β-GLOB</b>	1.10 ± 0.000	1.10 ± 0.321	1.10 ± 0.115	1.10 ± 0.424	1.43 ± 0.306	1.43 ± 0.416	0.67-1.21	g/dL

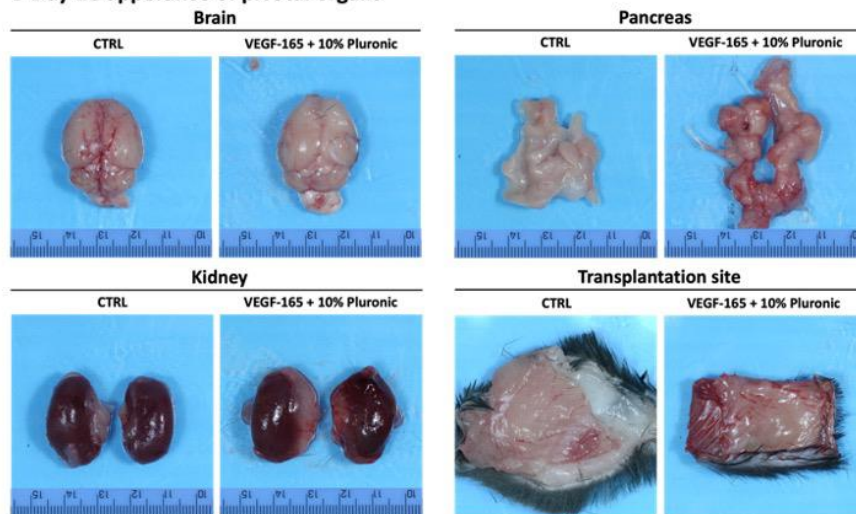
ALB: Albumin; ALP: Alkaline Phosphatase; ALT: Alanine aminotransferase; AMY: Amylase; TBIL: Total bilirubin; BUN: Blood urea nitrogen; CA: Calcium; PHOS: Phosphorus; CRE: Creatinine; GLU: Glucose; NA<sup>+</sup>: Sodium, K<sup>+</sup>: Potassium; TP: Total protein; β-GLOB: beta Globulin.



### A Day-21 subcutaneous bead apperance



### B Day-21 apperance of pivotal organs



### C Day-42 apperance of pivotal organs

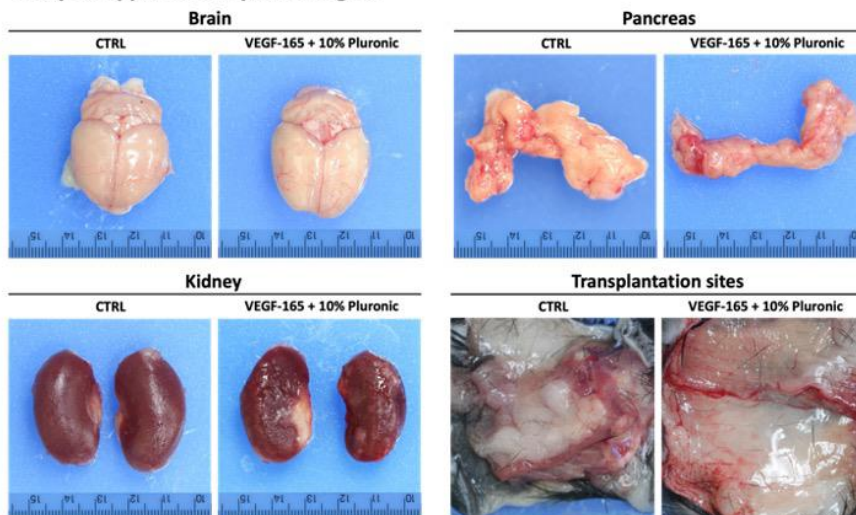


Figure S5 Gross apperance of mice undergone subcutaneous pocket formation and blank bead transplantaion. (A), (B), (C) Organ collection were compare between CTRL and VEGF-165+10%Pluronic mice at day-21.



## Global exploration of cytokine network in mice receiving blank bead

### transplantation

To dissect the inflammatory response during transplantation, normal CTRL mice and VEGF-165 + 10% Pluronic mice were detected 40 cytokine proteins in plasma via inflammation antibodies array. The dot dots were matched with manufactory array map; then, the array was analyzed the heat dots and intensity by ImageJ. The intensity was calculated by formula ( $X = (X(y)\text{-negative}) * P1/P(y)$ ) following the manufactory provide (Fig.6A and Fig.S10). Heat map was generated basing on relative intensity using a R software, which demonstrated 40 cytokine detections in both groups. There was quite similar inflammatory reaction with foreign factors in CTRL and VEGF-165 + 10% Pluronic. The 40 cytokines were consisted of chemokines, interleukins and others functioning inflammatory modulation. However, tumor necrosis factor receptor II (sTNF-RII) was extremely high at day-42 in CTRL mice (Fig.6B). In the results, the sTNF-RII was strong active pro-inflammation and anti-inflammation during blank bead transplantation. VEGF-165 + 10% Pluronic (VP) might mitigate the autoimmune response prolonging 42-day post-transplantation. The blank bead engraftment in VP mice was not rejected by autoimmune aggression without supplying the anti-rejected drugs.

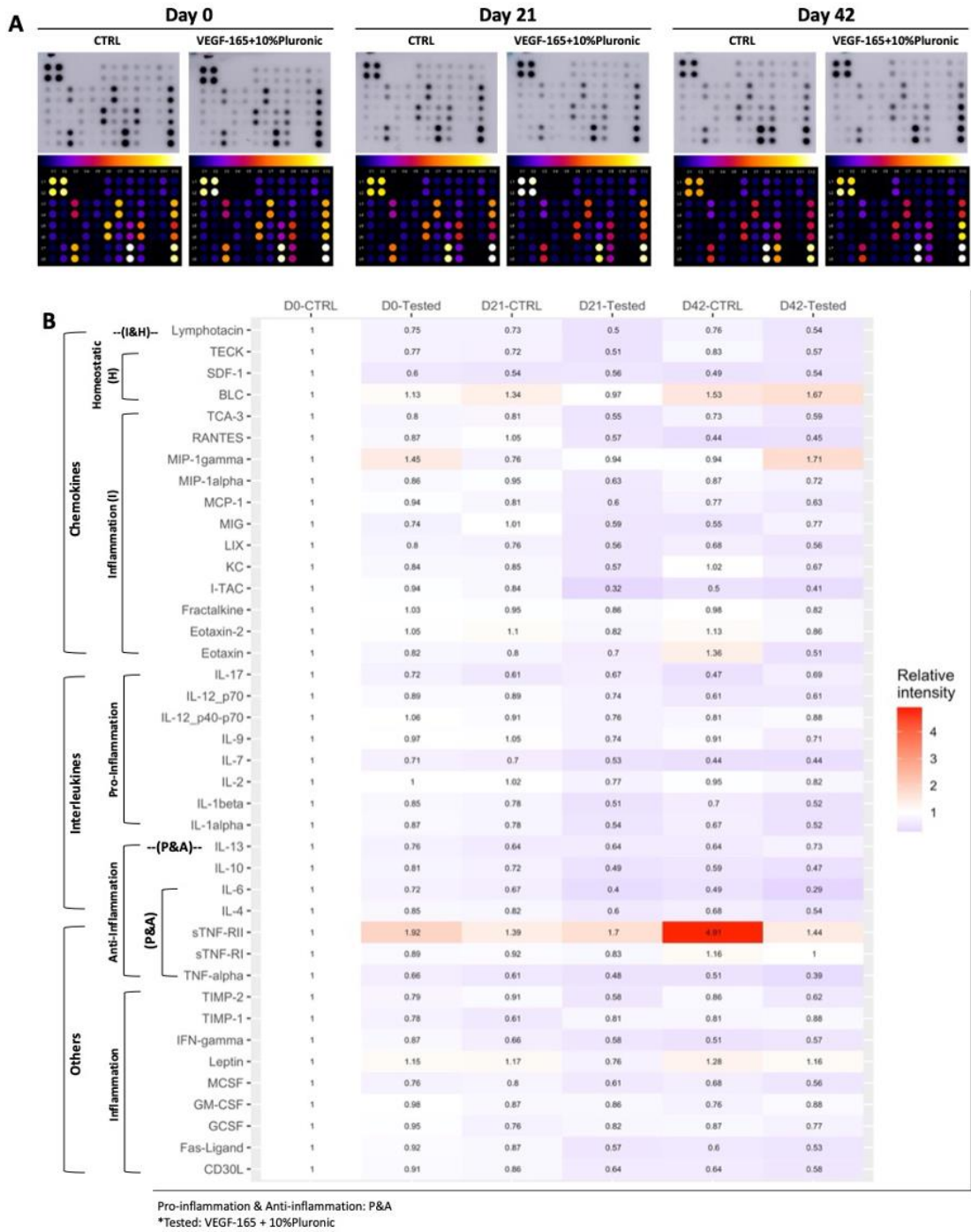


Figure 6 Global exploration of cytokine network in mice receiving blank bead transplantation

(A) The cytokine arrays were detected in CTRL and VEGF-165 + 10% Pluronic mice from day-0 to day-42. Then, the heat map of clot dots and intensity were generated by an ImageJ software. (B) Basing on the intensity of clot dots, 40 cytokines were expressed via a heat map using a R software. This cytokine array was an inflammation panel consisting of interleukins, chemokines, and others which contributed to dynamic stimulation in autoimmune response.

Abbreviations; BLC: B lymphocyte chemoattractant, GCSF: granulocyte colony-stimulating factor, GM-CSF: granulocyte-macrophage colony-stimulating factor, IFN: interferon, IL: interleukin, I-TAC: interferon-inducible T-cell alpha chemoattractant, CXC: Chemokine, KC: Keratinocyte chemoattractant (chemokine ligand 1), LIX: lipopolysaccharide-induced chemokine, MCP: monocyte chemoattractant protein, MCSF: macrophage colony-stimulating factor, MIG: monokine induced by gamma interferon, MIP: macrophage inflammatory protein, RANTES: Regulated on activation, normal T-cell expressed and secreted, SDF: stromal cell-derived factor, TCA: T-cell activation gene, TECK: thymus expressed chemokine, TIMP: Tissue inhibitor of metalloproteinase, TNF(R): tumor necrosis factor (receptor), CD30L: CD30 ligand (a member of TNF superfamily), Pos: Positive spot, Neg: negative spot.

### The transplantation platform shows no effect on insulin-dependent tissues

To prove histopathological insulin-dependent tissues during subcutaneous pocket formation and post-transplantation, the organs including pancreas, brain, kidney, muscle, and fat were stained hemoxilyn and eosin (H&E) at day-0, day-21, and day-42 (Fig.7A, 7B, 7C, 7D, 7F). The pancreatic islets were well performed with big size in both CTRL and 250 ng/ml VEGF-165 + 10% Pluronic-F127 (VP) group (Fig.7A). Hippocampus is a specific area for controlling neuroendocrine; however, led to hippocampal neurogenesis degradation in diabetes patients (Ho et al. 2013). The staining of hippocampus was normally shown from day-0 to day -42 in all animals (Fig.7B). Diabetic nephropathy was significantly severe complication of chronic kidney disease and globally renal failure at end-stage (Gross et al. 2005; Lim 2014). Less muscle mass associated with provoker diabetes prevalence and insulin resistance (Hong et al. 2017; Haines et al. 2022). In obese people, they are commonly considered a diabetes disease, then leading diabetes-related and obesity-related complications (Van der Schueren et al. 2021). In histopathological muscle, there were well construction and distribution in all mice (Fig.7D). Especially, the adipose cells were surrounded by thick wall of hyperplastic fibroblastic tissues. They were also invaded blood vessel generation in VP mice at day-21, day-42 (Fig.7F).

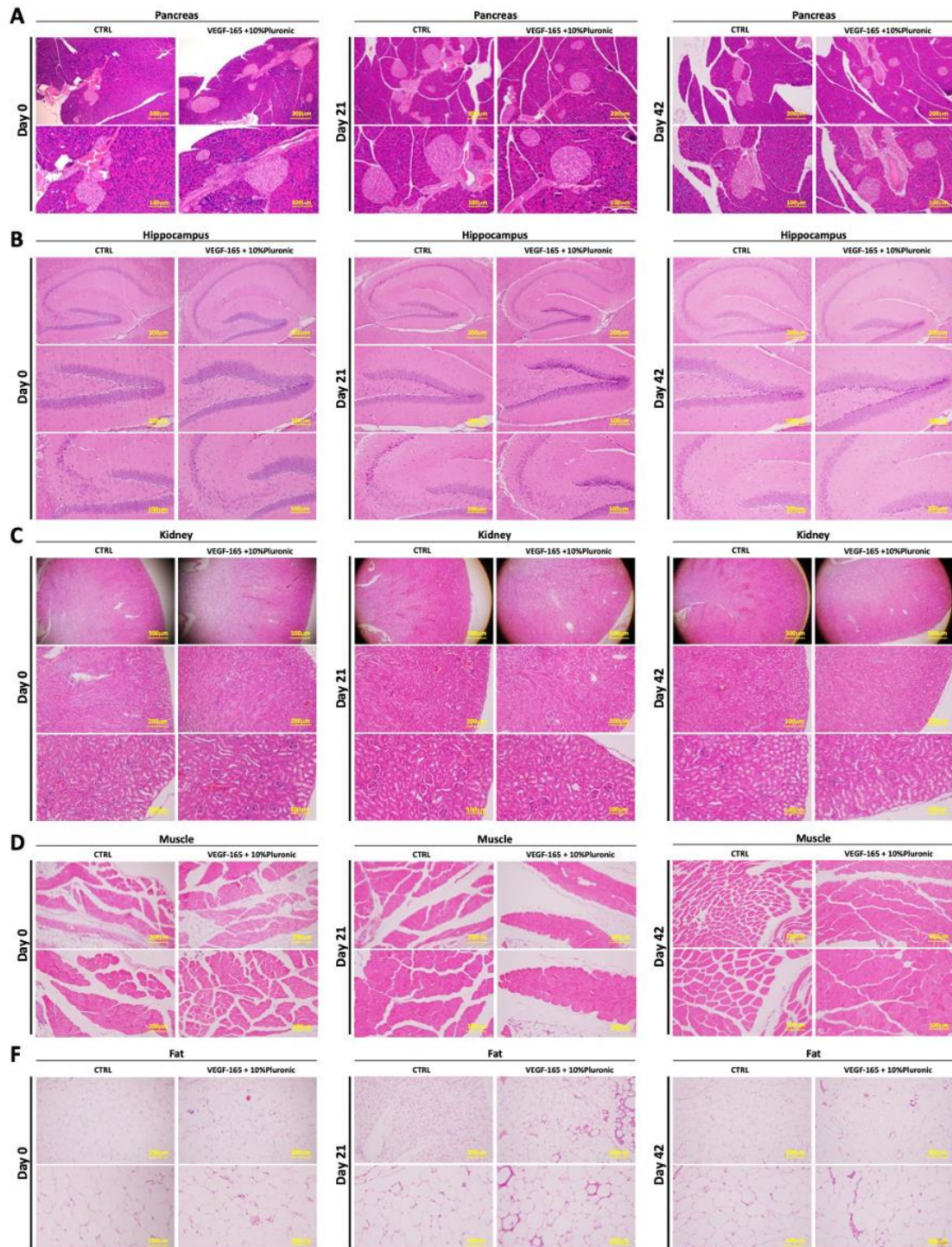


Figure 7 The mixture of 250 ng/ml VEGF-165 + 10% Pluronic-F127 normally reacted in histopathological insulin-dependent tissues

(A), (B), (C), (D), (E) Pancreas, Hippocampus, Kidney, Muscle, and Fat were stained H&E at day-0, day-21, day 42 in CTRL and VEGF-165 + 10% Pluronic mice.

### **Subcutaneous IPC-bead transplantation alleviates hyperglycemic condition and sustains survival rate in STZ-induced diabetic mice**

To study anti-diabetic property of encapsulated mouse induced pluripotent stem cell-derived insulin-producing cells (miPSC-IPCs) in type 1 diabetes mouse model, all animals were induced type 1 diabetes (T1D) by single high-dose streptozotocin (STZ) injection. The STZ-induced diabetic mice (DM) were divided into two study groups consist of i) STZ-induced-diabetic VEGF-165+10%Pluronic mice + IPC-bead transplantation mice (DM-VP + IPC-bead Tx) and ii) STZ-induced-diabetic VEGF-165+10%Pluronic mice + blank bead transplantation (DM-VP + Blank bead Tx). IPC encapsulation or IPC-bead were generated following the protocol VIII description. Otherwise, IPC-beads and blank beads were produced at the same time and equivalent manipulation, which were transplanted to DM-VP + IPC-bead Tx mice or DM-VP + Blank bead Tx mice. Consequently, they were monitored for 21-day and 42-day (Fig.8A). The C-peptide, relative C-peptide levels, and HOMA-beta in plasma were properly eliminated by STZ-treated, where insulin resistance oriented to increase (Fig.8D). However, the level of pancreatic C-peptide was maintained during IPC-bead

post-transplantation (Fig.8D). After STZ injection, all mice were lost the body weight. In DM-VP + IPC-bead Tx mice, they can gain weigh during subcutaneous pocket formation and IPC-bead transplantation duration (Fig.8B). In CBC, and BC parameters, IPC-bead have toward the DM-VP mice that gradually turning to conventional indexes (Table 3, Table 4). In IPGTT, DM-VP + IPC-bead Tx mice well responded with glucose stimulation at day-14 post-transplantation (Fig.8E). Remarkably, IPC-beads alleviated hyperglycemia, health condition and elongating survival in DM-VP mice (Fig.8C, 8E, 8F). The insulin protein was detected in day-21 and day-42 (Fig.8G, 8K). The subcutaneous pocket formation and IPC-bead or blank bead transplantation at transplantation sites were proved angiogenesis and neovascularization surrounding pocket space with CD31+ marker staining (Fig.8L, Fig.S7). Here, VEGF-165 + 10% Pluronic assisted subcutaneous pocket formation and the blood vessel generation in T1D mice. Insulin-producing cell secretion lengthened the survival of T1D mice. Remarkably, pancreatic beta-cell residue was preserved in DM-VP mice until day-42.



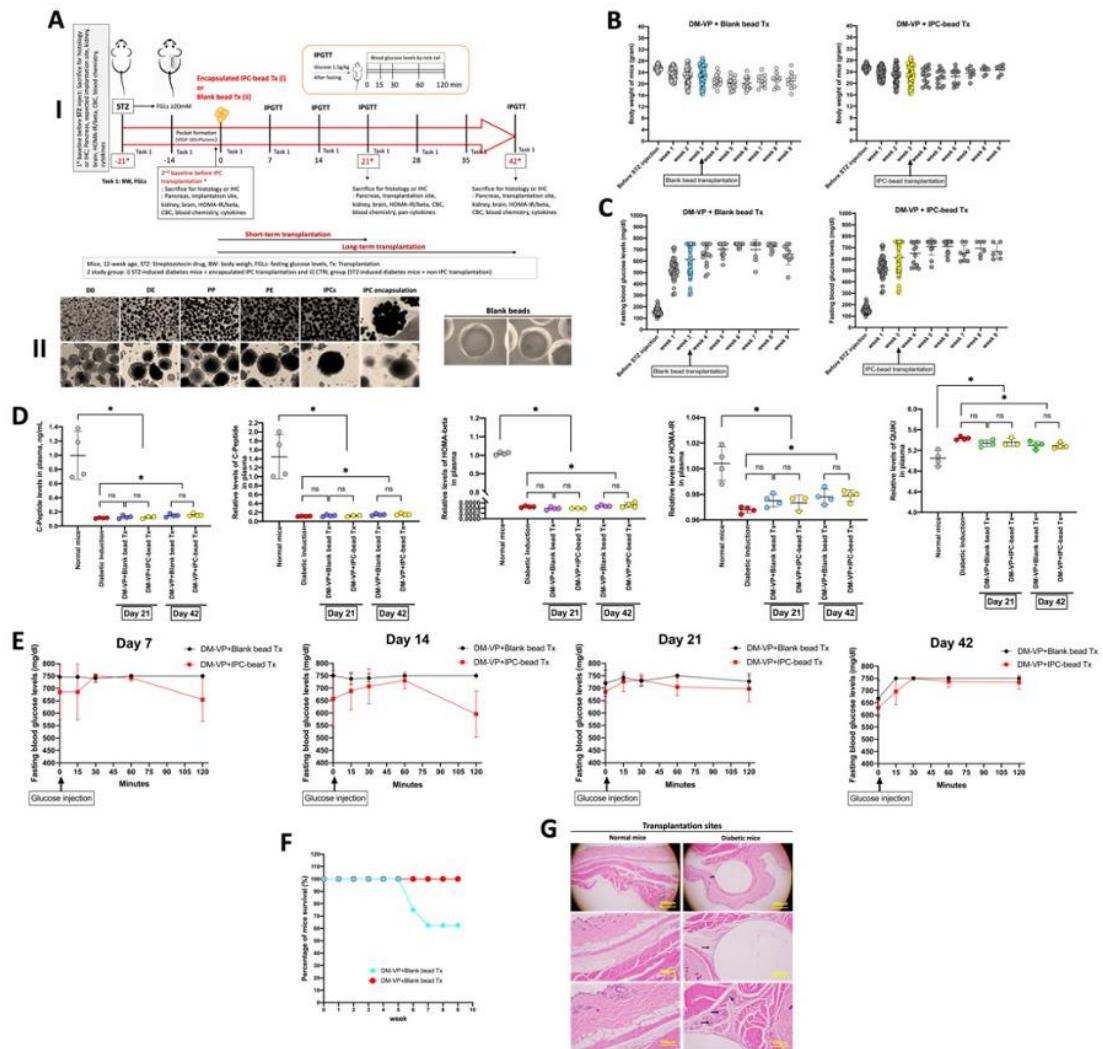


Figure 8 Subcutaneous IPC-bead transplantation alleviates hyperglycemic condition and sustains survival rate in STZ-induced diabetic mice

(A) Scheme of IPC-bead transplantation procedure. (B) The body weight of all mice was measured by a digital weight machine, gram (g). (C) Fasting blood glucose levels were checked by a glucose meter, dL/mg. (D) The C-peptide levels, relative C-peptide levels, HOMA-beta, HOMA-IR, QUKI indexes. (E) The mice were examined the



sensitivity of subcutaneous IPC-bead transplantation by intraperitoneal glucose tolerance test (IPGTT) at day-7, day-14, day-21, and day-42. (F) The survival mice were measured in DM-VP + Blank bead Tx, and DM-VP + IPC-bead Tx mice during subcutaneous pocket formation until post-transplantation. (G) The staining of transplantation sites.

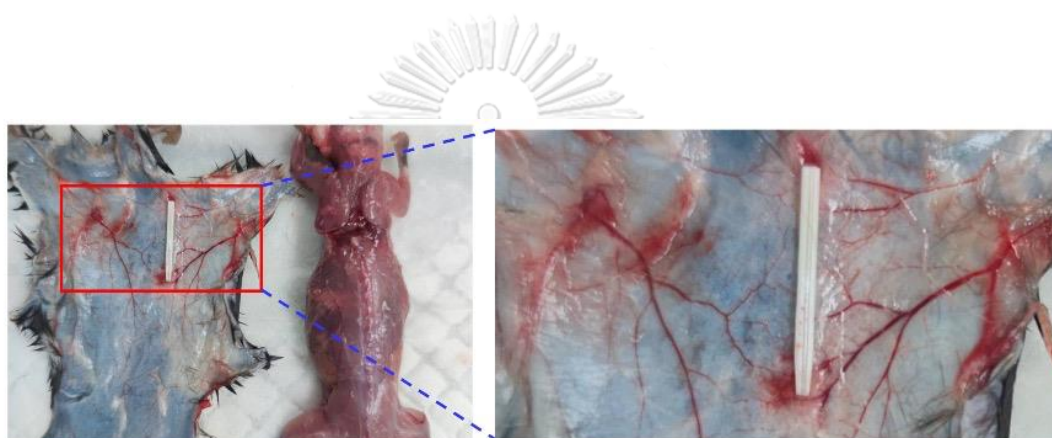


Figure S6 Blood vessel generation at the subcutaneous pocket formation site.

After 2 weeks, VEGF-165 stimulated the angiogenesis around the implantation site comparing with the other areas. It was implied that VEGF-165 showed the retention time into 10%Pluronic-127 gel at subcutaneous pocket formation site.

Table 3 Completed blood count parameters in DM-VP + Blank bead Tx and DM-VP + IPC-bead Tx mice

Table 4 Blood chemistry parameters in DM-VP + Blank bead Tx and DM-VP + IPC-bead Tx mice

**Table 3.** Completed blood count (CBC) parameters were demonstrated in normal mice at day -21, and DM + VEGF-165+10%Pluronic (DM-VP) mice after 1-week STZ-induction and 2-week catheter implantation with VEGF-165 + 10%Pluronic infiltration at day 0. The mice of DM-VP + Blank bead Tx, and DM-VP + IPCs-bead Tx mice were compared the CBC parameters at day 21 and day 42.

Parameter	Day -21	Day 0	Day 21		Day 42		Ranges	Unit
	Normal mice (n=5)	DM + VEGF-165+ 10%Pluronic (DM-VP) (n=5)	DM-VP + Blank bead Tx (CTRL), (n=3)	DM-VP + IPC-bead Tx (n=3)	DM-VP + Blank bead Tx (CTRL)	DM-VP + IPC-bead Tx		
<b>HB</b>	14.40 ± 1.564	13.63 ± 1.363	13.90 ± 0.755	15.67 ± 0.231	15.73 ± 0.252	16.07 ± 0.666	2.6-5.4	g/dL
<b>HCT</b>	46.40 ± 6.865	47.98 ± 5.279	41.70 ± 2.265	51.30 ± 5.910	52.33 ± 6.568	51.10 ± 1.308	16-200	U/L
<b>WBC animal count</b>	9.30 ± 3.436	6.35 ± 0.861	6.00 ± 0.000	6.16 ± 0.283	7.66 ± 2.244	6.77 ± 0.893	22-133	U/L
<b>RBC animal count</b>	9.60 ± 0.926	9.00 ± 0.919	10.08 ± 0.546	10.98 ± 0.101	11.27 ± 0.087	11.39 ± 0.618	608-1200	U/L
<b>PMN</b>	5.40 ± 1.517	29.50 ± 25.130	10.00 ± 5.000	8.67 ± 3.512	41.67 ± 19.655	26.33 ± 2.887	0.1-0.9	mg/dL
<b>LYMPHOCYTE</b>	90.40 ± 1.517	64.33 ± 23.872	57.33 ± 14.742	53.00 ± 15.875	46.00 ± 21.166	69.33 ± 7.024	2.0-71	mg/dL
<b>MONOCYTE</b>	0.40 ± 0.548	5.33 ± 8.710	7.67 ± 6.429	5.67 ± 1.528	1.67 ± 1.155	3.00 ± 3.464	6.8-11.9	mg/dL
<b>EOSINOPHIL</b>	0.00	0.00	0.00	0.67 ± 1.155	0.00 ± 0.000	0.67 ± 1.155	6.0-11.3	mg/dL
<b>BASOPHIL</b>	3.80 ± 2.490	0.83 ± 1.169	25.00 ± 10.149	32.00 ± 12.166	10.67 ± 2.082	0.67 ± 0.577	0.1-1.8	mg/dL
<b>RBC MORPHOLOGY</b>				<b>Normochromic/Normocytic</b>				
<b>MCV</b>	48.20 ± 3.865	53.32 ± 0.760	38.03 ± 6.012	46.73 ± 5.341	44.57 ± 2.542	45.00 ± 3.724	153-175	fmo/L
<b>MCH</b>	15.00 ± 0.381	15.17 ± 0.463	13.77 ± 0.115	14.27 ± 0.252	13.97 ± 0.231	14.10 ± 0.173	6.5-9.7	fmo/L
<b>MCHC</b>	31.30 ± 1.741	28.47 ± 1.271	25.13 ± 0.208	28.87 ± 3.272	32.63 ± 0.058	31.50 ± 2.078	4.6-7.3	g/dL
<b>BLOOD PARASITE</b>				<b>Not found</b>				
<b>PLATELET COUNT</b>	464.00 ± 362.724	728.67 ± 265.340	950.00 ± 77.660	798.00 ± 240.576	936.53 ± 54.669	665.67 ± 428.724	59.00 – 2633.00	10 <sup>3</sup> *cell/μL

HB: Hemoglobin; HCT: Hematocrit; WBC: White Blood Cells; PMNs: Polymorphonuclear leukocytes; RBC: Red Blood Cells; MCV: Mean Corpuscular Volume; MCH: Mean Corpuscular Hemoglobin; MCHC: Mean Corpuscular Hemoglobin Concentration.

**Table 4.** Blood Chemistry parameter were demonstrated in normal mice at day -21, and DM + VEGF-165+10%Pluronic (DM-VP) mice after 1-week STZ-induction and 2-week catheter implantation with VEGF-165 + 10%Pluronic infiltration at day 0. The mice of DM-VP + Blank bead Tx, and DM-VP + IPCs-bead Tx mice were compared the CBC parameters at day 21 and day 42.

Parameter	Day -21		Day 0		Day 21		Day 42		Ranges	Unit
	Normal mice (n=5)	DM + VEGF-165+10%Pluronic (DM-VP) (n=5)	DM-VP + Blank bead Tx (CTRL), (n=3)	DM-VP + IPC-bead Tx (n=3)	DM-VP + Blank bead Tx (CTRL), (n=3)	DM-VP + IPC-bead Tx (n=3)	DM-VP + Blank bead Tx (CTRL), (n=3)	DM-VP + IPC-bead Tx (n=3)		
ALB	4.80 ± 0.342	3.22 ± 0.259	3.17 ± 0.586	3.63 ± 0.153	4.03 ± 0.208	3.87 ± 0.153	4.03 ± 0.208	3.87 ± 0.153	2.6-5.4	g/dL
ALP	54.00 ± 12.349	126.60 ± 50.693	127.33 ± 8.386	83.33 ± 72.176	136.33 ± 17.786	133.67 ± 13.051	136.33 ± 17.786	133.67 ± 13.051	16-200	U/L
ALT	98.20 ± 32.337	141.00 ± 28.700	790.33 ± 670.709	139.00 ± 66.189	149.00 ± 70.739	106.00 ± 8.000	149.00 ± 70.739	106.00 ± 8.000	22-133	U/L
AMY	1010.20 ± 253.820	820.00 ± 193.808	626.33 ± 214.311	896.33 ± 308.234	737.00 ± 61.147	1131.33 ± 488.848	737.00 ± 61.147	1131.33 ± 488.848	608-1200	U/L
TBIL	0.20 ± 0.055	0.36 ± 0.251	0.33 ± 0.06	0.33 ± 0.058	0.30 ± 0.000	0.30 ± 0.000	0.30 ± 0.000	0.30 ± 0.000	0.1-0.9	mg/dL
BUN	19.60 ± 1.817	52.20 ± 17.370	68.33 ± 26.312	42.00 ± 13.856	27.67 ± 8.021	37.67 ± 8.505	27.67 ± 8.021	37.67 ± 8.505	2.0-71	mg/dL
CA	12.00 ± 0.400	10.98 ± 0.589	10.47 ± 0.416	7.90 ± 4.678	11.67 ± 0.208	11.00 ± 0.173	11.67 ± 0.208	11.00 ± 0.173	6.8-11.9	mg/dL
PHOS	11.80 ± 1.818	16.60 ± 9.673	12.40 ± 0.400	11.47 ± 1.815	13.80 ± 2.193	11.50 ± 1.473	13.80 ± 2.193	11.50 ± 1.473	6.0-11.3	mg/dL
CRE	0.00 ± 0.045	0.16 ± 0.251	0.17 ± 0.153	0.23 ± 0.208	0.07 ± 0.058	0.27 ± 0.462	0.07 ± 0.058	0.27 ± 0.462	0.1-1.8	mg/dL
GLU	261.60 ± 50.058	929.00 ± 61.278	973.67 ± 45.611	952.00 ± 78.000	631.33 ± 31.390	786.00 ± 103.523	631.33 ± 31.390	786.00 ± 103.523	114-279	mg/dL
NA+	157.40 ± 3.050	154.40 ± 3.435	151.00 ± 4.000	153.00 ± 4.359	151.00 ± 1.000	146.67 ± 1.528	151.00 ± 1.000	146.67 ± 1.528	153-175	mmol/L
K+	9.00 ± 0.923	9.86 ± 2.519	9.97 ± 0.651	8.40 ± 4.851	10.90 ± 0.100	10.23 ± 1.159	10.90 ± 0.100	10.23 ± 1.159	6.5-9.7	mmol/L
TP	6.00 ± 0.295	4.28 ± 0.466	4.47 ± 0.416	4.53 ± 0.208	5.23 ± 0.306	5.13 ± 0.115	5.23 ± 0.306	5.13 ± 0.115	4.6-7.3	g/dL
β-GLOB	1.20 ± 0.195	1.10 ± 0.316	1.30 ± 0.755	0.90 ± 0.100	1.23 ± 0.115	1.27 ± 0.058	1.23 ± 0.115	1.27 ± 0.058	0.67-1.21	g/dL

ALB: Albumin; ALP: Alkaline Phosphatase; ALT: Alanine aminotransferase; AMY: Amylase; TBIL: Total bilirubin; BUN: Blood urea nitrogen; CA: Calcium; PHOS: Phosphorus; CRE: Creatinine; GLU: Glucose; NA+: Sodium, K+: Potassium; TP: Total protein; β-GLOB: beta Globulin.

### Subcutaneous IPC-bead engraftment shows no immune response in post-transplantation

To elucidate the reaction between immune destruction and IPC-bead engraftment during transplanted time, 40 cytokines were expressed in plasma using antibody array in normal mice, diabetes mice, DM-VP + Blank bead Tx mice, and DM-VP + IPC-bead Tx mice (Fig.9A). In normal mice, all 40 cytokines were manifested the different levels in plasma, which served as a control. STZ-induced diabetic mice were indicated the highest inflammatory expression of granulocyte colony-stimulating factor (GCSF); then, B lymphocyte chemoattractant (BLC or CXCL13), macrophage inflammatory protein (MIP)-1gamma, Keratinocyte chemoattractant (KC or CXCL1/2), and the list of interleukins (IL-17, IL-12 p70, IL-12 p40/p70, IL9, IL-7, IL-2, IL-1alpha, IL-1beta, IL-13) were significantly expressed (Fig.9B). Continuously, at day-21, day-42, the inflammation reactivity was distinctly dynamic expression in both DM-VP + Blank bead Tx mice, and DM-VP + IPC-bead Tx mice (Fig.9B). It might show no immune response at subcutaneous IPC-bead engraftment during post-transplantation.

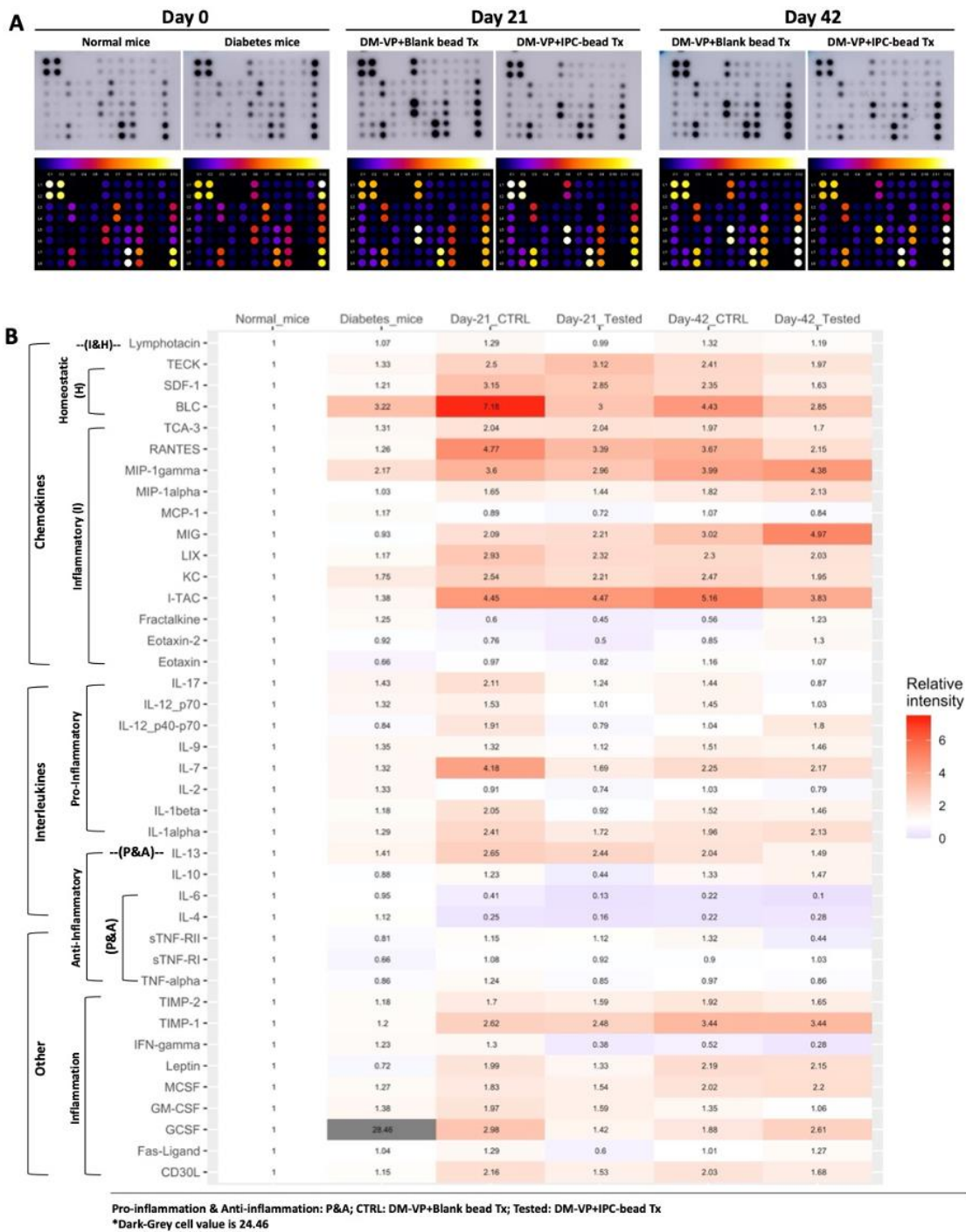


Figure 9 Subcutaneous IPC-bead engraftment shows no immune response in post-transplantation

(A) The cytokine arrays were detected in normal mice, diabetic mice, DM-VP + Blank bead Tx mice, and DM-VP + IPC-bead Tx mice at baseline, day-21, and day-42. Then, the heat map of clot dots and intensity were generated by an ImageJ software. (B) Basing on the intensity of clot dots, 40 cytokines were expressed via a heat map using a R software. This cytokine array was an inflammation panel consisting of interleukins, chemokines, and others which contributed to dynamic stimulation in autoimmune response.

Abbreviations; BLC: B lymphocyte chemoattractant, GCSF: granulocyte colony-stimulating factor, GM-CSF: granulocyte-macrophage colony-stimulating factor, IFN: interferon, IL: interleukin, I-TAC: interferon-inducible T-cell alpha chemoattractant, CXC: Chemokine, KC: Keratinocyte chemoattractant (chemokine ligand 1), LIX: lipopolysaccharide-induced chemokine, MCP: monocyte chemoattractant protein, MCSF: macrophage colony-stimulating factor, MIG: monokine induced by gamma interferon, MIP: macrophage inflammatory protein, RANTES: Regulated on activation, normal T-cell expressed and secreted, SDF: stromal cell-derived factor, TCA: T-cell activation gene, TECK: thymus expressed chemokine, TIMP: Tissue inhibitor of metalloproteinase, TNF(R): tumor necrosis factor (receptor), CD30L: CD30 ligand (a member of TNF superfamily), Pos: Positive spot, Neg: negative spot.



### Recovery pathogenesis of insulin-dependent tissues in IPC-bead mice

In diabetes mice, the pancreatic islets were severe atrophic. The blood vessels in interstitial space were replaced to connective tissues, where was located in islet complex destruction. Moreover, the acinar cells were degeneration due to dark and small pyknotic nucleus (Fig.10A). Kidney tissues were mild damaged in cortex and medulla. The epithelial cells of tubulous were erosion in diabetic nephropathy mice (Fig.10B). The granule cells were severe necrosis with pyknotic nucleus at CA3 area in hippocampus (Fig.10C). Degeneration of muscles was found in diabetic mice, which created large space between muscle cells (Fig.10D). The adipose cells were smaller and thinner layer (Fig.10E).

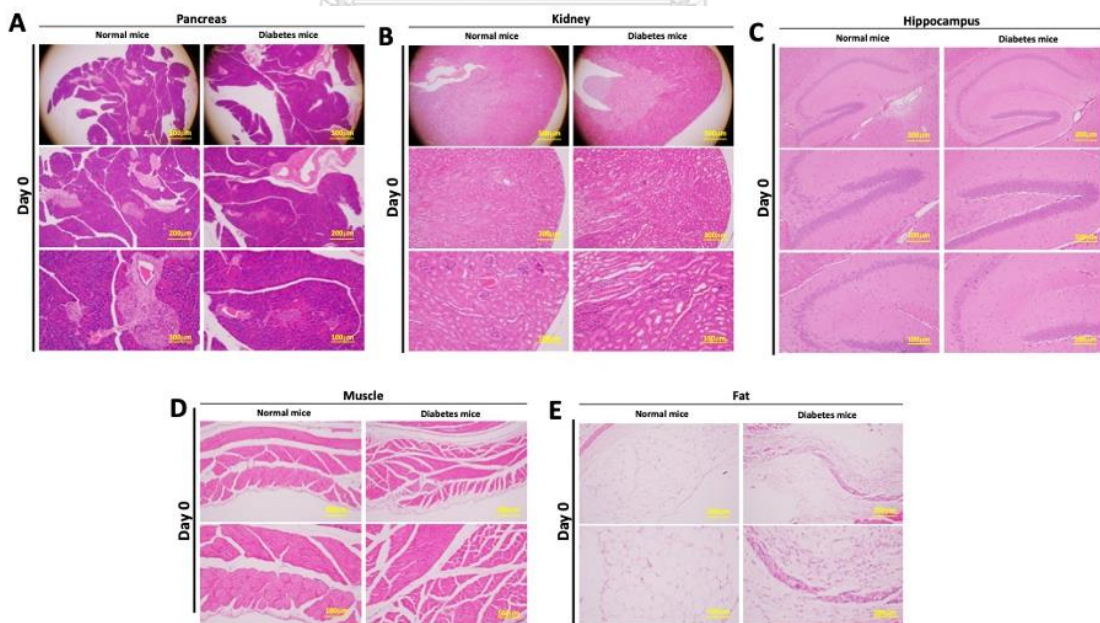


Figure 10 Insulin-dependent tissues were performed via H&E staining

(A), (B), (C), (D), (E) Pancreas, Hippocampus, Kidney, Muscle, and Fat were stained H&E

in normal mice and diabetic mice.





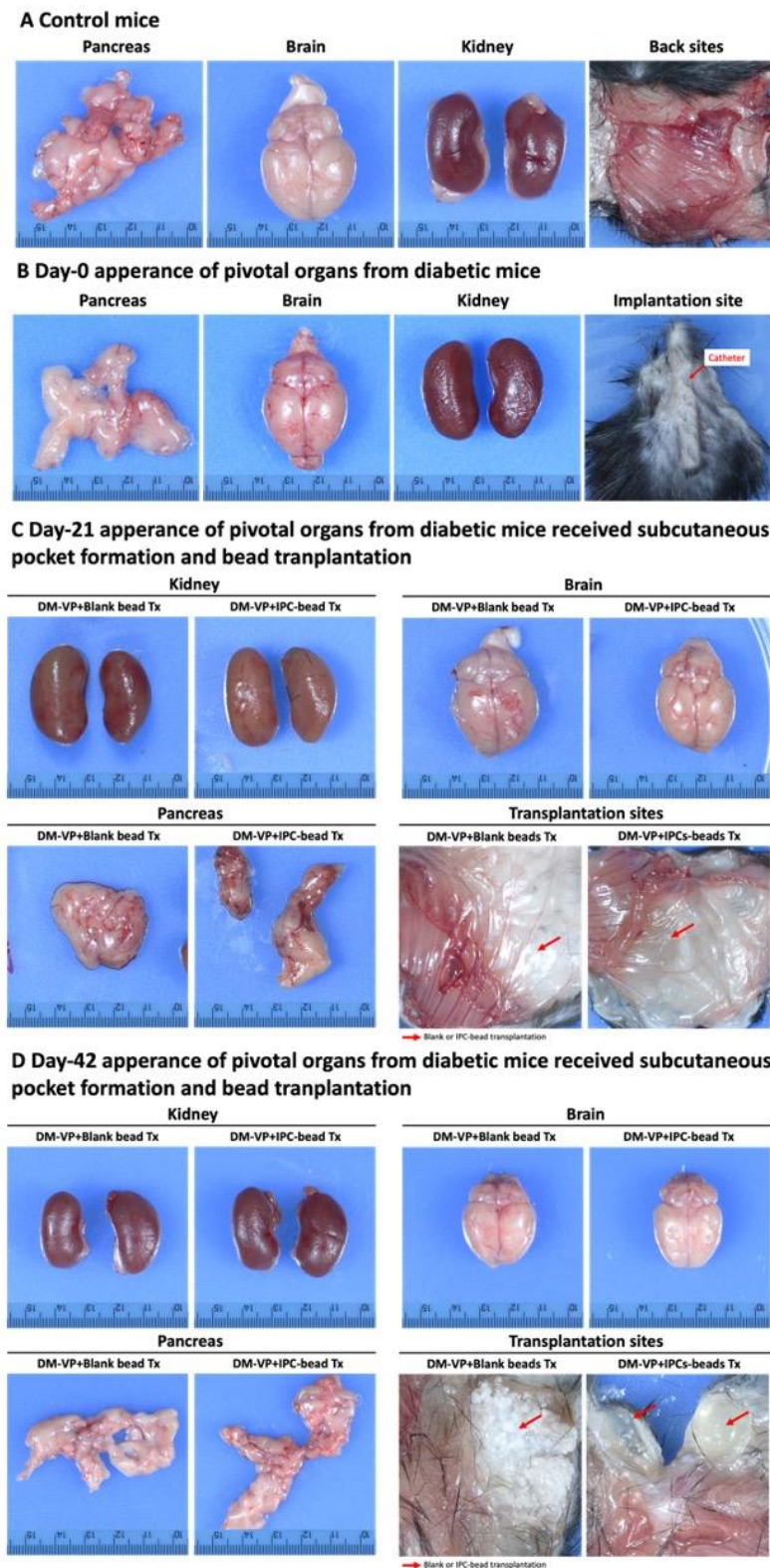


Figure S7 Gross appearance of diabetic mice undergone subcutaneous pocket formation and IPC-bead transplantation

## DISCUSSION

Insulin is a critical metabolism regulator, which is produced in pancreatic beta-cell and a major self-antigen in T1D insulin-based immunotherapies (Roep and Peakman 2012). Pancreatic beta-cell dysfunction promotes in pathogenesis of diabetes diseases (Fu et al. 2013). In diabetes treatment, the strategy of Insulin-producing cells (IPCs) transplantation was fashionably applied (Srivastava and Kilian 2019). To generate the high effective IPCs, in protocol VIII, the EBs were formed in Sterilin™ Petri Dish which were nice shape and parameter (Fig.S1). Here, they had the potential of IPC differentiation and survival in the long-term (Fig.1). Expectedly, IPCs showed the high level of endogenous Pro-insulin, Insulin expression (Fig.2J). Our data indicated a remarkable developing of IPCs from early IPCs (11-day), IPCs (13-day) to matured IPC evaluation (20-day) checking by the glucose stimulation Insulin/C-peptide secretion test (Fig.2H). Even though total Insulin protein expression was a low level at day-20 and highest level at day-34. In whiles, the mRNA levels of IPC markers (Insulin 1, Insulin 2, IIs1, Mafa, Glp1r, Glut2, Nkx6.1, and glucagon) were decreasing from day-27 to day-48. Especially, Insulin 1 and Insulin 2 mRNA levels were different expression in IPC colonies during IPC development. Remarkably, mRNA of Insulin 1 was high level at day-20 and day-27, which can compare with mouse pancreas (Fig.2E). However, Glut2

mRNA level was high at day-20, subsequently decreasing at day-27, day-34, day-48 in the following time points. Importantly, in rodents, Insulin gene have two non-allelic Insulin genes (Insulin1 and Insulin 2), which are different number of introns, and differ on chromosomal loci (Soares et al. 1985). In previous studies, Insulin gene encodes a 110 amino acid precursor that is called pre-proinsulin (Weiss et al. 2000). Then, undergoing modification pathways, the proinsulin preserved at immature secretory granules and is cleaved to yield C-peptide and Insulin proteins. In granules, C-peptide and Insulin maintains with islet amyloid polypeptide and other less abundant beta-cell secretory products (Taylor 1972; Nishi et al. 1990; Weiss et al. 2000; Liu et al. 2018). Here, the Glut2 expression or insulin-supporting secretory factors might reduce its activity or function in the progress of IPC secretion. IPCs can survive over 60 days with high glucose in maintaining medium corresponding low dead-cell detection (Fig.2K). It implied that the NEAAs and beta-mercaptoethanol were worked as essential nutrients for prolonging the live cells. Besides, high glucose remained the Insulin mRNA or Insulin protein stability during Insulin-producing cell production. It is well documented that insulin biosynthesis is regulated by multifactor, and glucose metabolism. In vitro studies, under low glucose concentration, Insulin mRNA stability is reduced; in contrast, high glucose concentration increases the stability of Insulin

mRNA (Welsh et al. 1985). In 3-day fated rat, proinsulin mRNA expression is lifted three- or four-fold within 24 hours after glucose injection (Giddings et al. 1982; Poitout et al. 2006). In the conclusion, the IPC biosynthesis based on several factors including embryo bodies (EBs) formation, balance chemical combination, and nutrients in maintaining medium. The results proved that the IPCs were correctly produced from EBs to matured IPCs as autologous cells.

Islet equivalent from large human islets secrete Insulin concentration that is significantly lower than from smaller islets in high glucose solution by Insulin Single islet glucose-stimulated Insulin release test (Lehmann et al. 2007; Fujita et al. 2011). In diabetic animals, small islets are 80% successful transplantation outcomes compared to large islets (MacGregor et al. 2006; Su et al. 2010). To fabricate a small size of transplantable IPCs and remain functionalities, the 0.25% trypsin-EDTA solution was treated day-4 Embryoid body (EBs) stage to single cells before IPC induction following protocol VIII (Fig.3). However, IPC generation was reduced the quantity and quality at the end-stage (Fig.3). In day-20 IPC differentiation, Pdx1, Glut2, Nkx6.1 mRNA levels were distinctly decreased comparing with protocol VIII (Fig.3). Insulin production pathways are well modulated by Insulin gene transcription factors including homeodomain protein pancreas duodenum homeobox 1 (Pdx1), homeobox protein

Nxk6.1 (Macfarlane et al. 2000; Rafiq et al. 2000; Aigha and Abdelalim 2020). Glucose transporter 2 (Glut2) is a pancreatic beta-cell-surface expression that is essential for glucose stimulated Insulin releasing (Pang et al. 1994; Low et al. 2021). It means that 0.25% trypsin-EDTA residue might cause the cytotoxins in all IPC differentiation stages. Otherwise, using the protocol VIII, the responsible chemical and nutrient combination totally supported IPC formation. Here, we can suggest that single cell of day-4 EBs still provokes to IPC colony induction, which IPC colonies showed the insulin activity and secretion. However, the capacity of these IPCs was lower than protocol VIII; then we used the protocol VIII for IPC differentiation that was applied for IPC transplantation. Cell encapsulation is an advance technique for living cell-based therapy (Steele et al. 2014). The encapsulated capsules should provide a bio-transport of oxygens, nutrients, and metabolic wastes (Zhang and He 2011). Cell encapsulation prevents the autoimmune destruction to engraftment donors (Dang et al. 2013; Wang et al. 2021). To immobilization of cells into biocompatible and semipermeable membranes, IPCs were encapsulated by two layers of 2% alginate and 30% Pluronic-F127. In the results, IPC encapsulation or IPC-beads were displayed the survival inside the beads with well preservation of mRNA levels (Fig.4). Our studies elucidate that IPC-beads prolonged the time of IPC maturation. In encapsulated IPCs, the trend of GSCS test was increasing

when the increasing glucose concentration. It is suggested that the insulin can reuptake in the cells during incubated timing in GSCS experiments. In whiles, double layers of encapsulation lengthen the reuptake timing of insulin.

In the VEGF family of growth factors, there are VEGF-A (121, 145, 165, 183, 189, 206), VEGF-B, VEGF-C, VEGF-D, VEGF-E, VEGF-F isoforms (Apte et al. 2019). They transport to the intracellular by the plenty of receptors as VEGFR-1, VEGFR-2, VEGFR-3, Neuropilin-1 (NRP-1), and NRP-2 (Simons et al. 2016; Castaneda-Cabral et al. 2019). Moreover, VEGF-A165 can access four receptors including VEGFR-1, VEGFR-2, NRP-1, and NRP-2 (Simons et al. 2016). In case, the ligands bind to VEGFR-1 which presses on the VEGF sequestration or decoy effects monocyte chemotaxis (Koizumi et al. 2022). Besides, the ligands bind to VEGFR-2 which triggers the pathways of migration, vascular permeability, endothelial cell proliferation, and survival (Masoumi Moghaddam et al. 2012; de Vries et al. 2019; Murata et al. 2022). In the results, we suggested VEGF-165

showed the retention time at the transplantation sites, which stimulated the angiogenesis activation until 42-day (VEGF-165 was not measured the retention time or release concentration of VEGF-165). However, the blood vessels were generated which elucidated on histopathology at D0, D21, D42. Dual-function of a glycogen synthase kinase 3 beta (GSK3 $\beta$ ) inhibitor, 6-bromoindirubin-3'-oxime (BIO), was loaded

in Pluronic F127 (PF127) nanoparticles for initial release to mitigate the inflammatory response and reduce cell apoptosis, while vascular endothelial growth factor (VEGF) was loaded in poly (lactic-co-glycolic acid) (PLGA) porous microspheres that enabled sustained release for continuous angiogenesis induction (Liu et al. 2022). In this study, VEGF-165 was loaded in Pluronic F127 nanoparticles for initial releasing to alleviate the immunology reaction, reduce cell apoptosis, and constitutively induce angiogenesis.

Inflammatory response is driven by pro-inflammatory cytokines and anti-inflammatory cytokines when immune cells are activated (Matsumoto et al. 2018). Pro-inflammatory cytokines are happened through activated macrophages. IL-1b, IL-6, IL-15, IL-17, IL-18 and TNF-alpha are popular involving in the upregulation of inflammatory reactions (Zhang and An 2007). On the other hand, the anti-inflammatory cytokines are secreted proteins for controlling the inflammation including the pro-inflammatory cytokine response. IL-1R antagonist, IL-4, IL-10, IL-11, and IL-13 are major in anti-inflammatory cytokines; besides, leukemia inhibitory factor, interferon-alpha, IL-6, TGF-beta are involved in either anti-inflammatory or pro-inflammatory cytokines (Cavaillon 2001; Wojdasiewicz et al. 2014). The normal development of CTRL and VEGF-165 + 10% Pluronic mice were properly monitored (Fig.5). The pathogenesis or blood chemistry

of VEGF-165 + 10% Pluronic mice was not significantly altered during subcutaneous pocket formation and post-transplantation (Fig. 7, Table 2). Besides, the autoimmune response was still activated due to subcutaneous 18-G catheter insertion in the normal mice. sTNF-receptor II was high activated during blank bead post-transplantation (Fig.6). Correspondingly, the basophil cells were also increased the level in completed blood count test (Table 1). It is well cited that immunosuppressive TNF-TNF receptor II interactions modulates the allergic inflammation. TNF receptor II agonist enhances proliferation and suppresses capacity of Treg cells (Ahmad et al. 2018). B Lymphocyte chemokine (BLC or CXCL13), macrophage inflammatory protein-1 gamma (MIP-1gamma or CCL9) were dynamic changed until day-42 in both CTRL and VEGF-165 + 10% Pluronic groups. In this study, the transplantation platform was successfully and safely established.

Single high-dose of streptozotocin injection caused completed type 1 diabetes in mice.

The pancreatic beta-cells were eliminated the function and activity via C-peptide detection and HOMA-indexes (Fig.8C, 8D). In diabetic mice, the inflammatory cells were globally activation in blood circulation (Fig.9). Especially, granulocyte colony-stimulating factor (GCSF) was extremely highest level (Fig.9B). The diabetic mice were developed the pathogenesis tissues and severe damaged pancreas (Fig.10).



In previous studies, GCSF is a regulator of granulocyte synthesis, which is inflammatory produced by endothelial cells, fibroblasts, bone marrow stromal cells, macrophages (Lawlor et al. 2004). Low-dose immunotherapy of GCSF and antithymocyte globulin (ATG) conserves C-peptide for 2 years. Then, the patients are continuously follow-up of 5 years, the low dose of GCSF/ATG delay progression of T1D from phase 2 (autoantibody positive with dysglycemia) to stage 3 of clinical T1D (Lin et al. 2021). In parallelly, BLC, RANTES (CCL5), MIP-1gamma, Interferon-inducible T-cell alpha chemoattractant (I-TAC or CXCL11), or KC (CXCL1/2) expression was strong in diabetic mice, and blank bead Tx mice; was reduced the level in DM-VP + IPC-bead Tx mice. B Lymphocyte chemokine (BLC or CXCL13) is aberrantly high expressed by myeloid dendritic cells which may break immune tolerance in the thymus (Ishikawa et al. 2001). CXCL13 and its receptor CXCR5 were increased the expression as well as pro-inflammatory cytokine of Tumor Necrosis factor (TNF)-alpha and IL6 in spinal cord of db/db type 2 diabetes mice (Liu et al. 2019). The tertiary lymphoid organs of B lymphocytes in islets are disrupted by CXCL13 blockade (Henry and Kendall 2010). Interferon-inducible T-cell alpha chemoattractant (I-TAC or CXCL11) is a non-ELR CXC chemokine, is regulated by interferon (IFN) and has potent chemotactic activity for interleukin (IL)-2-activated T cells. I-TAC selectively interacts affinity with CXCR3

(CXCR3 is a receptor for IFN-inducible chemokines, IFN-gamma-inducible 10-kD protein (IP10) and IFN-gamma-induced human monokine) (Cole et al. 1998). In atherogenesis, CXC chemokine ligands including I-TAC is suppressed by adiponectin via RNA profiling of lipopolysaccharide in macrophage (Okamoto et al. 2008). Eotaxin (CCL11) and Eotaxin-2 (CCL24) are chemokines acting via CCR3 which induces recruitment of basophils, eosinophils, neutrophils, and macrophages (Menzies-Gow et al. 2002). Eotaxin, RANTES, MCP-4 activate CCR3 receptor on eosinophils, Th2 cells, and mast cells which predisposition in development of T1D (Hessner et al. 2004). The researches documented the chemokines such as CCL-3/MIP-1 $\alpha$ , CCL-5/RANTES, CCL-7/MCP-3, CCL-8/MCP-2, CCL-11/eotaxin-1, CCL-13/MCP-4, and CCL-24/eotaxin-2 have been found to induce the eosinophil migration and activation in inflammatory diseases (Carvalho et al. 2018). In the results, IPC transplantation was somehow response the glucose stimulation via IPGTT test; however, it was not completely inversed the hyperglycemia in STZ-induced diabetic mice. The CBC and blood chemistry in IPC-bead Tx were gradually turn to normal indexes (Table 3, Table 4). Furthermore, the percentage of mice survival was maintained in DM-VP + IPC transplantation mice; it implied that IPC transplantation supported the health condition in STZ-induced diabetic mice.

In this study, we have presented the high capacity of the insulin-producing cell (IPC) differentiation protocols from mGF-iPSCs including accurate endogenous IPC biosynthesis and function. 10% Pluronic-F127 carrying-VEGF-165 significantly elevated the blood vessel network surrounding blank or IPC bead location, and subcutaneous pocket boundary. IPC-beads were translated for rescuing the insulin-dependent tissues, parameters and somehow recovering the hyperglycemia symptoms in STZ-induced-diabetic mice-VEGF-165+10%Pluronic + IPC-bead transplantation (DM-VP+IPC-bead Tx mice). Moreover, IPC-bead transplantation maintained the health condition. The 40 inflammatory cytokines were globally explored in the blood circulation which reduced the expression levels. Here, the results are used for a reference strategy of IPC differentiation protocol. The achievement of high-performance IPC engraftment is applied as a clinical protocol for diabetes treatment using cell-based therapy without using anti-rejection drugs.

## CHAPTER V

### CONCLUSION

The results indicate that mGF-iPSC-derived is a promising model for an improvement of pancreatic IPC differentiation protocol. IPC production obtained the Insulin biosynthesis correction. 10% Pluronic-carrying-VEGF-165 gel generates the blood vessel network for supporting the engraftment. Subcutaneous IPC-bead transplantation achieves the essential functionalities and biocompatibilities. IPC transplantation enhanced the health condition in diabetic mice. The gained results can be used as an effective IPC induction protocol for encapsulated-cell transplantation. In this study, we suggest that the transplantation platform can be a clinical pilot protocol for T1D treatment using cell-based therapy.



จุฬาลงกรณ์มหาวิทยาลัย  
**CHULALONGKORN UNIVERSITY**

## REFERENCES



จุฬาลงกรณ์มหาวิทยาลัย  
**CHULALONGKORN UNIVERSITY**

Ahmad S, Azid NA, Boer JC, Lim J, Chen X, Plebanski M, Mohamud R. 2018. The Key Role of TNF-TNFR2 Interactions in the Modulation of Allergic Inflammation: A Review. *Front Immunol* 9: 2572.

Aigha, II, Abdelalim EM. 2020. NKX6.1 transcription factor: a crucial regulator of pancreatic beta cell development, identity, and proliferation. *Stem Cell Res Ther* 11: 459.

Amimoto N, Nishimura K, Shimohama S, Takata K. 2021. Generation of striatal neurons from human induced pluripotent stem cells by controlling extrinsic signals with small molecules. *Stem Cell Res* 55: 102486.

Amjad S, Nisar S, Bhat AA, Shah AR, Frenneaux MP, Fakhro K, Haris M, Reddy R, Patay Z, Baur J et al. 2021. Role of NAD(+) in regulating cellular and metabolic signaling pathways. *Mol Metab* 49: 101195.

An D, Chiu A, Flanders JA, Song W, Shou D, Lu YC, Grunnet LG, Winkel L, Ingvorsen C, Christophersen NS et al. 2018. Designing a retrievable and scalable cell encapsulation device for potential treatment of type 1 diabetes. *Proc Natl Acad Sci U S A* 115: E263-E272.

Andorko JI, Jewell CM. 2017. Designing biomaterials with immunomodulatory properties for tissue engineering and regenerative medicine. *Bioeng Transl Med* 2: 139-155.

Apte RS, Chen DS, Ferrara N. 2019. VEGF in Signaling and Disease: Beyond Discovery and Development. *Cell* 176: 1248-1264.

Assoc AD. 2006. Pancreas and islet transplantation in type 1 diabetes. *Diabetes Care* 29: 935-935.

Audouard E, Rousselot L, Folcher M, Cartier N, Piguat F. 2021. Optimized Protocol for Subcutaneous Implantation of Encapsulated Cells Device and Evaluation of Biocompatibility. *Front Bioeng Biotechnol* 9: 620967.

Bai L, Meredith G, Tuch BE. 2005. Glucagon-like peptide-1 enhances production of insulin in insulin-producing cells derived from mouse embryonic stem cells. *J Endocrinol* 186: 343-352.

Billotey C, Aspod C, Beuf O, Piaggio E, Gazeau F, Janier MF, Thivolet C. 2005. T-cell homing to the pancreas in autoimmune mouse models of diabetes: in vivo MR imaging. *Radiology* 236: 579-587.



- Blanter M, Sork H, Tuomela S, Flodstrom-Tullberg M. 2019. Genetic and Environmental Interaction in Type 1 Diabetes: a Relationship Between Genetic Risk Alleles and Molecular Traits of Enterovirus Infection? *Curr Diabetes Rep* 19.
- Bode BW, Boyd J, Shah A, Parkes D, Ghosh S, Cherrington AD. 2020. Insulin and Glucagon Coadministration in Type 1 Diabetes Prevents Hypoglycemia without Worsening Hyperglycemia. *Diabetes* 69.
- Brickman JM, Serup P. 2017. Properties of embryoid bodies. *Wires Dev Biol* 6.
- Bromberg JS. 2015. Islet implantation in a pocket. *Nat Biotechnol* 33: 493-494.
- Brun PJ, Grijalva A, Rausch R, Watson E, Yuen JJ, Das BC, Shudo K, Kagechika H, Leibel RL, Blaner WS. 2015. Retinoic acid receptor signaling is required to maintain glucose-stimulated insulin secretion and beta-cell mass. *Faseb Journal* 29: 671-683.
- Brunet-Maheu JM, Fernandes JC, de Lacerda CA, Shi Q, Benderdour M, Lavigne P. 2009. Pluronic F-127 as a cell carrier for bone tissue engineering. *J Biomater Appl* 24: 275-287.
- Calafiore R, Basta G. 2014. Clinical application of microencapsulated islets: Actual perspectives on progress and challenges. *Adv Drug Deliver Rev* 67-68: 84-92.

- Carpenedo RL, Sargent CY, McDevitt TC. 2007. Rotary suspension culture enhances the efficiency, yield, and homogeneity of embryoid body differentiation. *Stem Cells* 25: 2224-2234.
- Carrageta DF, Oliveira PF, Barros A, Monteiro MP, Alves MG. 2021. Glucose stimuli prompts insulin secretion by human spermatozoa. *Febs Open Bio* 11: 181-181.
- Carvalho VF, Barreto EO, Arantes ACS, Serra MF, Ferreira TPT, Jannini-Sa YAP, Hogaboam CM, Martins MA, Silva PMR. 2018. Diabetes Downregulates Allergen-Induced Airway Inflammation in Mice. *Mediators Inflamm* 2018: 6150843.
- Castaneda-Cabral JL, Beas-Zarate C, Rocha-Arrieta LL, Orozco-Suarez SA, Alonso-Vanegas M, Guevara-Guzman R, Urena-Guerrero ME. 2019. Increased protein expression of VEGF-A, VEGF-B, VEGF-C and their receptors in the temporal neocortex of pharmacoresistant temporal lobe epilepsy patients. *J Neuroimmunol* 328: 68-72.
- Cavillon JM. 2001. Pro- versus anti-inflammatory cytokines: myth or reality. *Cell Mol Biol (Noisy-le-grand)* 47: 695-702.
- Cayabyab F, Nih LR, Yoshihara E. 2021. Advances in Pancreatic Islet Transplantation Sites for the Treatment of Diabetes. *Front Endocrinol (Lausanne)* 12: 732431.
- Chen CS, Pegan J, Luna J, Xia B, McCloskey K, Chin WC, Khine M. 2008. Shrinky-dink hanging drops: a simple way to form and culture embryoid bodies. *J Vis Exp*.

- Chen D, Thayer TC, Wen L, Wong FS. 2020. Mouse Models of Autoimmune Diabetes: The Nonobese Diabetic (NOD) Mouse. *Methods Mol Biol* 2128: 87-92.
- Chen Y, Shu Z, Qian K, Wang J, Zhu H. 2019. Harnessing the Properties of Biomaterial to Enhance the Immunomodulation of Mesenchymal Stem Cells. *Tissue Eng Part B Rev* 25: 492-499.
- Cheng Y, Liu YF, Zhang JL, Li TM, Zhao N. 2007. Elevation of vascular endothelial growth factor production and its effect on revascularization and function of graft islets in diabetic rats. *World J Gastroenterol* 13: 2862-2866.
- Cherkashova EA, Leonov GE, Namestnikova DD, Solov'eva AA, Gubskii IL, Bukharova TB, Gubskii LV, Goldstein DV, Yarygin KN. 2020. Methods of Generation of Induced Pluripotent Stem Cells and Their Application for the Therapy of Central Nervous System Diseases. *Bull Exp Biol Med* 168: 566-573.
- Cole KE, Strick CA, Paradis TJ, Ogborne KT, Loetscher M, Gladue RP, Lin W, Boyd JG, Moser B, Wood DE et al. 1998. Interferon-inducible T cell alpha chemoattractant (I-TAC): a novel non-ELR CXC chemokine with potent activity on activated T cells through selective high affinity binding to CXCR3. *J Exp Med* 187: 2009-2021.
- Dang TT, Thai AV, Cohen J, Slosberg JE, Siniakowicz K, Doloff JC, Ma M, Hollister-Lock J, Tang KM, Gu Z et al. 2013. Enhanced function of immuno-isolated islets in diabetes

therapy by co-encapsulation with an anti-inflammatory drug. *Biomaterials* 34:

5792-5801.

de Vries MR, Parma L, Peters HAB, Schepers A, Hamming JF, Jukema JW, Goumans M,

Guo L, Finn AV, Virmani R et al. 2019. Blockade of vascular endothelial growth factor

receptor 2 inhibits intraplaque haemorrhage by normalization of plaque neovessels. *J*

*Intern Med* 285: 59-74.

Deeds MC, Anderson JM, Armstrong AS, Gastineau DA, Hiddinga HJ, Jahangir A,

Eberhardt NL, Kudva YC. 2011. Single dose streptozotocin-induced diabetes:

considerations for study design in islet transplantation models. *Lab Anim* 45: 131-140.

Diniz IMA, Chen C, Xu XT, Ansari S, Zadeh HH, Marques MM, Shi ST, Moshaverinia A.

2015. Pluronic F-127 hydrogel as a promising scaffold for encapsulation of

dental-derived mesenchymal stem cells. *J Mater Sci-Mater M* 26.

Driver JP, Serreze DV, Chen YG. 2011. Mouse models for the study of autoimmune

type 1 diabetes: a NOD to similarities and differences to human disease. *Semin*

*Immunopathol* 33: 67-87.

Dufrane D, Gianello P. 2012. Macro- or microencapsulation of pig islets to cure type 1

diabetes. *World J Gastroenterol* 18: 6885-6893.

Egusa H, Okita K, Kayashima H, Yu GN, Fukuyasu S, Saeki M, Matsumoto T, Yamanaka S, Yatani H. 2010. Gingival Fibroblasts as a Promising Source of Induced Pluripotent Stem Cells. *Plos One* 5.

Escurat M, Djabali K, Huc C, Landon F, Becourt C, Boitard C, Gros F, Portier MM. 1991. Origin of the beta cells of the islets of Langerhans is further questioned by the expression of neuronal intermediate filament proteins, peripherin and NF-L, in the rat insulinoma RIN5F cell line. *Dev Neurosci* 13: 424-432.

Faideau B, Larger E, Lepault F, Carel JC, Boitard C. 2005. Role of beta-cells in type 1 diabetes pathogenesis. *Diabetes* 54 Suppl 2: S87-96.

Fu Z, Gilbert ER, Liu D. 2013. Regulation of insulin synthesis and secretion and pancreatic Beta-cell dysfunction in diabetes. *Curr Diabetes Rev* 9: 25-53.

Fujita Y, Takita M, Shimoda M, Itoh T, Sugimoto K, Noguchi H, Naziruddin B, Levy MF, Matsumoto S. 2011. Large human islets secrete less insulin per islet equivalent than smaller islets in vitro. *Islets* 3: 1-5.

Furman BL. 2015. Streptozotocin-Induced Diabetic Models in Mice and Rats. *Curr Protoc Pharmacol* 70: 5 47 41-45 47 20.

- 2021. Streptozotocin-Induced Diabetic Models in Mice and Rats. *Curr Protoc* 1: e78.

Garcia Barrado MJ, Iglesias Osma MC, Blanco EJ, Carretero Hernandez M, Sanchez

Robledo V, Catalano Iniesta L, Carrero S, Carretero J. 2015. Dopamine modulates

insulin release and is involved in the survival of rat pancreatic beta cells. PLoS One

10: e0123197.

Garcia KO, Ornellas FL, Martin PK, Patti CL, Mello LE, Frussa-Filho R, Han SW, Longo

BM. 2014. Therapeutic effects of the transplantation of VEGF overexpressing bone

marrow mesenchymal stem cells in the hippocampus of murine model of

Alzheimer's disease. Front Aging Neurosci 6: 30.

Giarratana N, Penna G, Adorini L. 2007. Animal models of spontaneous autoimmune

disease: type 1 diabetes in the nonobese diabetic mouse. Methods Mol Biol 380:

285-311.

Giddings SJ, Chirgwin J, Permutt MA. 1982. Effects of glucose on proinsulin messenger

RNA in rats in vivo. Diabetes 31: 624-629.

Graham ML, Janecek JL, Kittredge JA, Hering BJ, Schuurman HJ. 2011. The

Streptozotocin-Induced Diabetic Nude Mouse Model: Differences between Animals

from Different Sources. Comparative Med 61: 356-360.

Gram GJ, Nielsen SD, Hansen JE. 1998. Spontaneous silencing of humanized green fluorescent protein (hGFP) gene expression from a retroviral vector by DNA methylation. *J Hematother* 7: 333-341.

Gross JL, de Azevedo MJ, Silveiro SP, Canani LH, Caramori ML, Zelmanovitz T. 2005. Diabetic nephropathy: diagnosis, prevention, and treatment. *Diabetes Care* 28: 164-176.

Gunaseeli I, Doss MX, Antzelevitch C, Hescheler J, Sachinidis A. 2010. Induced Pluripotent Stem Cells as a Model for Accelerated Patient- and Disease-specific Drug Discovery. *Current Medicinal Chemistry* 17: 759-766.

Gunawardana SC, Benninger RKP, Piston DW. 2009. Subcutaneous transplantation of embryonic pancreas for correction of type 1 diabetes. *Am J Physiol-Endoc M* 296: E323-E332.



Hahn M, van Krieken PP, Nord C, Alanentalo T, Morini F, Xiong Y, Eriksson M, Mayer J,

Kostromina E, Ruas JL et al. 2020. Topologically selective islet vulnerability and self-sustained downregulation of markers for beta-cell maturity in

streptozotocin-induced diabetes. *Commun Biol* 3: 541.

Haines MS, Leong A, Porneala BC, Meigs JB, Miller KK. 2022. Association between muscle mass and diabetes prevalence independent of body fat distribution in adults under 50 years old. *Nutr Diabetes* 12: 29.

Halberstadt CR, Williams D, Emerich D, Goddard M, Vasconcellos AV, Curry W, Bhatia A, Gores PF. 2005. Subcutaneous transplantation of islets into streptozocin-induced diabetic rats. *Cell Transplantation* 14: 595-605.

Haridhasapavalan KK, Borgohain MP, Dey C, Saha B, Narayan G, Kumar S, Thummer RP. 2019. An insight into non-integrative gene delivery approaches to generate transgene-free induced pluripotent stem cells. *Gene* 686: 146-159.

Henquin JC. 2000. Triggering and amplifying pathways of regulation of insulin secretion by glucose. *Diabetes* 49: 1751-1760.

- . 2021. Glucose-induced insulin secretion in isolated human islets: Does it truly reflect beta-cell function in vivo? *Molecular Metabolism* 48.

Henry L, Labied S, Fransolet M, Kirschvink N, Blacher S, Noel A, Foidart JM, Nisolle M, Munaut C. 2015. Isoform 165 of vascular endothelial growth factor in collagen matrix improves ovine cryopreserved ovarian tissue revascularisation after xenotransplantation in mice. *Reprod Biol Endocrinol* 13: 12.



Henry RA, Kendall PL. 2010. CXCL13 blockade disrupts B lymphocyte organization in tertiary lymphoid structures without altering B cell receptor bias or preventing diabetes in nonobese diabetic mice. *J Immunol* 185: 1460-1465.

Hessner MJ, Wang X, Meyer L, Geoffrey R, Jia S, Fuller J, Lenmark A, Ghosh S. 2004. Involvement of eotaxin, eosinophils, and pancreatic predisposition in development of type 1 diabetes mellitus in the BioBreeding rat. *J Immunol* 173: 6993-7002.

Ho CK, Sriram G, Dipple KM. 2016. Insulin sensitivity predictions in individuals with obesity and type II diabetes mellitus using mathematical model of the insulin signal transduction pathway. *Mol Genet Metab* 119: 288-292.

Ho N, Sommers MS, Lucki I. 2013. Effects of diabetes on hippocampal neurogenesis: links to cognition and depression. *Neurosci Biobehav Rev* 37: 1346-1362.

Hong S, Chang Y, Jung HS, Yun KE, Shin H, Ryu S. 2017. Relative muscle mass and the risk of incident type 2 diabetes: A cohort study. *PLoS One* 12: e0188650.

Hosoya M, Kunisada Y, Kurisaki A, Asashima M. 2012. Induction of differentiation of undifferentiated cells into pancreatic beta cells in vertebrates. *Int J Dev Biol* 56: 313-323.

Hotta A, Ellis J. 2008. Retroviral vector silencing during iPS cell induction: an epigenetic beacon that signals distinct pluripotent states. *J Cell Biochem* 105: 940-948.

Huang W, Wang GL, Delaspre F, Vitery MDC, Beer RL, Parsons MJ. 2014. Retinoic acid plays an evolutionarily conserved and biphasic role in pancreas development.

*Developmental Biology* 394: 83-93.

Hussain MA, Porras DL, Rowe MH, West JR, Song WJ, Schreiber WE, Wondisford FE.

2006. Increased pancreatic beta-cell proliferation mediated by CREB binding protein gene activation. *Mol Cell Biol* 26: 7747-7759.

Hwang DH, Lee HJ, Park IH, Seok JI, Kim BG, Joo IS, Kim SU. 2009. Intrathecal

transplantation of human neural stem cells overexpressing VEGF provide behavioral improvement, disease onset delay and survival extension in transgenic ALS mice.

*Gene Ther* 16: 1234-1244.

Ishihara M, Kishimoto S, Nakamura S, Fukuda K, Sato Y, Hattori H. 2018. Biomaterials

as cell carriers for augmentation of adipose tissue-derived stromal cell

transplantation. *Bio-Med Mater Eng* 29: 567-585.

Ishikawa S, Sato T, Abe M, Nagai S, Onai N, Yoneyama H, Zhang Y, Suzuki T,

Hashimoto S, Shirai T et al. 2001. Aberrant high expression of B lymphocyte

chemokine (BLC/CXCL13) by C11b+CD11c+ dendritic cells in murine lupus and preferential chemotaxis of B1 cells towards BLC. *J Exp Med* 193: 1393-1402.

Jaafarpour Z, Soleimani M, Hosseinkhani S, Karimi MH, Yaghmaei P, Mobarra N, Geramizadeh B. 2016. Differentiation of Definitive Endoderm from Human Induced Pluripotent Stem Cells on hMSCs Feeder in a Defined Medium. *Avicenna J Med Biotechnol* 8: 2-8.

Janowski M, Lyczek A, Engels C, Xu J, Lukomska B, Bulte JW, Walczak P. 2013. Cell size and velocity of injection are major determinants of the safety of intracarotid stem cell transplantation. *J Cereb Blood Flow Metab* 33: 921-927.

Jeon K, Lim H, Kim JH, Thuan NV, Park SH, Lim YM, Choi HY, Lee ER, Kim JH, Lee MS et al. 2012. Differentiation and Transplantation of Functional Pancreatic Beta Cells Generated from Induced Pluripotent Stem Cells Derived from a Type 1 Diabetes Mouse Model. *Stem Cells and Development* 21: 2642-2655.

Jiang FX, Li K, Archer M, Mehta M, Jamieson E, Charles A, Dickinson JE, Matsumoto M, Morahan G. 2017. Differentiation of Islet Progenitors Regulated by Nicotinamide into Transcriptome-Verified beta Cells That Ameliorate Diabetes. *Stem Cells* 35: 1341-1354.

Juang JH, Bonner-Weir S, Ogawa Y, Vacanti JP, Weir GC. 1996. Outcome of subcutaneous islet transplantation improved by polymer device. *Transplantation* 61: 1557-1561.

Justice MJ, Dhillon P. 2016. Using the mouse to model human disease: increasing validity and reproducibility. *Disease Models & Mechanisms* 9: 101-103.

Kant V, Gopal A, Kumar D, Gopalkrishnan A, Pathak NN, Kurade NP, Tandan SK, Kumar D. 2014. Topical pluronic F-127 gel application enhances cutaneous wound healing in rats. *Acta Histochem* 116: 5-13.

Katsarou A, Gudbjornsdottir S, Rawshani A, Dabelea D, Bonifacio E, Anderson BJ, Jacobsen LM, Schatz DA, Lernmark A. 2017. Type 1 diabetes mellitus. *Nat Rev Dis Primers* 3: 17016.

Kim MJ, Lee EY, You YH, Yang HK, Yoon KH, Kim JW. 2020a. Generation of iPSC-derived insulin-producing cells from patients with type 1 and type 2 diabetes compared with healthy control. *Stem Cell Res* 48: 101958.

Kim PTW, Hoffman BG, Plesner A, Helgason CD, Verchere CB, Chung SW, Warnock GL,

Mui ALF, Ong CJ. 2010. Differentiation of Mouse Embryonic Stem Cells into Endoderm without Embryoid Body Formation. *Plos One* 5.

Kim YH, Ko JH, Lee S, Oh JY, Jeong GS, Park SN, Shim IK, Kim SC. 2020b. Long-term reversal of diabetes by subcutaneous transplantation of pancreatic islet cells and adipose-derived stem cell sheet using surface-immobilized heparin and engineered collagen scaffold. *Bmj Open Diab Res Ca* 8.

Koizumi K, Shintani T, Hayashido Y, Hamada A, Higaki M, Yoshioka Y, Sakamoto A, Yanamoto S, Okamoto T. 2022. VEGF-A promotes the motility of human melanoma cells through the VEGFR1-PI3K/Akt signaling pathway. *In Vitro Cell Dev Biol Anim*.

Krevelen DW, Hoftyzer PJ. 1976. Properties of polymers, their estimation and correlation with chemical structure. Elsevier Scientific Pub. Co., Amsterdam ; New York.

Kubo A, Shinozaki K, Shannon JM, Kouskoff V, Kennedy M, Woo S, Fehling HJ, Keller G. 2004. Development of definitive endoderm from embryonic stem cells in culture. *Development* 131: 1651-1662.

Kumar SS, Alarfaj AA, Munusamy MA, Singh AJ, Peng IC, Priya SP, Hamat RA, Higuchi A. 2014. Recent developments in beta-cell differentiation of pluripotent stem cells induced by small and large molecules. *Int J Mol Sci* 15: 23418-23447.

Kuncorojakti S, Rodprasert W, Yodmuang S, Osathanon T, Pavasant P, Srisuwatanasagul S, Sawangmake C. 2020. Alginate/Pluronic F127-based

encapsulation supports viability and functionality of human dental pulp stem cell-derived insulin-producing cells. *J Biol Eng* 14: 23.

Kusumoto M, Ooka T, Nishiya Y, Ogura Y, Saito T, Sekine Y, Iwata T, Akiba M, Hayashi T. 2011. Insertion sequence-excision enhancer removes transposable elements from bacterial genomes and induces various genomic deletions. *Nature Communications* 2.

Lai MI, Wendy-Yeo WY, Ramasamy R, Nordin N, Rosli R, Veerakumarasivam A, Abdullah S. 2011. Advancements in reprogramming strategies for the generation of induced pluripotent stem cells. *J Assist Reprod Genet* 28: 291-301.

Lanner JT, Bruton JD, Katz A, Westerblad H. 2008. Ca<sup>2+</sup> and insulin-mediated glucose uptake. *Curr Opin Pharmacol* 8: 339-345.

Lanner JT, Katz A, Tavi P, Sandstrom ME, Zhang SJ, Wretman C, James S, Fauconnier J,

Lannergren J, Bruton JD et al. 2006. The role of Ca<sup>2+</sup> influx for insulin-mediated glucose uptake in skeletal muscle. *Diabetes* 55: 2077-2083.

Lawlor KE, Campbell IK, Metcalf D, O'Donnell K, van Nieuwenhuijze A, Roberts AW,

Wicks IP. 2004. Critical role for granulocyte colony-stimulating factor in inflammatory arthritis. *Proc Natl Acad Sci U S A* 101: 11398-11403.

Lee JM, Kim BS, Lee H, Im GI. 2012. In Vivo Tracking of Mesenchymal Stem Cells Using Fluorescent Nanoparticles in an Osteochondral Repair Model. *Molecular Therapy* 20: 1434-1442.

Lee KY, Mooney DJ. 2012. Alginate: Properties and biomedical applications. *Prog Polym Sci* 37: 106-126.

Lee MH, Mamillapalli SS, Keiper BD, Cha DS. 2016. A systematic mRNA control mechanism for germline stem cell homeostasis and cell fate specification. *BMB Rep* 49: 93-98.

Lehmann R, Zuellig RA, Kugelmeier P, Baenninger PB, Moritz W, Perren A, Clavien PA, Weber M, Spinas GA. 2007. Superiority of small islets in human islet transplantation. *Diabetes* 56: 594-603.

Lim A. 2014. Diabetic nephropathy - complications and treatment. *Int J Nephrol Renovasc Dis* 7: 361-381.

Lin A, Mack JA, Bruggeman B, Jacobsen LM, Posgai AL, Wasserfall CH, Brusko TM, Atkinson MA, Gitelman SE, Gottlieb PA et al. 2021. Low-Dose ATG/GCSF in Established Type 1 Diabetes: A Five-Year Follow-up Report. *Diabetes* 70: 1123-1129.

Lin Y, Chen G. 2008. Embryoid body formation from human pluripotent stem cells in chemically defined E8 media. in *StemBook*, Cambridge (MA).

Lipes MA, Eisenbarth GS. 1990. Transgenic mouse models of type I diabetes. *Diabetes* 39: 879-884.

Liu H, Li R, Liao HK, Min Z, Wang C, Yu Y, Shi L, Dan J, Hayek A, Martinez Martinez L et al. 2021. Chemical combinations potentiate human pluripotent stem cell-derived 3D pancreatic progenitor clusters toward functional beta cells. *Nat Commun* 12: 3330.

Liu H, Ye Z, Kim Y, Sharkis S, Jang YY. 2010. Generation of endoderm-derived human induced pluripotent stem cells from primary hepatocytes. *Hepatology* 51: 1810-1819.

Liu M, Weiss MA, Arunagiri A, Yong J, Rege N, Sun J, Haataja L, Kaufman RJ, Arvan P. 2018. Biosynthesis, structure, and folding of the insulin precursor protein. *Diabetes Obes Metab* 20 Suppl 2: 28-50.

Liu S, Liu X, Xiong H, Wang W, Liu Y, Yin L, Tu C, Wang H, Xiang X, Xu J et al. 2019.

CXCL13/CXCR5 signaling contributes to diabetes-induced tactile allodynia via activating pERK, pSTAT3, pAKT pathways and pro-inflammatory cytokines production in the spinal cord of male mice. *Brain Behav Immun* 80: 711-724.

Liu Y, Zhang F, Long L, Li J, Liu Z, Hu C, Chen X, Zan X, Xu J, Wang Y. 2022.

Dual-function hydrogels with sequential release of GSK3 $\beta$  inhibitor and VEGF inhibit inflammation and promote angiogenesis after stroke. *Chemical Engineering Journal* 433: 133671.



Low BSJ, Lim CS, Ding SSL, Tan YS, Ng NHJ, Krishnan VG, Ang SF, Neo CWY, Verma CS,

Hoon S et al. 2021. Decreased GLUT2 and glucose uptake contribute to insulin

secretion defects in MODY3/HNF1A hiPSC-derived mutant beta cells. Nat Commun

12: 3133.

Ma X, Zhu S. 2017. Chemical strategies for pancreatic beta cell differentiation,

reprogramming, and regeneration. Acta Biochim Biophys Sin (Shanghai) 49: 289-301.

Macfarlane WM, Shepherd RM, Cosgrove KE, James RF, Dunne MJ, Docherty K. 2000.

Glucose modulation of insulin mRNA levels is dependent on transcription factor

PDX-1 and occurs independently of changes in intracellular Ca<sup>2+</sup>. Diabetes 49:

418-423.

MacGregor RR, Williams SJ, Tong PY, Kover K, Moore WV, Stehno-Bittel L. 2006. Small

rat islets are superior to large islets in in vitro function and in transplantation

outcomes. Am J Physiol Endocrinol Metab 290: E771-779.

Magisson J, Sassi A, Xhema D, Kobalyan A, Gianello P, Mourer B, Tran N, Burcez CT,

Aoun RB, Sigrist S. 2020. Safety and function of a new pre-vascularized bioartificial

pancreas in an allogeneic rat model. J Tissue Eng 11.

Manov A. 1991. [The role of the inadequate expression of HLA class-II molecules on pancreatic beta cells in the pathogenesis of type-1 diabetes mellitus]. *Vutr Boles* 30: 14-18.

Masoumi Moghaddam S, Amini A, Morris DL, Pourgholami MH. 2012. Significance of vascular endothelial growth factor in growth and peritoneal dissemination of ovarian cancer. *Cancer Metastasis Rev* 31: 143-162.

Matsumoto H, Ogura H, Shimizu K, Ikeda M, Hirose T, Matsuura H, Kang S, Takahashi K, Tanaka T, Shimazu T. 2018. The clinical importance of a cytokine network in the acute phase of sepsis. *Sci Rep* 8: 13995.

Matsuoka K, Saito M, Shibata K, Sekine M, Shitara H, Taya C, Zhang X, Takahashi TA, Kohno K, Kikkawa Y et al. 2013. Generation of mouse models for type 1 diabetes by selective depletion of pancreatic beta cells using toxin receptor-mediated cell knockout. *Biochem Biophys Res Commun* 436: 400-405.

McCrimmon RJ, Sherwin RS. 2010. Hypoglycemia in type 1 diabetes. *Diabetes* 59: 2333-2339.

Meng Y, Ren Z, Xu F, Zhou X, Song C, Wang VY, Liu W, Lu L, Thomson JA, Chen G. 2018. Nicotinamide Promotes Cell Survival and Differentiation as Kinase Inhibitor in Human Pluripotent Stem Cells. *Stem Cell Reports* 11: 1347-1356.

Menzies-Gow A, Ying S, Sabroe I, Stubbs VL, Soler D, Williams TJ, Kay AB. 2002.

Eotaxin (CCL11) and eotaxin-2 (CCL24) induce recruitment of eosinophils, basophils, neutrophils, and macrophages as well as features of early- and late-phase allergic reactions following cutaneous injection in human atopic and nonatopic volunteers. *J Immunol* 169: 2712-2718.

Mfopou JK, Geeraerts M, Dejene R, Van Langenhoven S, Aberkane A, Van Grunsven LA, Bouwens L. 2014. Efficient definitive endoderm induction from mouse embryonic stem cell adherent cultures: a rapid screening model for differentiation studies. *Stem Cell Res* 12: 166-177.

Min CK, Kim SY, Lee MJ, Eom KS, Kim YJ, Kim HJ, Lee S, Cho SG, Kim DW, Lee JW et al. 2006. Vascular endothelial growth factor (VEGF) is associated with reduced severity of acute graft-versus-host disease and nonrelapse mortality after allogeneic stem cell transplantation. *Bone Marrow Transplant* 38: 149-156.

Mitrousis N, Fokina A, Shoichet MS. 2018. Biomaterials for cell transplantation. *Nat Rev Mater* 3: 441-456.

Murata M, Noda K, Kase S, Hase K, Wu D, Ando R, Ishida S. 2022. Placental growth factor stabilizes VEGF receptor-2 protein in retinal pigment epithelial cells by downregulating glycogen synthase kinase 3 activity. *J Biol Chem*: 102378.

Murry CE, Keller G. 2008. Differentiation of embryonic stem cells to clinically relevant populations: lessons from embryonic development. *Cell* 132: 661-680.

Nishi M, Sanke T, Nagamatsu S, Bell GI, Steiner DF. 1990. Islet amyloid polypeptide. A new beta cell secretory product related to islet amyloid deposits. *J Biol Chem* 265: 4173-4176.

Oh SI, Lee CK, Cho KJ, Lee KO, Cho SG, Hong S. 2012. Technological progress in generation of induced pluripotent stem cells for clinical applications. *ScientificWorldJournal* 2012: 417809.

Ohsugi T, Maejima K, Urano T. 1991. Bacterial translocation from the gastrointestinal tract in various mouse models for human diabetes. *Microbiol Immunol* 35: 789-794.

Okamoto Y, Folco EJ, Minami M, Wara AK, Feinberg MW, Sukhova GK, Colvin RA,

Kihara S, Funahashi T, Luster AD et al. 2008. Adiponectin inhibits the production of CXC receptor 3 chemokine ligands in macrophages and reduces T-lymphocyte

recruitment in atherogenesis. *Circ Res* 102: 218-225.

Oliver-Krasinski JM, Stoffers DA. 2008. On the origin of the beta cell. *Genes Dev* 22: 1998-2021.

Omami M, McGarrigle JJ, Reedy M, Isa D, Ghani S, Marchese E, Bochenek MA, Longi M, Xing Y, Joshi I et al. 2017. Islet Microencapsulation: Strategies and Clinical Status in Diabetes. *Curr Diab Rep* 17: 47.

Osathanon T, Manokawinchoke J, Egusa H, Pavasant P. 2017. Notch signaling partly regulates the osteogenic differentiation of retinoic acid-treated murine induced pluripotent stem cells. *Journal of Oral Science* 59: 405-413.

Ostrom M, Loffler KA, Edfalk S, Selander L, Dahl U, Ricordi C, Jeon J, Correa-Medina M, Diez J, Edlund H. 2008. Retinoic Acid Promotes the Generation of Pancreatic Endocrine Progenitor Cells and Their Further Differentiation into beta-Cells. *Plos One* 3.

Pagliuca FW, Millman JR, Gurtler M, Segel M, Van Dervort A, Ryu JH, Peterson QP, Greiner D, Melton DA. 2014. Generation of functional human pancreatic beta cells in vitro. *Cell* 159: 428-439.

Pan G, Liu J. 2019. Small molecules and extrinsic factors promoting differentiation of stem cells into insulin-producing cells. *Ann Endocrinol (Paris)* 80: 128-133.

Pang K, Mukonoweshuro C, Wong GG. 1994. Beta cells arise from glucose transporter type 2 (Glut2)-expressing epithelial cells of the developing rat pancreas. *Proc Natl Acad Sci U S A* 91: 9559-9563.

Pavathuparambil Abdul Manaph N, Sivanathan KN, Nitschke J, Zhou XF, Coates PT, Drogemuller CJ. 2019. An overview on small molecule-induced differentiation of mesenchymal stem cells into beta cells for diabetic therapy. *Stem Cell Res Ther* 10: 293.

Pepper A, Gala-Lopez B, Pawlick R, Shapiro A. 2014. A Prevascularized Subcutaneous 'Device-Less' Site for Islet Transplantation. *American Journal of Transplantation* 14: 331-331.

Pepper AR, Gala-Lopez B, Pawlick R, Merani S, Kin T, Shapiro AM. 2015a. A prevascularized subcutaneous device-less site for islet and cellular transplantation. *Nat Biotechnol* 33: 518-523.

Pepper AR, Gala-Lopez B, Pawlick R, Merani S, Kin T, Shapiro AMJ. 2015b. A prevascularized subcutaneous device-less site for islet and cellular transplantation. *Nature Biotechnology* 33: 518-U233.

Perlman RL. 2016. Mouse models of human disease: An evolutionary perspective. *Evol Med Public Health* 2016: 170-176.

Pettinato G, Wen X, Zhang N. 2014a. Formation of well-defined embryoid bodies from dissociated human induced pluripotent stem cells using microfabricated cell-repellent microwell arrays. *Sci Rep* 4: 7402.

- 2015. Engineering Strategies for the Formation of Embryoid Bodies from Human Pluripotent Stem Cells. *Stem Cells Dev* 24: 1595-1609.

Pettinato G, Wen XJ, Zhang N. 2014b. Formation of Well-defined Embryoid Bodies from Dissociated Human Induced Pluripotent Stem Cells using Microfabricated Cell-repellent Microwell Arrays. *Scientific Reports* 4.

Poitout V, Hagman D, Stein R, Artner I, Robertson RP, Harmon JS. 2006. Regulation of the insulin gene by glucose and fatty acids. *J Nutr* 136: 873-876.

Pomposelli T, Schuetz C, Wang P, Yamada K. 2021. A Strategy to Simultaneously Cure Type 1 Diabetes and Diabetic Nephropathy by Transplant of Composite Islet-Kidney Grafts. *Front Endocrinol (Lausanne)* 12: 632605.

Proescholdt MA, Heiss JD, Walbridge S, Muhlhauser J, Capogrossi MC, Oldfield EH, Merrill MJ. 1999. Vascular endothelial growth factor (VEGF) modulates vascular permeability and inflammation in rat brain. *J Neuropathol Exp Neurol* 58: 613-627.

Qu X, Afelik S, Jensen JN, Bukys MA, Kobberup S, Schmerr M, Xiao F, Nyeng P,

Veronica Albertoni M, Grapin-Botton A et al. 2013. Notch-mediated post-translational control of Ngn3 protein stability regulates pancreatic patterning and cell fate commitment. *Dev Biol* 376: 1-12.

Rafiq I, da Silva Xavier G, Hooper S, Rutter GA. 2000. Glucose-stimulated preproinsulin gene expression and nuclear trans-location of pancreatic duodenum homeobox-1 require activation of phosphatidylinositol 3-kinase but not p38 MAPK/SAPK2. *J Biol Chem* 275: 15977-15984.

Raikwar SP, Zavazava N. 2009. Insulin producing cells derived from embryonic stem cells: are we there yet? *J Cell Physiol* 218: 256-263.

Roder PV, Wu B, Liu Y, Han W. 2016. Pancreatic regulation of glucose homeostasis. *Exp Mol Med* 48: e219.

Rodrigues CG, Plentz RD, Dipp T, Salles FB, Giusti, II, Sant'Anna RT, Eibel B, Nesralla IA, Markoski M, Beyer NN et al. 2013. VEGF 165 gene therapy for patients with refractory angina: mobilization of endothelial progenitor cells. *Arq Bras Cardiol* 101: 149-153.

Roep BO, Peakman M. 2012. Antigen targets of type 1 diabetes autoimmunity. *Cold Spring Harb Perspect Med* 2: a007781.

Roep BO, Thomaidou S, van Tienhoven R, Zaldumbide A. 2021. Type 1 diabetes mellitus as a disease of the beta-cell (do not blame the immune system?). *Nature Reviews Endocrinology* 17: 150-161.



Rosmalen JG, Leenen PJ, Katz JD, Voerman JS, Drexhage HA. 1997. Dendritic cells in the autoimmune insulinitis in NOD mouse models of diabetes. *Adv Exp Med Biol* 417: 291-294.

Rungarunlert S, Techakumphu M, Purity MK, Dinnyes A. 2009. Embryoid body formation from embryonic and induced pluripotent stem cells: Benefits of bioreactors. *World J Stem Cells* 1: 11-21.

Saini V. 2010. Molecular mechanisms of insulin resistance in type 2 diabetes mellitus. *World J Diabetes* 1: 68-75.

Sakiyama-Elbert S, Johnson P. 2012. Keynote: Biomaterials for cell transplantation and drug delivery after spinal cord injury. *J Tissue Eng Regen M* 6: 85-85.

Satoh T. 2014. Molecular mechanisms for the regulation of insulin-stimulated glucose uptake by small guanosine triphosphatases in skeletal muscle and adipocytes. *Int J Mol Sci* 15: 18677-18692.

Seki T, Fukuda K. 2015. Methods of induced pluripotent stem cells for clinical application. *World J Stem Cells* 7: 116-125.

Shahjalal HM, Abdal Dayem A, Lim KM, Jeon TI, Cho SG. 2018. Generation of pancreatic beta cells for treatment of diabetes: advances and challenges. *Stem Cell Res Ther* 9: 355.

Shapiro AMJ, Lakey JRT, Ryan EA, Korbitt GS, Toth E, Warnock GL, Kneteman NM,

Rajotte RV. 2000. Islet transplantation in seven patients with type 1 diabetes mellitus

using a glucocorticoid-free immunosuppressive regimen. *New Engl J Med* 343:

230-238.

Shevchenko EK, Makarevich PI, Tsokolaeva ZI, Boldyreva MA, Syssoeva VY, Tkachuk VA,

Parfyonova YV. 2013. Transplantation of modified human adipose derived stromal

cells expressing VEGF165 results in more efficient angiogenic response in ischemic

skeletal muscle. *J Transl Med* 11: 138.

Shibuya M. 2011. Vascular Endothelial Growth Factor (VEGF) and Its Receptor (VEGFR)

Signaling in Angiogenesis: A Crucial Target for Anti- and Pro-Angiogenic Therapies.

*Genes Cancer* 2: 1097-1105.

Sigrist S, Mechine-Neuville A, Mandes K, Calenda V, Braun S, Legeay G, Bellocq JP,

Pinget M, Kessler L. 2003. Influence of VEGF on the viability of encapsulated

pancreatic rat islets after transplantation in diabetic mice. *Cell Transplant* 12:

627-635.

Simons M, Gordon E, Claesson-Welsh L. 2016. Mechanisms and regulation of

endothelial VEGF receptor signalling. *Nat Rev Mol Cell Biol* 17: 611-625.

- Smink AM, de Vos P. 2018. Therapeutic Strategies for Modulating the Extracellular Matrix to Improve Pancreatic Islet Function and Survival After Transplantation. *Curr Diabetes Rep* 18.
- Soares MB, Schon E, Henderson A, Karathanasis SK, Cate R, Zeitlin S, Chirgwin J, Efstratiadis A. 1985. RNA-mediated gene duplication: the rat preproinsulin I gene is a functional retroposon. *Mol Cell Biol* 5: 2090-2103.
- Son MY, Kim HJ, Kim MJ, Cho YS. 2011. Physical passaging of embryoid bodies generated from human pluripotent stem cells. *PLoS One* 6: e19134.
- Souza YE, Chaib E, Lacerda PG, Crescenzi A, Bernal-Filho A, D'Albuquerque LA. 2011. Islet transplantation in rodents. Do encapsulated islets really work? *Arq Gastroenterol* 48: 146-152.
- Srivastava P, Kilian KA. 2019. Micro-Engineered Models of Development Using Induced Pluripotent Stem Cells. *Front Bioeng Biotechnol* 7: 357.
- Stabler CL, Li Y, Stewart JM, Keselowsky BG. 2019. Engineering immunomodulatory biomaterials for type 1 diabetes. *Nat Rev Mater* 4: 429-450.
- Stankov K, Benc D, Draskovic D. 2013. Genetic and epigenetic factors in etiology of diabetes mellitus type 1. *Pediatrics* 132: 1112-1122.

Steele JA, Halle JP, Poncelet D, Neufeld RJ. 2014. Therapeutic cell encapsulation techniques and applications in diabetes. *Adv Drug Deliv Rev* 67-68: 74-83.

Steineck IK, Ranjan A, Schmidt S, Clausen TR, Hoist JJ, Norgaard K. 2019. Preserved glucose response to low-dose glucagon after exercise in insulin-pump-treated individuals with type 1 diabetes: a randomised crossover study. *Diabetologia* 62: 582-592.

Stendahl JC, Kaufman DB, Stupp SI. 2009. Extracellular Matrix in Pancreatic Islets: Relevance to Scaffold Design and Transplantation. *Cell Transplantation* 18: 1-12.

Su X, Huang L, Xiao D, Qu Y, Mu D. 2018. Research Progress on the Role and Mechanism of Action of Activin A in Brain Injury. *Front Neurosci* 12: 697.

Su Z, Xia J, Shao W, Cui Y, Tai S, Ekberg H, Corbascio M, Chen J, Qi Z. 2010. Small islets are essential for successful intraportal transplantation in a diabetes mouse model. *Scand J Immunol* 72: 504-510.

Sulzbacher S, Schroeder IS, Truong TT, Wobus AM. 2009. Activin A-Induced

Differentiation of Embryonic Stem Cells into Endoderm and Pancreatic

Progenitors-The Influence of Differentiation Factors and Culture Conditions. *Stem Cell*

*Reviews and Reports* 5: 159-173.

Sun JC, Tan HP. 2013. Alginate-Based Biomaterials for Regenerative Medicine

Applications. *Materials* 6: 1285-1309.

Takahashi K, Okita K, Nakagawa M, Yamanaka S. 2007a. Induction of pluripotent stem cells from fibroblast cultures. *Nat Protoc* 2: 3081-3089.

Takahashi K, Tanabe K, Ohnuki M, Narita M, Ichisaka T, Tomoda K, Yamanaka S. 2007b.

Induction of pluripotent stem cells from adult human fibroblasts by defined factors.

*Cell* 131: 861-872.

Takahashi K, Yamanaka S. 2006. Induction of pluripotent stem cells from mouse embryonic and adult fibroblast cultures by defined factors. *Cell* 126: 663-676.

Takeuchi H, Nakatsuji N, Suemori H. 2014. Endodermal differentiation of human pluripotent stem cells to insulin-producing cells in 3D culture. *Scientific Reports* 4.

Tatarkiewicz K, Hollister-Lock J, Quickel RR, Colton CK, Bonner-Weir S, Weir GC. 1999.

Reversal of hyperglycemia in mice after subcutaneous transplantation of macroencapsulated islets. *Transplantation* 67: 665-671.

Taylor KW. 1972. The biosynthesis and secretion of insulin. *Clin Endocrinol Metab* 1: 601-622.

Tengholm A. 2012. Cyclic AMP dynamics in the pancreatic beta-cell. *Ups J Med Sci* 117: 355-369.

Thakur G, Lee HJ, Jeon RH, Lee SL, Rho GJ. 2020. Small Molecule-Induced Pancreatic beta-Like Cell Development: Mechanistic Approaches and Available Strategies. *Int J Mol Sci* 21.

Tomei AA, Manzoli V, Fraker CA, Giraldo J, Velluto D, Najjar M, Pileggi A, Molano RD, Ricordi C, Stabler CL et al. 2014. Device design and materials optimization of conformal coating for islets of Langerhans. *Proc Natl Acad Sci U S A* 111: 10514-10519.

Van Belle TL, Taylor P, von Herrath MG. 2009. Mouse Models for Type 1 Diabetes. *Drug Discov Today Dis Models* 6: 41-45.

Van der Schueren B, Ellis D, Faradji RN, Al-Ozairi E, Rosen J, Mathieu C. 2021. Obesity in people living with type 1 diabetes. *Lancet Diabetes Endocrinol* 9: 776-785.

Vlahos AE, Talior-Volodarsky I, Kinney SM, Sefton MV. 2021a. A scalable device-less biomaterial approach for subcutaneous islet transplantation. *Biomaterials* 269: 120499.

- 2021b. A scalable device-less biomaterial approach for subcutaneous islet transplantation. *Biomaterials* 269.

Walczak MP, Drozd AM, Stoczynska-Fidelus E, Rieske P, Grzela DP. 2016. Directed differentiation of human iPSC into insulin producing cells is improved by induced expression of PDX1 and NKX6.1 factors in IPC progenitors. *J Transl Med* 14: 341.

Wang CH, Chang CH, Lin TL, Fu RH, Huang YC, Chen SY, Shyu WC, Liu SP. 2020. The novel application of cordycepin in maintaining stem cell pluripotency and increasing iPS cell generation efficiency. *Sci Rep* 10: 2187.

Wang LH, Ernst AU, Flanders JA, Liu W, Wang X, Datta AK, Epel B, Kotecha M, Papas KK, Ma M. 2021. An inverse-breathing encapsulation system for cell delivery. *Sci Adv* 7.

Wang S, Chen Z, Tang X, Liu H, Yang L, Wang Y. 2015. Transplantation of vascular endothelial growth factor 165transfected endothelial progenitor cells for the treatment of limb ischemia. *Mol Med Rep* 12: 4967-4974.

Wei R, Yang J, Hou W, Liu G, Gao M, Zhang L, Wang H, Mao G, Gao H, Chen G et al.

2013. Insulin-producing cells derived from human embryonic stem cells: comparison of definitive endoderm- and nestin-positive progenitor-based differentiation strategies. *PLoS One* 8: e72513.

Weiss M, Steiner DF, Philipson LH. 2000. Insulin Biosynthesis, Secretion, Structure, and Structure-Activity Relationships. in *Endotext* (eds. KR Feingold, B Anawalt, A Boyce, G

Chrousos, WW de Herder, K Dhatariya, K Dungan, JM Hershman, J Hofland, S Kalra, et al.), South Dartmouth (MA).

Welsh M, Nielsen DA, MacKrell AJ, Steiner DF. 1985. Control of insulin gene expression in pancreatic beta-cells and in an insulin-producing cell line, RIN-5F cells.

II. Regulation of insulin mRNA stability. *J Biol Chem* 260: 13590-13594.

White AM, Shamul JG, Xu J, Stewart S, Bromberg JS, He X. 2020a. Engineering Strategies to Improve Islet Transplantation for Type 1 Diabetes Therapy. *ACS Biomater Sci Eng* 6: 2543-2562.

White AM, Shamul JG, Xu JS, Stewart S, Bromberg JS, He XM. 2020b. Engineering Strategies to Improve Islet Transplantation for Type 1 Diabetes Therapy. *Acs Biomater Sci Eng* 6: 2543-2562.

Wojdasiewicz P, Poniatowski LA, Szukiewicz D. 2014. The role of inflammatory and anti-inflammatory cytokines in the pathogenesis of osteoarthritis. *Mediators Inflamm* 2014: 561459.

Xiao X, Li N, Zhang D, Yang B, Guo H, Li Y. 2016. Generation of Induced Pluripotent Stem Cells with Substitutes for Yamanaka's Four Transcription Factors. *Cell Reprogram* 18: 281-297.



Xie C, Jiang WJ, Lacroix JJ, Luo Y, Hao JJ. 2020. Insight into Molecular Mechanism for Activin A-Induced Bone Morphogenetic Protein Signaling. *International Journal of Molecular Sciences* 21.

Yamanaka S. 2013. Shinya Yamanaka: purveyor of pluripotency. Interview by Ruth Williams. *Circ Res* 112: 233-235.

Yamanaka S, Blau HM. 2010. Nuclear reprogramming to a pluripotent state by three approaches. *Nature* 465: 704-712.

Yang H, Yang L. 2016. Targeting cAMP/PKA pathway for glycemic control and type 2 diabetes therapy. *J Mol Endocrinol* 57: R93-R108.

Yang HK, Ham DS, Park HS, Rhee M, You YH, Kim MJ, Shin J, Kim OY, Khang G, Hong TH et al. 2016. Long-term Efficacy and Biocompatibility of Encapsulated Islet

Transplantation With Chitosan-Coated Alginate Capsules in Mice and Canine Models of Diabetes. *Transplantation* 100: 334-343.

Yi CG, Xia W, Zhang LX, Zhen Y, Shu MG, Han Y, Guo SZ. 2007. VEGF gene therapy for the survival of transplanted fat tissue in nude mice. *J Plast Reconstr Aesthet Surg* 60: 272-278.

Yu G, Okawa H, Okita K, Kamano Y, Wang F, Saeki M, Yatani H, Egusa H. 2016. Gingival Fibroblasts as Autologous Feeders for Induced Pluripotent Stem Cells. *Journal of Dental Research* 95: 110-118.

Yu J, Vodyanik MA, Smuga-Otto K, Antosiewicz-Bourget J, Frane JL, Tian S, Nie J, Jonsdottir GA, Ruotti V, Stewart R et al. 2007. Induced pluripotent stem cell lines derived from human somatic cells. *Science* 318: 1917-1920.

Yu M, Agarwal D, Korutla L, May CL, Wang W, Griffith NN, Hering BJ, Kaestner KH, Velazquez OC, Markmann JF et al. 2020. Islet transplantation in the subcutaneous space achieves long-term euglycaemia in preclinical models of type 1 diabetes. *Nat Metab* 2: 1013-+.

Yue Z, Liu X, Coates PT, Wallace GG. 2016. Advances in printing biomaterials and living cells: implications for islet cell transplantation. *Curr Opin Organ Transplant* 21: 467-475.

Zeevaert K, Elsafi Mabrouk MH, Wagner W, Goetzke R. 2020. Cell Mechanics in Embryoid Bodies. *Cells* 9.

Zhang D, Jiang W, Liu M, Sui X, Yin X, Chen S, Shi Y, Deng H. 2009. Highly efficient differentiation of human ES cells and iPS cells into mature pancreatic insulin-producing cells. *Cell Res* 19: 429-438.

Zhang F, Citra F, Wang DA. 2011. Prospects of induced pluripotent stem cell technology in regenerative medicine. *Tissue Eng Part B Rev* 17: 115-124.

Zhang JM, An J. 2007. Cytokines, inflammation, and pain. *Int Anesthesiol Clin* 45: 27-37.

Zhang W, He X. 2011. Microencapsulating and Banking Living Cells for Cell-Based Medicine. *J Healthc Eng* 2: 427-446.

Zhou HY, Wu SL, Joo JY, Zhu SY, Han DW, Lin TX, Trauger S, Bien G, Yao S, Zhu Y et al. 2009. Generation of Induced Pluripotent Stem Cells Using Recombinant Proteins (vol 4, pg 381, 2009). *Cell Stem Cell* 4: 581-581.

Zhou S, Lei Y, Wang P, Chen J, Zeng L, Qu T, Maldonado M, Huang J, Han T, Wen Z et al. 2022. Human Umbilical Cord Mesenchymal Stem Cells Encapsulated with Pluronic F-127 Enhance the Regeneration and Angiogenesis of Thin Endometrium in Rat via Local IL-1beta Stimulation. *Stem Cells Int* 2022: 7819234.

## VITA

**NAME** Hong Thuan Tran

**DATE OF BIRTH** 17 August 1991

**PLACE OF BIRTH** Vinh Long, Vietnam

**INSTITUTIONS ATTENDED**

1. Tohoku University School of Dentistry, Sendai, Japan
2. Chulalongkorn University Laboratory Animal Center, Bangkok, Thailand
3. Ajou University, College of Medicine, Suwon, Korea.
4. Ton Duc Thang University, Ho Chi Minh City, Vietnam.
5. Pasteur Institute, Ho Chi Minh City, Vietnam.
6. Medicine and Pharmacy University, Ho Chi Minh City, Viet Nam.

**HOME ADDRESS** Ap 3, Hoa Thanh, Tam Binh, Vinh Long, Vietnam

**PUBLICATION**

1. Hong Thuan Tran, Anh Phu Nam Bui. 2022. Detection of novel genes on recessive heterozygous alleles in pig breeding. a Review. Indian Journal of Animal Research.
2. Adretta Soedarmanto, Watchareewan Rodprasert, Hong Thuan Tran, Nabila Syarifah Jamilah, Steven Dwi Purbantoro, Choopet Nitsakulthong, Anusak Kijawornrat, Pichit Suvanprakorn, Chenphop Sawangmake. 2021. Modification of the isolation protocol for retrieving small- sized islets of Langerhans. Thai J Vet Med. 51(Suppl.): 010-012.
3. Hong Thuan Tran, Eunjoo Cho, Seongsu Jeong, Eui Beom Jeong, Hae Sang Lee, Jin Soon Hwang, Seon Yong Jeong, Eun Young Kim. (2018). Makorin 1 regulates developmental timing in Drosophila. Mol.Cells. 41(12): 1024–1032.

**AWARD RECEIVED**

1. 09-2022 to 03-2023 Visiting trip at Tohoku University School of Dentistry, Japan. Grantee by Second Century Fund (C2F), Chulalongkorn University.
2. 2019-2022 Merit Second Century Fund (C2F) Ph.D. Scholarship, 100% scholarship and accommodation, Chulalongkorn University, Thailand
3. 09-2020 Virtual student exchange certificate via APRU program at Osaka University, Japan
4. 02-2019 Very Good Master Diploma from University President, Ajou University, Korea

5. 2016-2019 Ajou University 100% Scholarship, Suwon, Korea
6. 2016-2019 Key clock's Lab Scholarship for the stipend, Ajou University School of Medicine, Korea
7. 04-2014 Elite Engineer certification from University President, Ton Duc Thang University, Vietnam
8. 04-2014 Good Bachelor certification, Ton Duc Thang University, Vietnam

